

Markov staircases

Nikolas Adaloglou, Jo   Brendel, Jonny Evans,
Johannes Hauber and Felix Schlenk

December 5, 2025

Abstract

Rational homology ellipsoids are certain Liouville domains diffeomorphic to rational homology balls and having Lagrangian pin-wheels as their skeleta. From the point of view of almost toric fibrations, they are a natural generalisation of usual symplectic ellipsoids. We study symplectic embeddings of rational homology ellipsoids into the complex projective plane and we show that for each Markov triple, this problem gives rise to an infinite staircase. A key ingredient in the proof is the result that any two such embeddings are Hamiltonian isotopic. We also prove constraints on sizes for pairs of disjoint embeddings.

Contents

1	Introduction	2
2	Notation and definitions	14
2.1	Wahl singularities and their resolutions	14
2.2	Offcuts	17
2.3	Vianna triangles	18
2.4	The culet	20
3	Geometry and topology of pavilion blow-ups	21
3.1	Pavilion blow up and its geometric structures	21
3.2	Topology of the pavilion blow-up	24
4	Ruled 4-manifolds	27
4.1	Regulations and rulings	27
4.2	Broken rulings	29
5	Pin-ellipsoids in the complex projective plane	32
5.1	Goal and strategy	32
5.2	Proof of the Isotopy Theorem (Theorem 1.4.1)	35

5.3	Proof of the Staircase Theorem (Theorem 1.5.2)	43
5.4	Proof of Theorem 5.1.1 (Evans–Smith <i>sans</i> orbifolds)	47
5.5	Proof of the Two Pin-Ball Theorem (Theorem 1.6.1)	52
5.6	Proof of Theorem 5.1.4	54
6	Appendix	56
6.1	Alternative proof of Theorem 5.1.1	56

1 Introduction

1.1 Old questions for new domains

Let (X, ω) be a symplectic 4-manifold. By Darboux’s theorem, small enough patches of X are symplectomorphic to subsets of the standard symplectic vector space (\mathbb{C}^2, ω_0) . In particular one can always symplectically embed small enough symplectic ellipsoids

$$E(\alpha, \beta) = \left\{ (z_1, z_2) \in \mathbb{C}^2 : \frac{\pi|z_1|^2}{\alpha} + \frac{\pi|z_2|^2}{\beta} \leq 1 \right\} \quad (1.1)$$

into (X, ω) . This raises several natural questions:

- (Q1) **Isotopy problem.** Given two such embeddings of the same size, are they ambiently isotopic?
- (Q2) **Embedding problem.** For which values of the parameters $\alpha, \beta > 0$ do symplectic embeddings of $E(\alpha, \beta)$ exist?
- (Q3) **Ellipsoid packing problem.** Given several embeddings of differently-sized ellipsoids, when can they be made disjoint?

In the case of symplectic balls $B(\alpha) = E(\alpha, \alpha)$, these questions were raised in Gromov’s foundational work [22], and, ever since, the idea of using such embeddings to measure the symplectic sizes and quantitative properties of (X, ω) has been a central theme in symplectic topology. In the work of McDuff and Schlenk [37], it was shown that the set of pairs (α, β) for which there is a symplectic embedding of $E(\alpha, \beta)$ into the ball takes the shape of an infinite staircase, whose step-sizes are related to the sequence of odd-indexed Fibonacci numbers. Since then, the ellipsoid embedding question into various target spaces X has attracted a lot of attention, see for instance the survey [42]. In this paper, instead of looking at new target spaces, we consider new domains.

Our goal is to study symplectic embedding questions for a family of domains we call *pin-ellipsoids* $E_{p,q}(\alpha, \beta)$, where p and q are positive coprime integers with $q \leq p$. See Definition 1.2.1 for their definition. These domains arise naturally (1) in Milnor fibres of smoothings of certain surface singularities called *cyclic quotient T-singularities*, and (2) as building blocks of *almost toric fibrations*. The name pin-ellipsoid is derived from the fact that every pin-ellipsoid contains a so-called *Lagrangian pin-wheel*. The case $p = q = 1$

corresponds to the case of the *standard ellipsoid* in Equation (1.1), whereas $E_{2,1}(\alpha, \beta)$ can be identified with a neighbourhood of the zero-section of $T^*\mathbb{RP}^2$. We address the above questions (Q1)–(Q3) for all pin-ellipsoid embeddings into $X = \mathbb{CP}^2$. Theorem 1.4.1 affirmatively answers the isotopy question (Q1), Theorem 1.5.2 solves the embedding problem (Q2) in the “visible range” (see Remark 1.2.2 (d)), and Theorem 1.6.1 solves the multiple pin-ellipsoid problem (Q3) for the special case of *pin-balls* where $\alpha = \beta$, analogous to Gromov’s Two Ball Theorem [22, §0.3.B]. We begin by defining pin-ellipsoids and also quickly recall the Markov numbers, which will play a key role in the statements of all of our theorems.

1.2 Pin-ellipsoids, pin-balls and pin-wheels

Our definition of the pin-ellipsoid $E_{p,q}(\alpha, \beta)$ uses the theory of *almost toric fibrations* (ATFs), where the symplectic geometry of a 4-manifold is encoded in a 2-dimensional *almost toric base diagram*. These diagrams were introduced by Symington [46]; see the book [16] for more details about how to decode these diagrams.

Definition 1.2.1. Given positive integers $1 \leq q \leq p$ with $\gcd(p, q) = 1$ and positive real numbers α, β , let the *pin-ellipsoid* $E_{p,q}(\alpha, \beta)$ be the compact symplectic manifold corresponding to the almost toric base diagram $\mathfrak{A}_{p,q}(\alpha, \beta)$ shown in Figure 1. This base diagram has a slanted edge pointing in the $(p^2, pq - 1)$ -direction, having integral affine length α , and a vertical edge having integral affine length β ; it has a single focus-focus fibre joined to the origin by a branch cut parallel to the (p, q) -direction. The top side, drawn — — is included in the diagram but it is not part of the toric boundary; the preimage of this side under the almost toric fibration is the boundary of $E_{p,q}(\alpha, \beta)$, which is a 3-manifold diffeomorphic to the lens space $L(p^2, pq - 1)$.

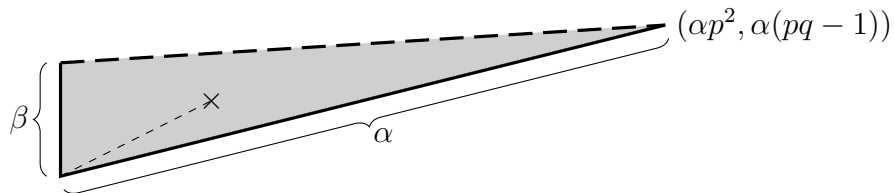


Figure 1: The almost toric base diagram $\mathfrak{A}_{p,q}(\alpha, \beta)$ for $E_{p,q}(\alpha, \beta)$. The branch cut is parallel to the (p, q) -direction. The toric boundary comprises the two solid edges (not the top side), whose affine lengths are α and β ; these are two segments of an unbroken straight line with respect to the integral affine structure on the base diagram.

Remark 1.2.2. (a) We distinguish between *edges* of an almost toric base diagram (which we draw as thick, unbroken lines —) which are part of the toric boundary (that is, the fibre over a point of an edge is a circle or a point), and *sides* (drawn as thick, long-dashed lines — —) which are not part of the toric boundary (that is, the fibre over a point of a side is a 2-torus). Thin, short-dashed lines - - - - on the interior of the polygon will represent branch cuts.

- (b) Note that $E_{p,q}(\alpha, \beta)$ is symplectomorphic to $E_{p,p-q}(\beta, \alpha)$: the almost toric base diagrams are related by an integral affine transformation with determinant -1 , which lifts to a symplectomorphism of the total spaces. It follows that pin-ellipsoid embedding problems in the case $(p, q) = (2, 1)$ will be symmetric with respect to swapping α and β , just like for standard ellipsoids. For other (p, q) this will no longer hold true, as will be evident from Theorem 1.5.2. Compare also Remark 1.5.3.
- (c) We call the pin-ellipsoid $E_{p,q}(\alpha, \alpha)$ the *pin-ball* $B_{p,q}(\alpha)$.
- (d) Given an almost toric base diagram which contains a subset integral-affine equivalent to $\mathfrak{A}_{p,q}(\alpha, \beta)$, its preimage under the almost toric fibration is an embedded copy of $E_{p,q}(\alpha, \beta)$ in the associated almost toric manifold. We refer to these as *visible pin-ellipsoids*.

Definition 1.2.3. Inside $E_{p,q}(\alpha, \beta)$ there is an immersed Lagrangian disc $L_{p,q}$ which lives over the branch cut. This immersion fails to be an embedding along its boundary circle which meets the toric boundary; here it is p -to-1 and modelled on a standard model immersion, described in [28, Equations (3.4) and (3.5)] or [16, Example 5.14]. This immersed disc is called a *Lagrangian (p, q) -pin-wheel*.

Remark 1.2.4. More generally, we call any immersed Lagrangian disc which is embedded away from its boundary and modelled on $L_{p,q}$ along its boundary a Lagrangian pin-wheel. Khodorovskiy [28, Lemma 3.4] shows that any Lagrangian pin-wheel admits a neighbourhood symplectomorphic to $E_{p,q}(\alpha, \beta)$ for any sufficiently small $\alpha, \beta > 0$. We will call a Lagrangian pin-wheel *visible* if it projects to an arc in the base of some almost toric fibration.

1.3 Markov numbers and their companions

Definition 1.3.1. Integer solutions to the Markov equation

$$p_1^2 + p_2^2 + p_3^2 = 3p_1p_2p_3$$

are called *Markov triples*. One can produce new Markov triples from a given one by three *mutations*, each of which substitutes a member of the triple by another Markov number. For example the mutation $(p_1, p_2, p_3) \rightarrow (p_1, p_2, 3p_1p_2 - p_3)$ replaces p_3 by $p'_3 = 3p_1p_2 - p_3$. All Markov triples are obtained in this way from iterated mutations of $(1, 1, 1)$. Thus they are naturally arranged according to the graph depicted in Figure 2.

Definition 1.3.2 (Companion numbers). Let p be a Markov number. A number q is called *companion number of p* if there exists a Markov triple (p, p_2, p_3) such that

$$q \equiv \pm 3p_2p_3^{-1} \pmod{p}. \quad (1.2)$$

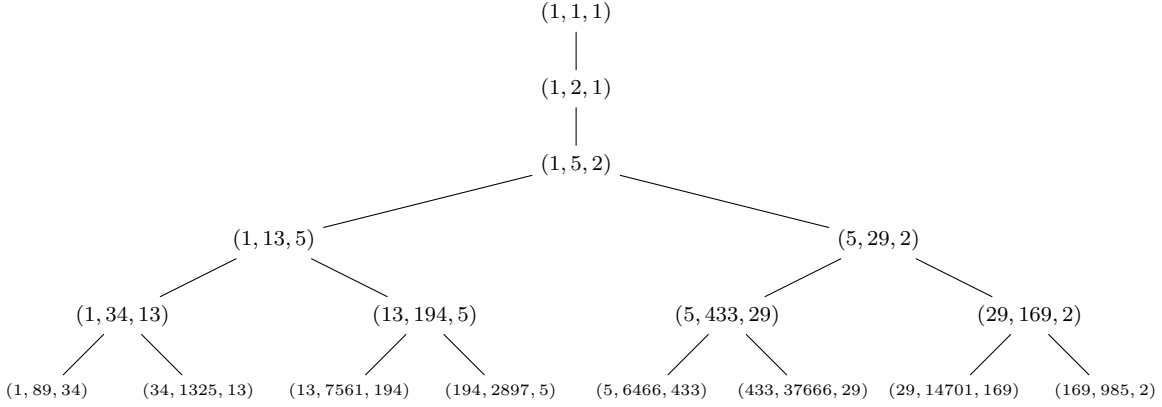


Figure 2: The beginning of the Markov graph, where we have omitted the repetitions at the first two Markov triples.

Remarks 1.3.3. (a) For a fixed triple, Equation (1.2) defines two companion numbers with $1 \leq q \leq p$ which are related to one another by $q \rightarrow p - q$. If $p \in \{1, 2\}$, then the two companion numbers are both equal to 1, and for all other Markov numbers they differ and are strictly less than p . Mutations of Markov triples containing p preserve its companion numbers.

(b) Conversely, there is a unique mutation branch in the Markov tree in which p appears with companion number q , see for example [5, Proposition 3.15]. It is conjectured that each Markov number has only one pair of companion numbers (see [5, §2.3]), but since this conjecture is famously open, we need to specify both p and q in everything that follows.

As was noticed by Vianna [50], the almost toric base diagrams of \mathbb{CP}^2 (up to integral affine equivalence and nodal slides) are in bijection with unordered Markov triples. This is closely related to the fact – due to Hacking–Prokhorov [23] – that the singular fibre of any \mathbb{Q} -Gorenstein degeneration of \mathbb{CP}^2 is (a partial smoothing of) a weighted projective plane $\mathbb{P}(p_1^2, p_2^2, p_3^2)$ where (p_1, p_2, p_3) is a Markov triple. Given a Markov triple, let us write $\mathfrak{D}(p_1, p_2, p_3)$ for the corresponding almost toric base diagram. We call these almost toric base diagrams *Vianna triangles*: see Section 2.3 for a full description. For now, the important feature is that Vianna triangles allow us to see *visible* pin-ellipsoids

$$E_{p_i, q_i}(\alpha_i, \beta_i) \subset \mathbb{CP}^2 \quad \text{for any} \quad \alpha_i < \frac{p_{i+2}}{p_i p_{i+1}}, \quad \beta_i < \frac{p_{i+1}}{p_i p_{i+2}}, \quad (1.3)$$

where q_i is the companion number $3p_{i+1}p_{i+2}^{-1} \bmod p_i$. Note that reordering the Markov triple by swapping p_{i+1} and p_{i+2} will swap the order of the bounds on α_i and β_i and also swap the companion numbers; this is consistent with Remark 1.2.2(b).

1.4 The isotopy problem

Evans and Smith [17] showed that $E_{p,q}(\alpha, \beta)$ admits a symplectic embedding into \mathbb{CP}^2 for some $\alpha, \beta > 0$ if and only if p is a Markov number and q is one of its companion numbers. Provided that $\alpha < \frac{p_3}{pp_2}$ and $\beta < \frac{p_2}{pp_3}$ for some Markov triple (p, p_2, p_3) with $q = 3p_2p_3^{-1} \bmod p$, there is a visible embedding $E_{p,q}(\alpha, \beta) \hookrightarrow \mathbb{CP}^2$ coming from the Vianna triangle $\mathfrak{D}(p, p_2, p_3)$. But there exist symplectic embeddings also outside the visible range; for instance, symplectic folding can be used to show that for any $\alpha > 0$ there exists $\beta > 0$ such that $E_{p,q}(\alpha, \beta)$ symplectically embeds into \mathbb{CP}^2 .

Theorem 1.4.1 (Isotopy Theorem). *Any two symplectic embeddings of a pin-ellipsoid $E_{p,q}(\alpha, \beta)$ into \mathbb{CP}^2 are isotopic through symplectic embeddings.*

In other words, the space of symplectic embeddings of a pin-ellipsoid into \mathbb{CP}^2 , if non-empty, is path-connected.

Remarks 1.4.2. (a) The problem whether the space of symplectic embeddings of $E_{p,q}(\alpha, \beta)$ into \mathbb{CP}^2 is non-empty is addressed in § 1.5.

(b) Since $H^1(E_{p,q}(\alpha, \beta); \mathbb{R})$ vanishes, it follows that any two embeddings which are symplectically isotopic are related by a Hamiltonian diffeomorphism of \mathbb{CP}^2 .

(c) In fact, we will reprove the results of Evans and Smith [17] along the way, avoiding the use of orbifold holomorphic curves. See Section 5.4.

Corollary 1.4.3. *Lagrangian (p, q) -pin-wheels in \mathbb{CP}^2 are unique up to Hamiltonian isotopy.*

Proof. Indeed, Khodorovskiy [28, Lemma 3.4] shows that a Lagrangian pin-wheel has a standard neighbourhood symplectomorphic to an embedded pin-ellipsoid. Therefore, two pin-wheels yield two embedded pin-ellipsoids. If we choose them sufficiently small and of equal sizes α, β , Theorem 1.4.1 shows that these pin-ellipsoids are Hamiltonian isotopic, and the restriction of this isotopy to the pin-wheel gives the desired isotopy of pin-wheels. \square

Since the $(2, 1)$ -pin-wheel is \mathbb{RP}^2 , this generalises the known result about the uniqueness of Lagrangian \mathbb{RP}^2 s in \mathbb{CP}^2 due to Hind [26] and Li–Wu [30, Section 6.4.1], see also Borman–Li–Wu [7, Theorem 1.3] and Adaloglou [3] for an approach closer to ours.

Remark 1.4.4. Every Lagrangian pin-wheel $L \subset \mathbb{CP}^2$ is a non-trivial Lagrangian barrier in the sense of Biran [6]: the Gromov width of the complement $\mathbb{CP}^2 \setminus L$ is strictly less than the Gromov width of \mathbb{CP}^2 . Indeed, by Corollary 1.4.3 any pin-wheel in \mathbb{CP}^2 is Hamiltonian isotopic to one of the *visible* Lagrangian pin-wheels studied by Brendel and Schlenk [9], who proved that these are barriers and moreover computed the Gromov width of the complement.

1.5 The embedding problem

Notation 1.5.1. Answering the embedding problem (Q2) for pin-ellipsoid embeddings into \mathbb{CP}^2 means determining the set

$$\mathcal{A}_{p,q} := \{(\alpha, \beta) \in \mathbb{R}_{>0}^2 : E_{p,q}(\alpha, \beta) \xrightarrow{s} \mathbb{CP}^2\}, \quad (1.4)$$

where p is a Markov number and q one of its companion numbers. By the definition of symplectic embedding, the set $\mathcal{A}_{p,q}$ is open in $\mathbb{R}_{>0}^2$. Let (p, m_0, m_1) be a Markov triple with $q \equiv 3m_0m_1^{-1} \pmod{p}$ and consider the recursion

$$m_{i+2} = 3pm_{i+1} - m_i, \quad (1.5)$$

defining a sequence $\{m_i\}_{i \in \mathbb{Z}}$. The set $\{(p, m_i, m_{i+1}) \mid i \in \mathbb{Z}\}$ consists of all Markov triples which can be obtained from (p, m_0, m_1) by mutations preserving p : in the Markov tree in Figure 2 this set forms a \wedge -shaped tree. Let

$$\square_i(p, q) := \left(0, \frac{m_{i+1}}{pm_i}\right) \times \left(0, \frac{m_i}{pm_{i+1}}\right), \quad \text{Stair}(p, q) := \bigcup_{i \in \mathbb{Z}} \square_i(p, q), \quad (1.6)$$

and

$$\sigma_p := \frac{1}{2} \left(3 + \sqrt{9 - \frac{4}{p^2}}\right).$$

Theorem 1.5.2 (Staircase Theorem). *Let p be a Markov number and q one of its companion numbers. Then*

$$\mathcal{A}_{p,q} \cap (0, \sigma_p)^2 = \text{Stair}(p, q). \quad (1.7)$$

Remarks 1.5.3. (a) Since $\text{vol}(E_{p,q}(\alpha, \beta)) = \frac{1}{2}p^2\alpha\beta$, the volume constraint for the symplectic embedding problem yields that $\mathcal{A}_{p,q}$ lies below the curve $\{p^2\alpha\beta = 1\}$.

(b) All the pin-ellipsoids in this staircase can be realised as visible pin-ellipsoids coming from Vianna triangles (compare with Equation (1.3)) and by Theorem 1.4.1 are isotopic to a visible pin-ellipsoid. Conversely, all visible embeddings of $E_{p,q}(\alpha, \beta)$ satisfy $\max\{\alpha, \beta\} < \sigma_p$. It is striking that visible constructions are often sharp for such quantitative problems.

(c) The sets in Equation (1.7) are infinite staircases whose outer corners lie on the volume constraint and accumulate at the boundary of the square $(0, \sigma_p)^2 \subset \mathbb{R}^2$, see Figures 4 and 5. The first such staircase, which we recover as the case $(p, q) = (1, 1)$, was found by McDuff and Schlenk [37]. Since then, similar staircases have been found for many different target spaces – we refer to [42] and the references therein for more on this and related problems. The usual convention is to use the normalisation freedom to reduce to the case $E(1, \beta) \hookrightarrow \mathbb{CP}^2(A)$, where $A > 0$ is the symplectic area of the line. In our case, we prefer the normalisation convention $E(\alpha, \beta) \hookrightarrow \mathbb{CP}^2(1)$. This is in part justified by the fact that the staircases we find in Theorem 1.5.2

are not symmetric with respect to swapping α and β , making it more natural to keep α and β on equal footing. In fact, the set obtained by swapping coordinates in $\text{Stair}(p, q)$ describes $\mathcal{A}_{p, p-q}$, the staircase associated to the second companion number $p - q$, by Remark 1.2.2(b).

- (d) We do not know the set $\mathcal{A}_{p,q}$ for $\alpha \geq \sigma_p$ or $\beta \geq \sigma_p$, except for $p = q = 1$ where it can be derived from [37, Sections 4 and 5]. For $p \geq 2$ we even do not know whether the intersection of the closure $\overline{\mathcal{A}_{p,q}}$ with the vertical segment at $\alpha = \sigma_p$ is a point or an interval of positive length. For $p = 1$ this intersection is a point, since the upper boundary of $\mathcal{A}_{1,1}$ on $\{\tau^2 \leq \alpha \leq \frac{21}{8}\}$ is given by $\beta = 3 - \alpha$.

For many (though not all, [13, Remark 5.1]) symplectic 4-manifolds (X, ω) , there are full symplectic fillings $E(\alpha, \beta) \hookrightarrow (X, \omega)$ by standard ellipsoids whenever $\frac{\alpha}{\beta}$ is sufficiently large or sufficiently small. For instance, the boundary of $\mathcal{A}_{1,1}$ over $\{\frac{17}{6} \leq \alpha < \infty\}$ is given by $\beta = \frac{1}{\alpha}$. Is this so for all Markov numbers p ? More precisely:

Question 1.5.4. Let (p, q) be as above. Are there full symplectic fillings $E_{p,q}(\alpha, \beta) \hookrightarrow \mathbb{CP}^2$ for all sufficiently small and all sufficiently large $\frac{\alpha}{\beta}$?

Example 1.5.5. Let us illustrate Theorem 1.5.2 by the example $p = 2, q = 1$, see Figures 3 and 4. We start with the Vianna triangle $\mathfrak{D}(1, 1, 1)$ appearing as the image of \mathbb{CP}^2 under the standard toric moment map. After one mutation, we obtain the triangle $\mathfrak{D}(2, 1, 1)$, containing a vertex which is integral affine equivalent to the cone spanned by the vectors $(0, -1)$ and $(4, -1)$ adjacent to edges which both have integral affine length $\frac{1}{2}$. Thus we deduce the existence of a volume filling embedding $E_{2,1}(\frac{1}{2}, \frac{1}{2}) \hookrightarrow \mathbb{CP}^2$. This domain is symplectomorphic to the codisc bundle $D_{1/2\pi}^* \mathbb{RP}^2$ of radius $\frac{1}{2\pi}$ in the round metric of curvature 1 on \mathbb{RP}^2 . One more mutation at another vertex yields the triangles $\mathfrak{D}(2, 1, 5)$ and $\mathfrak{D}(2, 5, 1)$ and hence volume filling embeddings of $E_{2,1}(\frac{5}{2}, \frac{1}{10})$ and $E_{2,1}(\frac{1}{10}, \frac{5}{2})$ into \mathbb{CP}^2 , respectively. This generates three steps of the $(2, 1)$ -staircase, as illustrated in Figure 4.

The rest of the $p = 2, q = 1$ staircase comes from the sequence:

$$\{m_i\}_{i \in \mathbb{Z}} = \{\dots, 29, 5, 1, 1, 5, 29, 169, \dots\}$$

of odd-index Pell numbers, which yields the staircase depicted in Figure 4. This staircase is symmetric with respect to swapping the coordinate axes.

Example 1.5.6. For $(p, q) = (5, 1)$, we obtain

$$\{m_i\}_{i \in \mathbb{Z}} = \{\dots, 433, 29, 2, 1, 13, 194, 2897, \dots\},$$

yielding the staircase depicted in Figure 5. This staircase is not symmetric with respect to swapping the coordinate axes.

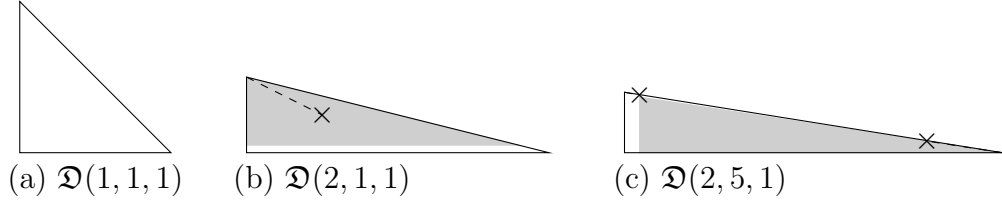


Figure 3: The first three Vianna triangles (a) $\mathfrak{D}(1, 1, 1)$, (b) $\mathfrak{D}(2, 1, 1)$ and (c) $\mathfrak{D}(2, 5, 1)$ together with the first two visible pin-ellipsoids (shaded in (b) and (c)) for the $p = 2, q = 1$ staircase. These visible embeddings can be made to fill an arbitrarily large portion of the triangle; in case (c) you need to use a nodal slide to shrink the other branch cut.

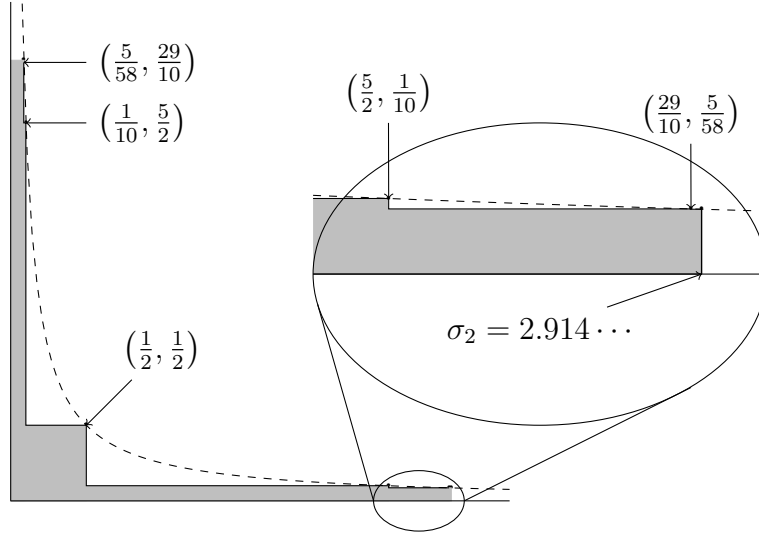


Figure 4: The staircase for $p = 2, q = 1$.

Remark 1.5.7. In particular, for a Markov number p with companion number q , Theorem 1.5.2 computes the largest (p, q) -pin-ball that symplectically embeds into \mathbb{CP}^2 :

$$\sup\{\alpha > 0 : B_{p,q}(\alpha) \xrightarrow{s} X\} = \min\left\{\frac{p_2}{pp_3}, \frac{p_3}{pp_2}\right\}$$

where (p, p_2, p_3) denotes the Markov triple in which p appears as largest entry with companion number q . The only pin-balls admitting volume-filling embeddings into \mathbb{CP}^2 are therefore those with $(p, q) = (1, 1)$ and $(p, q) = (2, 1)$.

1.6 Pin-ball packing problem

The following result generalizes Gromov's Two Ball Theorem in dimension four.

Theorem 1.6.1 (Two Pin-Ball Theorem). *Let p_1, p_2 be Markov numbers appearing in the*

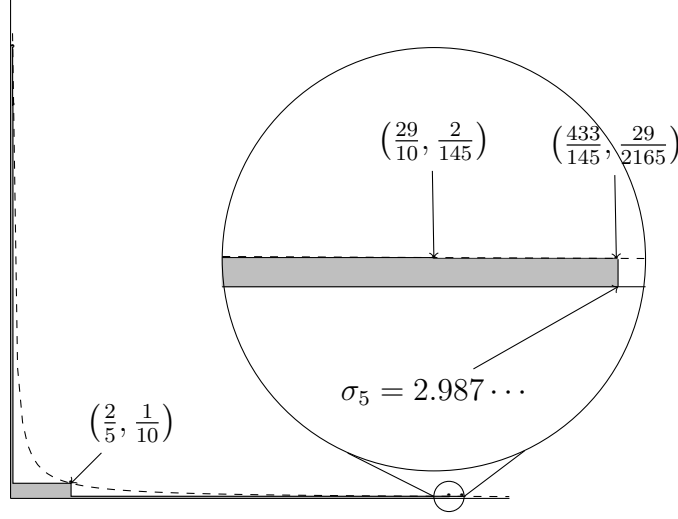


Figure 5: The staircase for $p = 5$, $q = 1$.

same Markov triple¹, and let p_3 be the smaller of the two Markov numbers completing the triple. Let $q_i = \pm 3p_{i+1}p_{i+2}^{-1} \bmod p_i$ for $i = 1, 2$ be companion numbers. Then there exists a symplectic embedding

$$B_{p_1, q_1}(\alpha_1) \sqcup B_{p_2, q_2}(\alpha_2) \hookrightarrow \mathbb{CP}^2, \quad (1.8)$$

if and only if $\alpha_1 < \frac{p_2}{p_1 p_3}$ and $\alpha_2 < \frac{p_1}{p_2 p_3}$ and $\alpha_1 + \alpha_2 < \frac{p_3}{p_1 p_2}$.

Remark 1.6.2. Note that one of the inequalities on the α_j s is implied by the bound on $\alpha_1 + \alpha_2$. To see this, assume that $p_2 = \max\{p_1, p_2, p_3\}$; the case $p_1 = \max\{p_1, p_2, p_3\}$ follows by exactly the same argument. Then, assuming that $\alpha_1 + \alpha_2 < p_3/(p_1 p_2)$, we get

$$\alpha_1 < \alpha_1 + \alpha_2 < \frac{p_3}{p_1 p_2} \leq \frac{p_2}{p_1 p_3},$$

which proves the inequality for α_1 . Moreover, Theorem 1.5.2 proves that $\alpha_2 < \frac{p_1}{p_2 p_3}$. This means that to establish the necessity of the inequalities in Theorem 1.6.1, we only need to prove the bound on $\alpha_1 + \alpha_2$.

Remark 1.6.3. The embeddings in Theorem 1.6.1 again appear as visible embeddings in Vianna triangles, see Figure 6. In general, if an embedding of the form (1.8) exists and $p_1, p_2 \geq 2$, then p_1 and p_2 are necessarily Markov numbers appearing in the same Markov triple and q_1 and q_2 are companion numbers of p_1 and p_2 , respectively, see [17, Theorem 1.2]. However if, say, $p_1 = 1$, then $B_{p_1, q_1}(\alpha_1)$ is a standard ball and embeddings of the type (1.8) exist even if the Markov numbers 1, p_2 do not appear in the same triple. In that case, constraints on α_1 and α_2 can be derived by the same methods as in [9].

¹Whenever such a triple exists, there are precisely two such triples, and they are related by a single mutation.

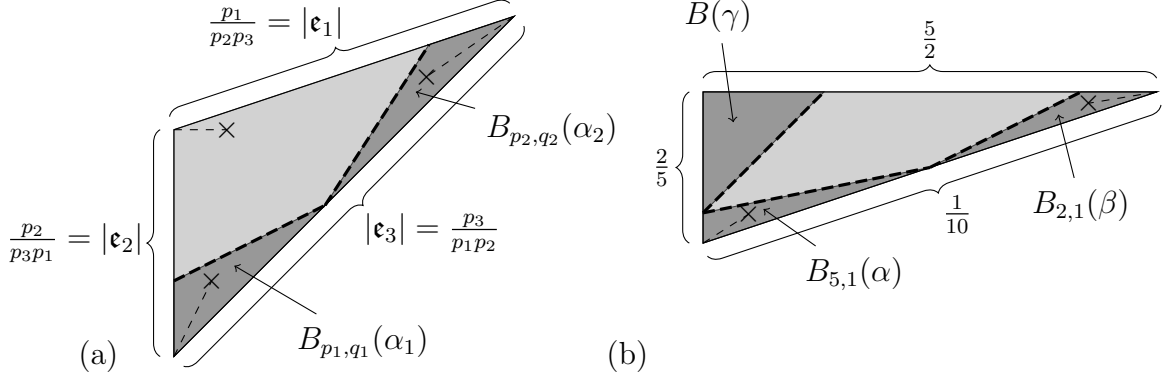


Figure 6: (a) The Vianna triangle $\mathfrak{D}(p_1, p_2, p_3)$ and an illustration of the constructive side of the Two Pin-Ball Theorem 1.6.1. (b) The Vianna triangle $\mathfrak{D}(5, 2, 1)$ and the pin-balls for the constructive side of the Two Pin-Ball Theorem for $\{p_1, p_2\} = \{1, 5\}$ and for $\{p_1, p_2\} = \{2, 5\}$ and of the Three Pin-Ball Theorem 1.6.4.

Corollary 1.6.4 (Three Pin-Ball Theorem). *Let (p_1, p_2, p_3) be a Markov triple with companion numbers q_1, q_2, q_3 . Then there exists a symplectic embedding*

$$B_{p_1, q_1}(\alpha_1) \sqcup B_{p_2, q_2}(\alpha_2) \sqcup B_{p_3, q_3}(\alpha_3) \hookrightarrow \mathbb{CP}^2, \quad (1.9)$$

if and only if $\alpha_1 + \alpha_2 < \frac{p_3}{p_1 p_2}$, $\alpha_1 + \alpha_3 < \frac{p_2}{p_1 p_3}$ and $\alpha_2 + \alpha_3 < \frac{p_1}{p_2 p_3}$.

Proof. If $p_1 = p_2 = p_3 = 1$, the claim follows directly from Theorem 1.6.1 (or also from Gromov's 2-ball theorem). We can therefore assume that $p_3 \leq p_2 < p_1$. By Theorem 1.6.1,

$$\alpha_1 + \alpha_2 < \frac{p_3}{p_1 p_2}.$$

If we mutate (p_1, p_2, p_3) at p_2 , then $p'_2 = 3p_1 p_3 - p_2 > p_2$. Hence Theorem 1.6.1 applied to p_1, p_3 yields

$$\alpha_1 + \alpha_3 < \frac{p_2}{p_1 p_3}.$$

Finally, if we mutate (p_1, p_2, p_3) at p_1 , then $p'_1 = 3p_2 p_3 - p_1 < p_1$. Hence Theorem 1.6.1 applied to p_2, p_3 yields

$$\alpha_2 + \alpha_3 < \frac{p'_1}{p_2 p_3} < \frac{p_1}{p_2 p_3}. \quad \square$$

Remark 1.6.5. Note that, by [17, Theorem 1.2], it is impossible to pack more than three pin-balls with $p_i \geq 2$.

1.7 Idea of proof for Theorem 1.4.1

Our proof builds on the idea of Hind [26] and Li-Wu [30, §6.1.1] who showed the Lagrangian uniqueness of \mathbb{RP}^2 in \mathbb{CP}^2 by turning this problem into the uniqueness problem of

symplectic -4 -spheres in $S^2 \times S^2$ obtained by a symplectic cut on the boundary of small codisc-bundle of an embedded \mathbb{RP}^2 in \mathbb{CP}^2 . Suppose we have two symplectic embeddings $\iota_1, \iota_2: E_{p,q}(\alpha, \beta) \hookrightarrow \mathbb{CP}^2$. We shall perform a rational blow-up along each of these pin-ellipsoids; this yields two 4-manifolds \tilde{X}_1 and \tilde{X}_2 containing configurations \mathcal{C}_1 and \mathcal{C}_2 of embedded symplectic spheres. We show that, for $i = 1, 2$, \tilde{X}_i is ruled, and that:

- in each case, one of the curves from \mathcal{C}_i is a section of this ruled surface,
- the other curves of \mathcal{C}_i (together with some additional curves) form one or two broken rulings.
- the configuration \mathcal{T}_i consisting of \mathcal{C}_i and these additional curves (and possibly one or two additional smooth rulings) is completely determined by p, q and the choice of data of the rational blow-up. In other words \mathcal{T}_1 and \mathcal{T}_2 have symplectomorphic neighbourhoods $\nu_1 \cong \nu_2$.
- the common boundary $\partial\nu_i$ is contactomorphic to $S^1 \times S^2$ and the complement of ν_i in \tilde{X}_i is minimal. In particular, uniqueness of symplectic fillings of these manifolds tells us that the symplectic completion of $\tilde{X}_i \setminus \nu_i$ is symplectomorphic to either \mathbb{R}^4 or $T^*S^1 \times \mathbb{C}$.

Since \tilde{X}_1 and \tilde{X}_2 are essentially obtained by gluing together symplectomorphic pieces, and there is only one way to glue these together, we find that \tilde{X}_1 and \tilde{X}_2 are symplectomorphic via a symplectomorphism taking \mathcal{C}_1 to \mathcal{C}_2 . This descends to give a symplectomorphism of the rational blow-down $\mathbb{CP}^2 \rightarrow \mathbb{CP}^2$ taking one pin-ellipsoid to the other. Finally, this symplectomorphism is Hamiltonian due to Gromov's classical result stating that the symplectomorphism group of \mathbb{CP}^2 is connected.

1.8 Idea of proof for Theorems 1.5.2 and 1.6.1

To explain the proof of the Staircase Theorem (Theorem 1.5.2), let p be a Markov number and q a companion number. As mentioned in Remark 1.5.3 (b), the points in $\text{Stair}(p, q)$ are realised by visible embeddings coming from Vianna triangles. It is therefore enough to show that for all $i \in \mathbb{Z}$, $E_{p,q}(\alpha, \beta)$ does not symplectically embed into \mathbb{CP}^2 whenever $\alpha > \frac{m_i}{pm_{i-1}}$ and $\beta > \frac{m_i}{pm_{i+1}}$. Here m_i denote the members of the sequence defined in (1.5). Note that these points correspond to the inner corners of the staircase $\text{Stair}(p, q)$.

Assuming that such an embedding $\iota: E_{p,q}(\alpha, \beta) \hookrightarrow \mathbb{CP}^2$ exists, we construct a one-parameter family of symplectic manifolds $(\tilde{X}, \tilde{\omega}_t)$ by rational symplectic blow-up² of a small neighbourhood of $\iota(tE_{p,q}(\alpha, \beta))$, where the parameter $t \in (0, 1]$ measures the size of the blow-up. For small enough t , we can assume, by Theorem 1.4.1, that the embedding coincides with the visible embedding coming from the Vianna triangle $\mathfrak{D}(p, m_{i-1}, m_i)$. In that case, we construct a *visible* symplectic -1 -sphere in the base diagram of $(\tilde{X}, \tilde{\omega}_t)$, see

²Technically, we need to take a blow-up of the rational blow-up which we refer to as a *pavilion blow-up*.

Figure 22.³ Hence we find a class $S \in H_2(\tilde{X}; \mathbb{Z})$ whose Gromov invariant is one. Furthermore, homological computations show that the symplectic area of S as measured by $\tilde{\omega}_t$ becomes negative for t close enough to 1. However, the Gromov invariant is a deformation invariant, meaning that S should be represented by a holomorphic curve for all $\tilde{\omega}_t$. If $\alpha > \frac{m_i}{pm_{i-1}}$ and $\beta > \frac{m_i}{pm_{i+1}}$ for some i then we show that t can be chosen large enough that the symplectic area of S is negative. Since holomorphic curves have positive area, we obtain a contradiction.

This idea of using visible curves to obstruct embeddings of standard ellipsoids can be found in McDuff–Siegel [38, Figure 4.2.1 and Corollary 6.1.4], so the main new input here is the Isotopy Theorem. Note that in the proof we only use a weak version of the Isotopy Theorem 1.4.1, namely that two pin-ellipsoid embeddings can be made to agree on an arbitrarily small pin-subellipsoid. For symplectic embeddings of balls ($p = 1$, where the pin-wheel becomes a point) this is an elementary fact; as a consequence, the proof of the Fibonacci staircase (in the visible range, below the aspect ratio ϕ^4) is immediate from almost toric geometry: the optimal embeddings are visible and the obstructions come from visible curves. This is implicit in [38].

The proof of the Two Pin-Ball Theorem (Theorem 1.6.1) also comes from positivity of area for a pseudoholomorphic curve, and can be seen as an elaborate version of Gromov’s proof of his Two Ball Theorem. Suppose we have disjoint symplectically embedded pin-balls $B_{p_1, q_1}(\alpha_1)$ and $B_{p_2, q_2}(\alpha_2)$ in \mathbb{CP}^2 . In this case, we rationally blow-up both pin-balls; this produces a manifold \tilde{X} containing two chains of symplectic spheres. We find a symplectic -1 -sphere \tilde{C} in \tilde{X} which connects these chains and whose symplectic area is bounded by $\frac{p_3}{p_1 p_2}$ where p_3 is the smaller Markov number making (p_1, p_2, p_3) a Markov triple. Contracting the chains yields an orbifold with two orbifold points, and the image of \tilde{C} passes through both of them. We then lift to the uniformising cover of each orbifold chart and apply the monotonicity formula for areas of minimal surfaces to get a lower bound of $\alpha_1 + \alpha_2$ on the symplectic area of \tilde{C} . In the case when the pin-balls are simultaneously visible, the sphere \tilde{C} is also visible as part of the toric boundary; see Figure 7. One could prove the existence of \tilde{C} in general by proving an isotopy theorem for pairs of pin-balls, but to save space we instead appeal to the paper of Evans and Smith [17, Theorem 4.16].

1.9 Outline of the paper

In Section 2, we introduce the basic constructions from almost toric geometry which are needed for the rest of the paper, including the Vianna triangles (almost toric base diagrams for \mathbb{CP}^2) which allow us to see the visible pin-ellipsoids, the *pavilion blow-up* (a mild generalisation of rational blow-up) and the *culet curve* (a distinguished curve in the pavilion blow-up of a pin-ellipsoid in \mathbb{CP}^2). In Section 3, we explain in detail how to equip the pavilion blow-up with a symplectic structure and compatible almost complex structure

³In the case $p = 1$ this curve corresponds to the unicuspidal curve in \mathbb{CP}^2 used in [38, Figure 4.2.1], but here it is found directly in \tilde{X} and hence it is a smoothly embedded -1 -curve.

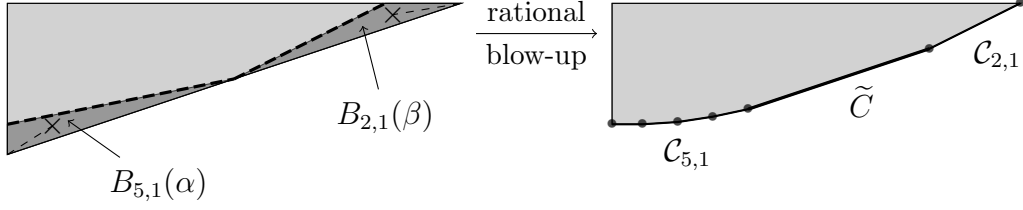


Figure 7: \tilde{C} is the exceptional curve used to prove the obstructive side of the Two Pin-Ball Theorem 1.6.1. The situation above is the visible situation for the $(5, 2)$ -case. The Wahl chains $\mathcal{C}_{5,1}$ and $\mathcal{C}_{2,1}$ are connected by the exceptional curve \tilde{C} . In general we will find the curve \tilde{C} by a neck stretching procedure.

and how to perform computations in the homology after blowing up. In Section 4, we collect some basic results about ruled symplectic 4-manifolds which will be used in the main argument. Section 5 contains the proofs of the main results:

- The main technical results are: the existence of a square zero holomorphic sphere in the rational blow-up (Theorem 5.1.1, proved in Section 5.4) and the description of how this sphere can degenerate to give broken rulings (Theorem 5.1.4, proved in Section 5.6).
- The proofs of the Isotopy Theorem 1.4.1 and the Staircase Theorem 1.5.2, assuming these technical results, are given in Section 5.2 and 5.3 respectively.
- The Two Pin-Ball Theorem (Theorem 1.6.1) is proved in Section 5.5.

Acknowledgements

The authors would like to thank Gerard Bargalló i Gómez, Marco Golla, Richard Hind, Paul Levy, Grisha Mikhalkin, Dusa McDuff, Federica Pasquotto, George Politopoulos, Joel Schmitz, Kyler Siegel, Laura Starkston, Giancarlo Urzúa, Renato Vianna and Weiyi Zhang for helpful conversations.

JB is supported by SNSF Ambizione Grant PZ00P2-223460.

JE is supported by EPSRC Standard Grant EP/W015749/1.

2 Notation and definitions

2.1 Wahl singularities and their resolutions

Definition 2.1.1 (Triangle $\Delta_{p,q}(\alpha, \beta)$). If we ignore the node and branch cut for the almost toric base diagram $\mathfrak{A}_{p,q}(\alpha, \beta)$ from Definition 1.2.1 then we get a triangle (see Figure 8):

$$\Delta_{p,q}(\alpha, \beta) := \{x \in \mathbb{R}^2 \mid \rho_0 \cdot x \geq 0, \quad \rho_{m+1} \cdot x \geq 0, \quad \gamma \cdot x \geq -\alpha\beta p^2\} \quad (2.1)$$

where ρ_0 , ρ_{m+1} and γ are the vectors

$$\rho_0 = (1, 0), \quad \rho_{m+1} = (1 - pq, p^2), \quad \text{and} \quad \gamma = (\alpha pq - \alpha - \beta, -\alpha p^2).$$

We use the index $m + 1$ here because we will soon add further edges with inward normals ρ_1, \dots, ρ_m ; see Definition 2.1.7.

Definition 2.1.2 (Girdled orbifold $\mathcal{O}_{p,q}(\alpha, \beta)$). This triangle is the moment map image of a compact toric orbifold $\mathcal{O}_{p,q}(\alpha, \beta)$ with boundary. As in Remark 1.2.2(a), the top side of $\Delta_{p,q}(\alpha, \beta)$ with inward normal γ is considered to be part of the boundary, not the toric boundary⁴. We refer to the top side as the *girdle*⁵ and we call this bounded toric orbifold the *girdled orbifold*.

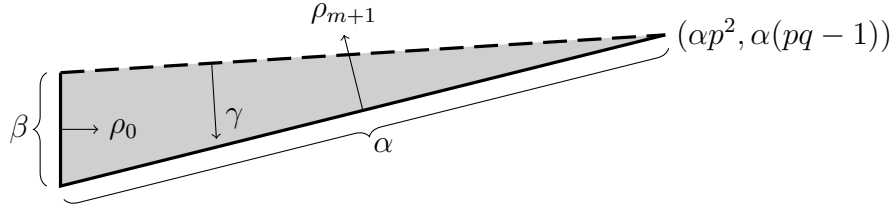


Figure 8: The moment image $\Delta_{p,q}(\alpha, \beta)$ of a toric orbifold. The toric boundary comprises the two solid edges, *not* the top side; the orbifold point is at the vertex of the polygon. We have also labelled the inward normals ρ_0 and ρ_{m+1} of the toric boundary and γ of the top side.

The girdled orbifold $\mathcal{O}_{p,q}(\alpha, \beta)$ has a singularity x living over the vertex of $\Delta_{p,q}(\alpha, \beta)$, locally modelled on the cyclic quotient singularity $\frac{1}{p^2}(1, pq - 1)$. This is the quotient of \mathbb{C}^2 by the action of $\mu_{p^2} = \{\xi \in \mathbb{C}^\times \mid \xi^{p^2} = 1\}$ where $\xi \cdot (x, y) = (\xi x, \xi^{pq-1} y)$. Singularities of this form are called *Wahl singularities*. These are precisely the cyclic quotient singularities which admit a \mathbb{Q} -Gorenstein smoothing of Milnor number zero. The Milnor fibre of this smoothing is a pin-ellipsoid, so whenever a smooth surface admits a \mathbb{Q} -Gorenstein degeneration with Wahl singularities, we can find symplectically embedded pin-ellipsoids in the smooth fibres.

Definition 2.1.3 (Resolutions). A *resolution* of $\mathcal{O}_{p,q}(\alpha, \beta)$ is a smooth complex manifold (\tilde{U}, \tilde{J}) together with a holomorphic map $\pi: \tilde{U} \rightarrow \mathcal{O}_{p,q}(\alpha, \beta)$ satisfying the following property. There exists a configuration \mathcal{C} of complex curves $C \subset \tilde{U}$ such that $\pi(C) = x$ for all $C \in \mathcal{C}$ and such that π restricts to a biholomorphism $\tilde{U} \setminus \bigcup_{C \in \mathcal{C}} C \rightarrow \mathcal{O}_{p,q}(\alpha, \beta) \setminus \{x\}$. We say that the resolution is *chain-shaped* if the curves $C \in \mathcal{C}$ are embedded spheres and form a chain, that is, $\mathcal{C} = \{C_1, C_2, \dots, C_m\}$ with

$$C_i \cdot C_j = \begin{cases} 1 & \text{if } |i - j| = 1 \\ 0 & \text{otherwise.} \end{cases}$$

⁴The boundary has real codimension 1; the toric boundary is a divisor, with complex codimension 1.

⁵The terminology we introduce in this paper (girdle, pavilion, culet) is standard for cut gems [10].

Definition 2.1.4 (Girdled resolution \tilde{U}_ρ). There is a standard family of chain-shaped resolutions of $\mathcal{O}_{p,q}(\alpha, \beta)$ which are themselves toric. They arise from subdivisions of the inward normal fan for the girdled orbifold. Recall that the inward normals to the two edges of $\Delta_{p,q}(\alpha, \beta)$ are ρ_0 and ρ_{m+1} . A subdivision ρ is a sequence of primitive integer vectors ρ_1, \dots, ρ_m in the convex sector bounded by ρ_0 and ρ_{m+1} with the property that $\rho_i \wedge \rho_{i+1} \geq 1$ for $i = 0, 1, \dots, m$. Here, $v \wedge w$ denotes the determinant of the 2-by-2 matrix with columns v and w . If the subdivision ρ satisfies $\rho_i \wedge \rho_{i+1} = 1$ the subdivided fan ρ determines the resolution as a normal toric variety, see for example [20, Section 2.6]. Since we are resolving a girdled orbifold, we will call this the *girdled resolution* \tilde{U}_ρ associated to ρ .

A general prescription for finding resolutions of a cyclic quotient singularity $\frac{1}{n}(a, 1)$ works as follows. The exceptional set of the minimal resolution is a chain of holomorphic spheres C_1, \dots, C_m with $C_i^2 = -b_i$ where $[b_1, \dots, b_m]$ is the Hirzebruch–Jung continued fraction expansion of n/a , that is:

$$[b_1, \dots, b_m] := b_1 - \frac{1}{b_2 - \frac{1}{\ddots - \frac{1}{b_m}}}.$$

Remark 2.1.5. Girdled resolutions all *dominate* a unique *minimal resolution*, meaning that they are obtained from it by a sequence of complex blow-ups. For the minimal resolution, the curves C_i are embedded spheres with self-intersection $C_i^2 = -b_i$ where $[b_1, \dots, b_m]$ is the Hirzebruch–Jung continued fraction expansion of $p^2/(pq - 1)$. Non-minimal resolutions are obtained from the minimal one by blowing up at intersection points between the exceptional spheres C_i .

Definition 2.1.6 (Wahl chains and duals). In the special case of Wahl singularities, we call $[b_1, \dots, b_m]$ a *Wahl chain*. Recall that the *dual* of the singularity $\frac{1}{n}(1, a)$ is the singularity $\frac{1}{n}(1, \bar{a})$ where $a\bar{a} = 1 \pmod{n}$; the continued fraction of n/\bar{a} is $[b_m, \dots, b_1]$, the *dual* of the chain for n/a .

Definition 2.1.7 (Pavilion). Let ρ be a subdivision and, for each $\rho_i \in \rho$, choose a positive real number $\lambda_i > 0$. We then consider the polygon

$$\text{Pav}_{\rho, \lambda}(\Delta_{p,q}(\alpha, \beta)) := \{x \in \Delta_{p,q}(\alpha, \beta) \mid \rho_i \cdot x \geq \lambda_i \text{ for } i = 1, \dots, m\}, \quad (2.2)$$

see Figure 9. We require that $\rho_i \cdot x > \lambda_i$ for all points x on the girdle (recall that this is the top side of the moment triangle). A choice of ρ and λ satisfying this requirement is called a *pavilion*. If, moreover, for every $i = 1, 2, \dots, m$ we have that (a) $\rho_i \wedge \rho_{i+1} = 1$ and (b) there is an edge f_i of the polygon with inward normal ρ_i and positive length, then we call the pavilion *Delzant*. We call a pavilion *minimal* if the corresponding toric girdled resolution \tilde{U}_ρ is the minimal resolution.

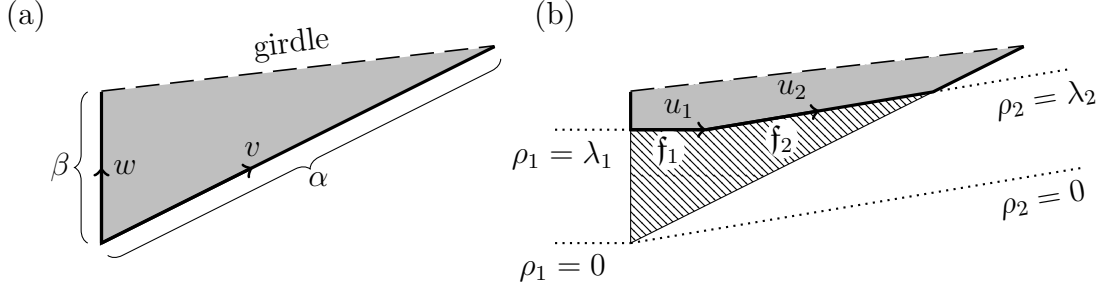


Figure 9: (a): $\Delta_{p,q}(\alpha, \beta)$ with its girdle. (b): A pavilion $\text{Pav}_{\rho, \lambda}(\Delta_{p,q}(\alpha, \beta))$ for $\Delta_{p,q}(\alpha, \beta)$.

If we choose a Delzant pavilion and a strictly convex function ψ on it (with suitable behaviour along the edges of the polygon) then we get a toric Kähler metric on the resolution constructed using the Hessian of ψ (see [1, Eq. (2.1)]; the boundary behaviour along edges is obtained from [1, Eq. (2.8)] by taking Legendre transform). Therefore, $\text{Pav}_{\rho, \lambda}(\Delta_{p,q}(\alpha, \beta))$ is the moment image for a toric Kähler structure on the girdled resolution \tilde{U}_{ρ} . We write $\tilde{\omega}_{\rho, \lambda, \psi}$ for the Kähler form.

Definition 2.1.8 (Pavilion blow-up). We call the symplectic manifold $(\tilde{U}_{\rho}, \tilde{\omega}_{\rho, \lambda, \psi})$ the *pavilion blow-up* of $E_{p,q}(\alpha, \beta)$.

Remark 2.1.9. The specific choices of α , β and λ will be important for some of the quantitative questions we consider. The freedom to choose non-minimal resolutions will help with finding holomorphic curves which give obstructions to pin-ellipsoid embeddings.

Remark 2.1.10. Although we construct the symplectic form in this way, one could also think of the pavilion blow-up as coming from a sequence of symplectic cuts. This would have the disadvantage that different choices of λ would yield symplectic forms on *different manifolds* (all diffeomorphic, but still different) making it harder to compare almost complex structures. Nonetheless, we will sometimes abuse language and talk about “making a pavilion cut”; we just mean picking a particular ρ and λ .

2.2 Offcuts

Definition 2.2.1. Given a pavilion ρ, λ for $\Delta_{p,q}(\alpha, \beta)$, we can think of the pavilion as a subset of the almost toric base diagram $\mathfrak{A}_{p,q}(\alpha, \beta)$, and nodally slide so that the focus-focus singularity lies below $\text{Pav}_{\rho, \lambda}(\Delta_{p,q}(\alpha, \beta))$. Define the *offcut*

$$\text{Off}_{\rho, \lambda}(\mathfrak{A}_{p,q}(\alpha, \beta)) := \mathfrak{A}_{p,q}(\alpha, \beta) \setminus \text{Pav}_{\rho, \lambda}(\Delta_{p,q}(\alpha, \beta)).$$

We call the associated almost toric domain the *almost toric offcut* $\text{Off}_{\rho, \lambda}(E_{p,q}(\alpha, \beta))$; see Figure 10.

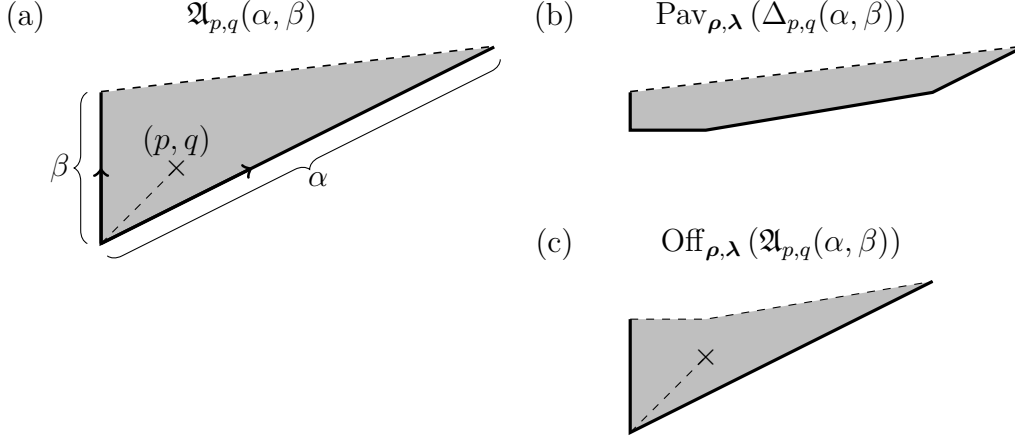


Figure 10: (a): The almost toric base diagram $\mathfrak{A}_{p,q}(\alpha, \beta)$. (b): The moment image of the pavilion blow-up \tilde{U}_ρ . (c): The almost toric offcut $\text{Off}_{\rho, \lambda}(E_{p,q}(\alpha, \beta))$.

2.3 Vianna triangles

Let $\mathfrak{D}(1, 1, 1)$ be the triangle with vertices $\mathbf{v}_1 = (0, 0)$, $\mathbf{v}_2 = (1, 0)$ and $\mathbf{v}_3 = (0, 1)$. This is the moment image of a Hamiltonian torus action on \mathbb{CP}^2 . We can make nodal trades at the three corners to get an almost toric base diagram with three nodes $\mathbf{n}_1, \mathbf{n}_2, \mathbf{n}_3$ where \mathbf{n}_i is connected to the vertex \mathbf{v}_i by a branch cut \mathbf{b}_i . The result is the base of an almost toric fibration on \mathbb{CP}^2 . We can perform mutations of this almost toric base diagram and we obtain a sequence of almost toric base diagrams called *Vianna triangles*. For a general introduction to Vianna triangles and their elementary properties see [16, Appendix I]. We continue to write $\mathbf{v}_1, \mathbf{v}_2, \mathbf{v}_3$ for the vertices (ordered anticlockwise) and \mathbf{b}_i for the branch cut connecting \mathbf{v}_i to the node \mathbf{n}_i . Recall that the determinant⁶ at the vertex \mathbf{v}_i is equal to p_i^2 for some positive integer p_i , and together, (p_1, p_2, p_3) form a *Markov triple*. Recall that (p_1, p_2, p_3) is called a Markov triple if

$$p_1^2 + p_2^2 + p_3^2 = 3p_1p_2p_3. \quad (2.3)$$

We will write $\mathfrak{D}(p_1, p_2, p_3)$ for the Vianna triangle corresponding to (p_1, p_2, p_3) . If we mutate $\mathfrak{D}(p_1, p_2, p_3)$ at the vertex p_2 , say, then the result is $\mathfrak{D}(p'_1, p'_2, p'_3)$ where

$$p'_1 = p_1, \quad p'_2 = p_3, \quad p'_3 = 3p_1p_3 - p_2. \quad (2.4)$$

Label the edges of $\mathfrak{D}(p_1, p_2, p_3)$ as $\mathbf{e}_1, \mathbf{e}_2, \mathbf{e}_3$, where \mathbf{e}_i is opposite vertex \mathbf{v}_i . The affine length of \mathbf{e}_i is $\frac{p_i}{p_{i+1}p_{i+2}}$, see [16, Corollary I.13].

If we ignore the nodes and branch cuts, then $\mathfrak{D}(p_1, p_2, p_3)$ is the moment image for the toric

⁶If the primitive integer vectors along the edges emanating from \mathbf{v}_i are u and v , then the determinant of \mathbf{v}_i is defined to be $|u \wedge v|$, that is the absolute value of the determinant of the matrix whose columns are u and v .

orbifold surface $\mathbb{P}(p_1^2, p_2^2, p_3^2)$ which has a $\frac{1}{p_i^2}(p_{i+2}^2, p_{i+1}^2)$ cyclic quotient singularity⁷ living over the vertex \mathbf{v}_i . Note that (taking indices modulo 3) $\frac{1}{p_i^2}(p_{i+2}^2, p_{i+1}^2) \cong \frac{1}{p_i^2}(p_{i+1}^2 p_{i+2}^{-2}, 1)$, where the inverse is computed modulo p_i^2 . Equation (2.3) tells us that $p_{i+1}^2 p_{i+2}^{-2} = 3p_i p_{i+2}^{-1} p_{i+1} - 1 \pmod{p_i^2}$. Furthermore, $p_{i+1}^2 p_{i+2}^{-2} = p_i q_i - 1 \pmod{p_i^2}$ since the singularity is Wahl. Therefore,

$$q_i = +3p_{i+1}p_{i+2}^{-1} \pmod{p_i}. \quad (2.5)$$

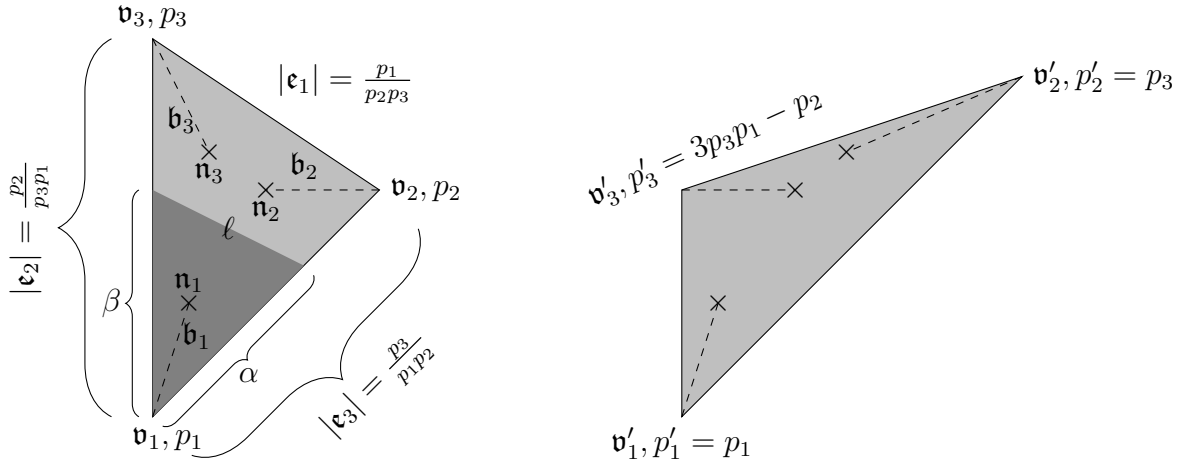


Figure 11: A Vianna triangle and its mutation at \mathbf{v}_2 ; quantities for the mutated triangle are written with primes. The darker shaded region bounded by the line ℓ is the visible $\mathfrak{A}_{p_1, q_1}(\alpha, \beta)$. Next to each vertex \mathbf{v}_i we also give the Markov number p_i with $\det(\mathbf{v}_i) = p_i^2$.

Lemma 2.3.1. *Given a Markov triple (p_1, p_2, p_3) , take the companion number $q_i = 3p_{i+1}p_{i+2}^{-1} \pmod{p_i}$ for $i = 1, 2, 3$ (indices taken modulo 3). Then \mathbb{CP}^2 contains a visible symplectic $E_{p_i, q_i}(\alpha, \beta)$ for any $\alpha < \frac{p_{i+2}}{p_i p_{i+1}}$ and $\beta < \frac{p_{i+1}}{p_i p_{i+2}}$.*

Proof. The constraints on α and β mean that we can pick the points \mathbf{p}_{i+2} on \mathbf{e}_{i+2} an affine length α from v_i and \mathbf{p}_{i+1} on \mathbf{e}_{i+1} an integral affine length β from v_i . Connect them with a straight line ℓ ; nodally slide \mathbf{n}_i so that it lives on one side of ℓ and \mathbf{n}_{i+1} and \mathbf{n}_{i+2} so that they live on the far side of ℓ . The line ℓ divides $\mathfrak{D}(p_1, p_2, p_3)$ into two pieces; the piece containing \mathbf{n}_i is integral-affine equivalent to $\mathfrak{A}_{p_i, q_i}(\alpha, \beta)$, so we obtain a visible embedding of $E_{p_i, q_i}(\alpha, \beta)$ as required; see Figure 11. \square

⁷Note that there is a confusing ordering issue here. The conventions we are using for the moment polygon ensure that the Hirzebruch–Jung chain appears in order if you read the self-intersections off anticlockwise. However, with this convention, the moment-preimage of the vertical edge in $\Delta_{p, q}(\alpha, \beta)$ is contained in the x -axis and the moment-preimage of the slanted edge is contained in the y -axis. Indeed, the affine change of coordinates in [16, Example 3.21] which finds the moment polygon for an orbifold singularity has negative determinant. This is why we write $\frac{1}{p_i^2}(p_{i+2}^2, p_{i+1}^2)$ rather than $\frac{1}{p_i^2}(p_{i+1}^2, p_{i+2}^2)$.

2.4 The culet

Once again, ignore the almost toric data and consider $\mathfrak{D}(p_1, p_2, p_3)$ as the moment image of the toric orbifold $\mathbb{P}(p_1^2, p_2^2, p_3^2)$. Suppose that p_1 is the biggest number in the Markov triple (p_1, p_2, p_3) and use an integral affine transformation to make the edge \mathfrak{e}_1 of $\mathfrak{D}(p_1, p_2, p_3)$ horizontal, with the rest of the triangle below.

Definition 2.4.1. Let us subdivide the fan of inward normals for the Vianna triangle by adding a ray pointing vertically upwards. This gives partial resolution of the $\frac{1}{p_1^2}(p_2^2, p_3^2)$ singularity introducing a single exceptional curve which we call the *culet curve*.⁸ If we fix a sufficiently small λ then we get a (non-Delzant) pavilion with a new horizontal edge at the bottom, which we call the *culet*; see Figure 12.

There are still (up to) two orbifold singularities on this edge at the new vertices \mathfrak{v}'_1 and \mathfrak{v}''_1 ; these are toric, with their moment images modelled on the *alternate angles* for the corners \mathfrak{v}_2 and \mathfrak{v}_3 and so are *dual* to these Wahl singularities [41, Proposition 6]. We can further (minimally) resolve these singularities by completing our subdivision to a Delzant pavilion ρ . Corresponding to these new rays in the fan, we have a chain of exceptional curves of the form $[W_0^\vee, w, W_1^\vee]$ where W_i^\vee are dual Wahl chains and $-w$ is the self-intersection of the culet curve. By a theorem of Urzúa and Zúñiga [49, Proposition 4.1], this is only possible if:

- both W_i^\vee are nonempty chains and $w = 10$,
- precisely one of the W_i^\vee is nonempty and $w = 7$, or
- both of the W_i^\vee are empty and $w = 4$.

Hence the chain $[W_0^\vee, w, W_1^\vee]$ does not contain any (-1) -spheres and is therefore minimal.

Remark 2.4.2. If we pick a non-minimal resolution, it dominates the minimal resolution. We will still refer to the proper transform of the culet curve as the culet curve, so the notion makes sense for arbitrary resolutions.

Definition 2.4.3. Given a chain-shaped resolution of the $\frac{1}{p_1^2}(p_2^2, p_3^2)$ singularity, we write C_1, \dots, C_m for the exceptional curves of this resolution and write i_{culet} for the index of the culet curve.

Definition 2.4.4. Let w be $-C_{i_{\text{culet}}}^2$ for the minimal resolution. We call this the *Manetti weight* of the pin-ellipsoid (note that it only makes sense when p is a Markov number and q a companion of p).

⁸We will continue to refer to the proper transform of this curve as the culet curve in any resolution dominating this one.

Remark 2.4.5. Recall that $w \in \{4, 7, 10\}$ by the aforementioned result of Urzúa and Zúñiga [49, Proposition 4.1]. The Manetti weights depend on the pairs (p, q) as follows. The pair $(p, q) = (2, 1)$ is the only one which yields $w = 4$. The Manetti weight is $w = 7$ if and only if (p, q) comes from a Markov triple containing a 1. In every other case it is $w = 10$. Note that the square of the culet curve in a non-minimal resolution will be bigger than the weight if our non-minimal resolution is obtained from the minimal one by blow up of points on the culet curve.

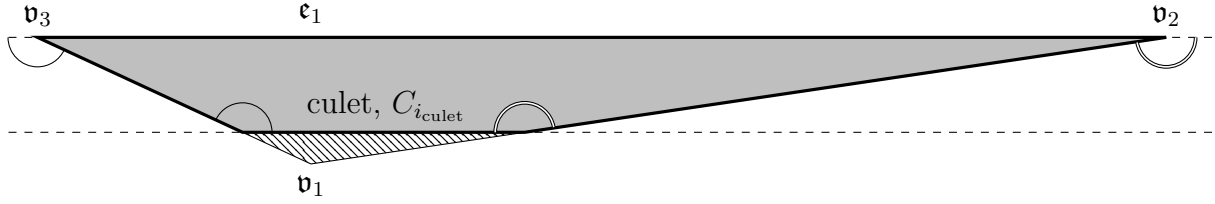


Figure 12: The culet cut is horizontal, parallel to the edge \mathfrak{e}_1 of affine length $p_1/(p_2p_3)$. The new corners are integral-affine dual to the corners at \mathfrak{v}_2 and \mathfrak{v}_3 .

Since the edge \mathfrak{e}_1 is parallel to the culet, there is a visible symplectic sphere in the sense of Symington [48, Definition 7.2] having square zero and living over a vertical arc connecting \mathfrak{e}_1 and the culet. One of the main ideas in what follows will be to find the analogue of this square zero sphere for an arbitrary symplectic embedding $E_{p,q}(\alpha, \beta) \hookrightarrow \mathbb{CP}^2$.

3 Geometry and topology of pavilion blow-ups

In Section 3.1, we explain in detail the almost complex and symplectic structures with which we will equip pavilion blow-ups. In Section 3.2, we explain how to compute in the cohomology ring of the pavilion blow-up.

3.1 Pavilion blow up and its geometric structures

Notation 3.1.1. Given a symplectic manifold (W, ω) with a convex (respectively concave) boundary, let \overline{W} denote its symplectic completion, obtained by gluing on copies of the positive (respectively negative) half of the symplectisation of the boundary. If J is an ω -compatible almost complex structure on W which is cylindrical near the ends then let \overline{J} denote the unique almost complex structure on \overline{W} extending J cylindrically to the ends. If W has both convex and concave ends then define \overline{W}_+ (respectively \overline{W}_-) to be the result of completing only the convex (respectively concave) ends.

Definition 3.1.2. A neighbourhood N of the boundary of $E_{p,q}(\alpha, \beta)$ is symplectomorphic to a neighbourhood of the boundary of the girdled orbifold $\mathcal{O}_{p,q}(\alpha, \beta)$, namely the moment-preimage of the shaded region in $\Delta_{p,q}(\alpha, \beta)$ shown in Figure 13. Since this toric orbifold is

a finite quotient of a compact set in \mathbb{C}^2 , it has a complex structure. Let J_N be the pullback of this complex structure to N .

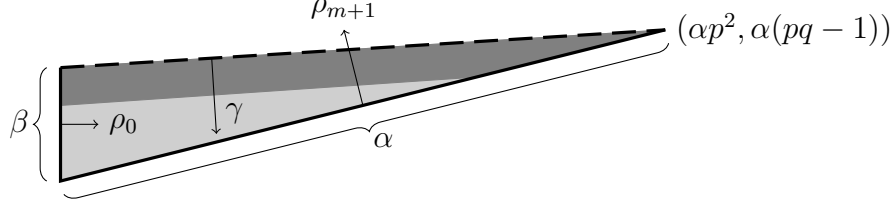


Figure 13: The moment image $\Delta_{p,q}(\alpha, \beta)$ of a toric orbifold. The preimage under the moment map of the shaded region is symplectomorphic to a neighbourhood of $\partial E_{p,q}(\alpha, \beta)$ in $E_{p,q}(\alpha, \beta)$. The toric boundary comprises the two solid edges, *not* the top side; the orbifold point is at the vertex of the polygon. We have also labelled the inward normals ρ_0 and ρ_{m+1} of the toric boundary and γ of the top side (girdle).

Definition 3.1.3. Let (X, ω) be a symplectic manifold and suppose that we have a symplectic embedding $\iota: E_{p,q}(\alpha, \beta) \hookrightarrow X$. Let \mathcal{J}_N be the space of compatible almost complex structures on X which coincide with $\iota_* J_N$ on $\iota(N)$.

These almost complex structures are *adjusted* to the neck region N in the sense of [8, Section 2.2] and so amenable to *neck-stretching*. Neck-stretching (or splitting) is a specific one-parameter deformation of the almost complex structure introduced in [15, Section 1.3]; neck-stretching for pin-ellipsoids is discussed in detail in [51, Sections 3.2–3.3] and [17, Section 3.1].

Definition 3.1.4. Given a $J \in \mathcal{J}_N$, we get a neck-stretching sequence of compatible almost complex structures J_t on X with $J_0 = J$; let us write $U = \iota(E_{p,q}(\alpha, \beta))$ and $V = X \setminus U$ and \bar{U}, \bar{V} for the symplectic completions. Since (\bar{N}_-, \bar{J}_N) is isomorphic to a punctured neighbourhood of the origin in \mathbb{C}^2/G , we can compactify (\bar{V}, \bar{J}) by adding in a point x to obtain an almost complex orbifold (\hat{X}, \hat{J}) . Let $\hat{N} := \bar{N}_- \cup \{x\}$; this is an embedded copy of the girdled orbifold $\mathcal{O}_{p,q}(\alpha, \beta)$.

We will now resolve \hat{X} using a pavilion as in Definition 2.1.8. We will need to choose a Delzant pavilion such that the image of the neck N under the moment map is contained in $\text{Pav}_{\rho, \lambda}(\Delta_{p,q}(\alpha, \beta))$; in practice, we will fix the choice of pavilion first, and then choose N sufficiently close to the girdle that it satisfies this condition.

Definition 3.1.5 (Pavilion blow-up). Given a Delzant pavilion ρ, λ for $E_{p,q}(\alpha, \beta)$ and a symplectic embedding $\iota: E_{p,q}(\alpha, \beta) \hookrightarrow X$, we obtain a resolution \tilde{X} of \hat{X} by replacing $\hat{N} \subset \hat{X}$ with the girdled resolution \tilde{U}_ρ of $\mathcal{O}_{p,q}(\alpha, \beta)$.

- (i) Let \tilde{J} be the almost complex structure on \tilde{X} which coincides with J on V and agrees with the complex structure on \tilde{U}_ρ .

- (ii) Note that if $J \in \mathcal{J}_N$, the associated almost Kähler metric $\omega(-, J-)$ is flat on N . Let ψ_0 be the convex function on the moment-image of N which encodes the Kähler potential of $\omega|_N$. Given a convex function ψ on $\text{Pav}_{\rho, \lambda}(\Delta_{p, q}(\alpha, \beta))$ which coincides with ψ_0 on the shaded region (moment-image of N) and has the correct behaviour along the edges, we obtain a symplectic form $\tilde{\omega}$ on \tilde{X} which coincides with ω on V and $\tilde{\omega}_{\rho, \lambda, \psi}$ on \tilde{U}_ρ ; this is well-defined because ψ is chosen to coincide with ψ_0 on the moment-image of N .

We call the manifold $\tilde{X} := V \cup \tilde{U}_\rho$, equipped with the almost complex structure \tilde{J} and the symplectic form $\tilde{\omega}$ the *pavilion blow-up* of X along the embedded pin-ellipsoid U . If we want to keep the dependence of \tilde{X} on the various choices explicit, we will write $\text{Pav}_{\rho, \lambda}^\ell(X)$ for \tilde{X} . We will sometimes abusively drop the subscript on \tilde{U} .

Remark 3.1.6. A pavilion blow-up with minimal Delzant pavilion is just the usual *symplectic rational blow-up* established by Symington [46, 47], which was elaborated upon by Khodorovskiy [28]. It is the inverse operation of the *rational blow-down*, introduced in the smooth category by Fintushel and Stern [19]; see also [16, Section 9.2] for an exposition in the symplectic category. In the last decade the symplectic rational blow-up was used by many authors to study Lagrangian pin-wheels and pin-ellipsoids. See for example the work of Borman–Li–Wu [7], Shevchishin–Smirnov [43] and Adaloglou [2, 3] on Lagrangian embeddings of \mathbb{RP}^2 ; the work of Khodorovskiy [27] and Evans–Smith [18] on bounding Wahl singularities; the work of Brendel–Schlenk on Lagrangian barriers [9] generalising Biran’s work [6]; and the work of Adaloglou [2] and Adaloglou–Hauber [4] on symplectic embeddings of $B_{n,1}$.

Figure 14 illustrates the spaces $X, \bar{V}, \hat{X}, \tilde{X}$, the subspaces $U, V, \tilde{U}, N, \bar{N}_-, \hat{N}$, and the relations between them all.

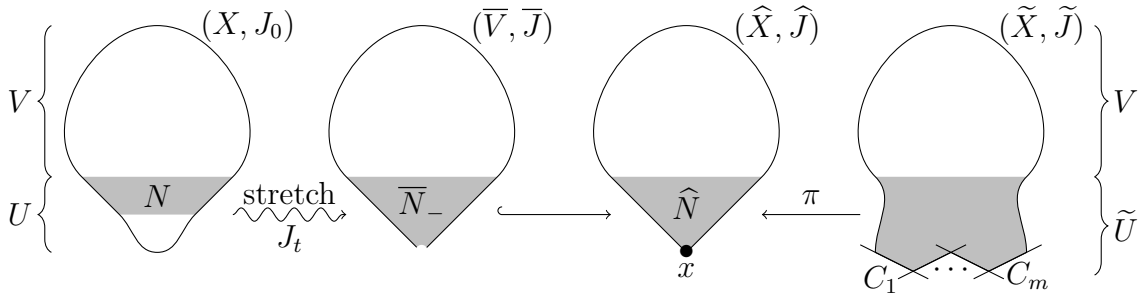


Figure 14: The spaces defined in Section 3.1

Lemma 3.1.7. *There are bijections between the following collections of objects:*

- irreducible finite energy punctured \bar{J} -holomorphic curves C in \bar{V} ,
- irreducible orbifold \hat{J} -holomorphic curves \hat{C} in \hat{X} ,

- irreducible \tilde{J} -holomorphic curves \tilde{C} in \tilde{X} other than C_1, \dots, C_m .

Proof. Given a finite energy punctured \bar{J} -holomorphic curve $C \subset \bar{V}$, we write \hat{C} for its closure in \hat{X} . The inverse operation is puncturing (removing x). Given an orbifold curve \hat{C} in \hat{X} , write \tilde{C} for the proper transform in \tilde{X} . The inverse operation is projection along π , which sends any curve other than C_1, \dots, C_m to an orbifold curve. \square

Lemma 3.1.8. (a) Any irreducible \tilde{J} -holomorphic curve in \tilde{X} which is not one of the C_i must enter the interior of V .

(b) By choosing J generically on V , we can ensure that all curves which enter V are regular⁹, so that the only irregular \tilde{J} -holomorphic curves are amongst¹⁰ the C_1, \dots, C_m .

Proof. (a) If $\tilde{C} \subset \tilde{X}$ is a \tilde{J} -curve other than C_1, \dots, C_m which does not enter the interior of V then the associated punctured curve C is contained in \bar{N}_- . Since the positive boundary of \bar{N}_- is convex, this contradicts the maximum principle.

(b) This follows from [36, Proposition 3.2.1 and Remark 3.2.3]. \square

Remark 3.1.9. Note that everything that was introduced and discussed within this section makes sense in the case where there are several disjoint pin-ellipsoids.

3.2 Topology of the pavilion blow-up

Given a symplectic embedding $\iota: E_{p,q}(\alpha, \beta) \hookrightarrow X$ and a choice of pavilion, we will need to understand how to compute intersection numbers of curves in the pavilion blow-up \tilde{X} by computing locally in \tilde{U} and $V = X \setminus \tilde{U}$ separately, and adding. In what follows, if A is a class in integral homology, we will write $A_{\mathbb{Q}}$ for the corresponding class in rational homology. Denote the interface between \tilde{U} and V by Σ and recall that Σ is topologically a lens space $L(p^2, pq - 1)$.

Lemma 3.2.1. We have $H_1(U, \Sigma; \mathbb{Z}) = H_3(U, \Sigma; \mathbb{Z}) = 0$ and $H_2(U, \Sigma; \mathbb{Z}) \cong \mathbb{Z}_p$.

Proof. This follows immediately from the long exact sequence of the pair (U, Σ) :

⁹A curve is called *regular* if its linearised Cauchy–Riemann operator is surjective; see [36, Section 3.1]. For an embedded holomorphic sphere C in a 4-manifold, [36, Lemma 3.3.3] implies that regularity is equivalent to the condition $C^2 \geq -1$.

¹⁰If the resolution is minimal then *all* the C_i are irregular ($C_i^2 \leq -2$). Otherwise there are also some -1 -spheres amongst them.

$$\begin{array}{ccccccc}
\cdots & \longrightarrow & H_3(U; \mathbb{Z}) & \longrightarrow & H_3(U, \Sigma; \mathbb{Z}) & & \\
& & \downarrow 0= & & \swarrow & & \\
0= & H_2(\Sigma; \mathbb{Z}) & \xleftarrow{\quad} & H_2(U; \mathbb{Z}) & \longrightarrow & H_2(U, \Sigma; \mathbb{Z}) & \\
& & \downarrow 0= & & \swarrow & & \\
\mathbb{Z}_{p^2}= & H_1(\Sigma; \mathbb{Z}) & \xleftarrow{\quad \text{mod } p} & H_1(U; \mathbb{Z}) & \longrightarrow & H_1(U, \Sigma; \mathbb{Z}) \longrightarrow 0. & \\
& & & \downarrow \cong \mathbb{Z}_p & & &
\end{array}$$

□

Lemma 3.2.2. *Given a class $A \in H_2(\tilde{X}; \mathbb{Z})$, there exist rational numbers a_1, \dots, a_m and a class $A_X \in H_2(X; \mathbb{Z})$ such that*

$$A_{\mathbb{Q}} = \frac{1}{p} A_X + \sum_{i=1}^m a_i [C_i]. \quad (3.1)$$

Here we are identifying $H_2(X; \mathbb{Q})$ as a subset of $H_2(\tilde{X}; \mathbb{Q})$ using the fact that $H_2(X; \mathbb{Q}) \cong H_2(V; \mathbb{Q})$. Moreover, the class pA_X is an integral class which can be represented by a cycle contained in V .

Proof. The Mayer–Vietoris sequence says:

$$0 = H_2(\Sigma; \mathbb{Z}) \rightarrow H_2(\tilde{U}; \mathbb{Z}) \oplus H_2(V; \mathbb{Z}) \rightarrow H_2(\tilde{X}; \mathbb{Z}) \rightarrow H_1(\Sigma; \mathbb{Z}) = \mathbb{Z}_{p^2} \rightarrow \cdots,$$

so if $A \in H_2(\tilde{X}; \mathbb{Z})$ then $p^2 A$ can be written as $A'_{\tilde{U}} + A'_V$. Therefore $A_{\mathbb{Q}} = \frac{1}{p^2} A'_{\tilde{U}} + \frac{1}{p^2} A'_V$. We will take $A_{\tilde{U}} := \frac{1}{p^2} A'_{\tilde{U}} = \sum_{i=1}^m a_i [C_i]$ for some rational numbers $a_i \in \frac{1}{p^2} \mathbb{Z}$. To understand A'_V , consider the exact sequence of the pair (X, V) :

$$0 = H_3(U, \Sigma; \mathbb{Z}) \rightarrow H_2(V; \mathbb{Z}) \rightarrow H_2(X; \mathbb{Z}) \rightarrow H_2(X, V; \mathbb{Z}) = H_2(U, \Sigma; \mathbb{Z}) = \mathbb{Z}_p,$$

where we used excision to identify $H_2(X, V)$ with $H_2(U, \Sigma)$. This means that $A'_V = pA_X$ for some $A_X \in H_2(X; \mathbb{Z})$. □

Remark 3.2.3. We can calculate the numbers a_j as follows if we know how A intersects the curves C_j . Let $\alpha_j = A \cdot [C_j] \in \mathbb{Z}$ and let $\boldsymbol{\alpha} = (\alpha_1, \dots, \alpha_m)^T$ and $\mathbf{a} = (a_1, \dots, a_m)$. Then

$$\alpha_j = \sum_{i=1}^m a_i C_i \cdot C_j, \text{ or } \boldsymbol{\alpha} = M \mathbf{a},$$

where M is the m -by- m matrix with entries $M_{ij} = C_i \cdot C_j$. Therefore $\mathbf{a} = M^{-1} \boldsymbol{\alpha}$. It will be useful to have formulas for the entries of M^{-1} .

Lemma 3.2.4. *Suppose that the Wahl chain for the minimal resolution of our singularity is*

$$[b_1, \dots, b_m], \quad \text{with } b_i = -C_i^2,$$

and fix an index i . Consider the continued fractions $e_i/e_{i-1} = [b_{i-1}, \dots, b_1]$ and $f_i/f_{i+1} = [b_{i+1}, \dots, b_m]$. The entries of M_{ij}^{-1} are

$$M_{ij}^{-1} = \begin{cases} -(e_i f_j)/p^2 & \text{if } i \leq j \\ -(e_j f_i)/p^2 & \text{if } i > j \end{cases}.$$

Proof. The continued fractions are computed as

$$\begin{aligned} \frac{e_{i+1}}{e_i} &= b_i - \frac{1}{[b_{i-1}, \dots, b_1]} & \frac{f_{i-1}}{f_i} &= b_i - \frac{1}{[b_{i+1}, \dots, b_m]} \\ &= \frac{b_i e_i - e_{i-1}}{e_i}, & &= \frac{b_i f_i - f_{i+1}}{f_i}, \end{aligned}$$

so

$$e_{i+1} + e_{i-1} = b_i e_i, \quad f_{i+1} + f_{i-1} = b_i f_i,$$

which are Fibonacci-like recursions with initial conditions

$$e_0 = 0, \quad e_1 = 1, \quad f_0 = p^2, \quad f_1 = pq - 1.$$

For the matrix M^{-1} as postulated in the lemma, the off-diagonal entries $(M^{-1}M)_{ij}$ above the diagonal are¹¹

$$-\frac{1}{p^2} (e_i f_{j-1} - e_i b_j f_j + e_i f_{j+1}) = 0.$$

Those below the diagonal are

$$-\frac{1}{p^2} (e_{j-1} f_i - e_j b_j f_i + e_{j+1} f_i) = 0.$$

Those on the diagonal are

$$-\frac{1}{p^2} (e_{i-1} f_i - b_i e_i f_i + e_i f_{i+1}) = \frac{1}{p^2} (e_i f_{i-1} - e_{i-1} f_i).$$

We can show that $e_i f_{i-1} - e_{i-1} f_i = p^2$ by induction: it holds when $i = 1$ and

$$e_{i+1} f_i - e_i f_{i+1} = \begin{vmatrix} e_{i+1} & f_{i+1} \\ e_i & f_i \end{vmatrix} = \begin{vmatrix} b_i e_i - e_{i-1} & b_i f_i - f_{i-1} \\ e_i & f_i \end{vmatrix} = \begin{vmatrix} e_i & f_i \\ e_{i-1} & f_{i-1} \end{vmatrix}$$

by subtracting b_i times row 2 from row 1 and swapping the rows.

This shows that $M^{-1}M$ is the identity matrix, as required. \square

¹¹The entries in the first and last column have only two terms, but the formula still holds true if we decide to set $e_0 = f_{m+1} = 0$.

Remark 3.2.5. We will only be concerned with the case when $X = \mathbb{CP}^2$. In this case, we write \mathcal{E} for the rational class $\frac{1}{p}H \in H_2(X; \mathbb{Q})$, where H is the class of the line, so $p^2\mathcal{E}$ can be represented by a cycle in V . We can write any class $A \in H_2(\tilde{X}; \mathbb{Q})$ in the form

$$A = a_0\mathcal{E} + \sum_{i=1}^m a_i[C_i]. \quad (3.2)$$

The square of A is then given by the formula

$$A^2 = \frac{a_0^2}{p^2} + \mathbf{a}^T M \mathbf{a}. \quad (3.3)$$

Remark 3.2.6. In the case of multiple embeddings $\iota: \bigsqcup_{j=1}^{\ell} E_{p_j, q_j}(\alpha_j, \beta_j) \hookrightarrow X$ we define $\Delta := \prod_{j=1}^{\ell} p_j$. Then, by performing a pavilion blow-up on all the ℓ embedded pin-ellipsoids, we obtain spaces \tilde{X}, \tilde{V} and V , and Equation (3.1) becomes

$$A_{\mathbb{Q}} = \frac{1}{\Delta} A_X + \sum_{j=1}^{\ell} \sum_{i=1}^{m_j} a_{j,i} [C_{j,i}].$$

Similarly, in the case that $X = \mathbb{CP}^2$, Equations (3.2) and (3.3) become:

$$A = a_0\mathcal{E} + \sum_{j=1}^{\ell} \sum_{i=1}^{m_j} a_{j,i} [C_{j,i}] \quad \text{and} \quad A^2 = \frac{a_0^2}{\Delta^2} + \sum_{j=1}^{\ell} \mathbf{a}_j^T M_j \mathbf{a}_j. \quad (3.4)$$

4 Ruled 4-manifolds

The results of this section are well-known to experts; we thank Weiyi Zhang for informing us that the methods of his paper [52] for irrational ruled surfaces can be adapted to the rational case.

4.1 Regulations and rulings

Definition 4.1.1. Given a stable J -holomorphic curve S , write $S = \sum_{i \in I} m_i S_i$ where S_i are the non-constant irreducible components of S , indexed by a set I , and m_i their covering multiplicities. The *dual graph* of S is the labelled graph Γ_S :

- whose vertex set is I ,
- whose vertex i is labelled by the self-intersection number S_i^2 ,
- and where there are $S_i \cdot S_j$ edges between the vertices $i \neq j$.

Definition 4.1.2. Let (Y, J) be a tamed almost complex 4-manifold. Given a homology class $A \in H_2(Y; \mathbb{Z})$, let $\overline{\mathcal{M}}_{0,n}(A, J)$ denote the moduli space of J -holomorphic stable maps in the class A having n marked points. We say that Y admits a J -holomorphic regulation¹² in the class A if all the following conditions hold:

- (a) $A^2 = 0$ and $c_1(Y) \cdot A = 2$
- (b) the evaluation map $\text{ev}: \overline{\mathcal{M}}_{0,1}(A, J) \rightarrow Y$ has degree 1.

The curves in the moduli space $\overline{\mathcal{M}}_{0,0}(A, J)$ are called *rulings*. Smooth curves corresponding to points of the (possibly empty) subspace $\mathcal{M}_{0,0}(A, J)$ we call *smooth rulings*; by the adjunction formula, these are embedded spheres. Curves corresponding to points of $\partial \overline{\mathcal{M}}_{0,0}(A, J) = \overline{\mathcal{M}}_{0,0}(A, J) \setminus \mathcal{M}_{0,0}(A, J)$ we call *broken rulings*. We call the regulation of Y *non-degenerate* if there is at least one smooth ruling.

Example 4.1.3. (1) The simplest example of a ruled surface is $\mathbb{CP}^1 \times \mathbb{CP}^1$: this admits two non-degenerate regulations, one in the class $[\mathbb{CP}^1 \times \{\mathfrak{p}\}]$ and one in the class $[\{\mathfrak{p}\} \times \mathbb{CP}^1]$. This ruled surface arises as a quadric surface in \mathbb{CP}^3 and the rulings in both regulations are lines.

- (2) If we degenerate the quadric to a nodal quadric then there is still a regulation (but now only one) consisting of lines $\{F_t \mid t \in \mathbb{CP}^1\}$ passing through the node: the two regulations of the smooth surface degenerate onto this regulation. If we resolve the node (introducing a -2 -curve σ_∞) then the result is the Hirzebruch surface \mathbb{F}_2 . The proper transforms \tilde{F}_t of the rulings of the nodal quadric yield the standard non-degenerate regulation of \mathbb{F}_2 ; there is another, degenerate, regulation whose rulings are $\tilde{F}_t + \sigma_\infty$.

Theorem 4.1.4. If Y contains a smoothly embedded J -holomorphic curve C with $[C]^2 = 0$ then C is part of a non-degenerate J -holomorphic regulation in the class $[C]$.

Proof. We get that $c_1(Y) \cdot [C] = 2$ by adjunction. Since $c_1(Y) \cdot [C] > 0$, automatic transversality guarantees that the moduli space $\mathcal{M}_{0,1}([C], J)$ is a smooth manifold of dimension 4 and the evaluation map $\text{ev}: \mathcal{M}_{0,1}([C], J) \rightarrow Y$ is a pseudocycle. The degree of this pseudocycle must be 1 because there is at most one smooth J -holomorphic sphere in the class $[C]$ passing through any point (by positivity of intersections because $[C]^2 = 0$) and for all points in a neighbourhood of C there is precisely one (namely C or its small deformations, which exist by automatic transversality). In particular, $\text{ev}: \overline{\mathcal{M}}_{0,1}([C], J) \rightarrow Y$ has degree 1. \square

¹²This would ordinarily be called a *ruling*, but ruling can also mean one of the curves in the regulation and this is how we will use it. Regulation is to *regula* (Latin for rule) as a triangulation is to *triangle*.

4.2 Broken rulings

Proposition 4.2.1. *Let (Y, J) be a tamed almost complex manifold admitting a non-degenerate regulation in the class $A \in H_2(Y; \mathbb{Z})$. Let C be a smooth ruling, and let $S = \sum m_i S_i$ be a broken ruling of the regulation.*

- (a) *The curves S_i are embedded rational curves disjoint from C .*
- (b) *The dual graph Γ_S is a tree.*
- (c) *The irreducible components S_i have $[S_i]^2 < 0$.*
- (d) *At least one irreducible component is a sphere of square -1 .*

Proof. (a) and (b). The existence of a smooth ruling of the regulation implies that the class A is J -nef in the sense of Li and Zhang [31, Lemma 2.8]. This implies that the dual graph is a tree and all the components are embedded spheres [31, Theorem 1.5]. Note that the components S_i are disjoint from any smooth ruling C , since $0 = A^2 = C \cdot \sum m_i S_i = \sum m_i (C \cdot S_i)$ and $C \cdot S_i \geq 0$ for all i , so $C \cdot S_i = 0$ for all components S_i .

(c) To see why $S_i^2 < 0$ for all i , we adapt the proof of [35, Lemma 3.3.1]. Suppose that S_i is a component which appears with multiplicity m_i in S . Since the curves $\sum_{j \neq i} m_j S_j$ and $C + m_i S_i$ are geometrically distinct, they intersect non-negatively; in fact, since the dual graph is connected with at least two vertices, S_i must intersect at least one S_j with $j \neq i$, so they have positive intersection. Therefore

$$0 < \sum_{j \neq i} m_j S_j \cdot (A + m_i S_i) = (A - m_i S_i) \cdot (A + m_i S_i) = -m_i^2 S_i^2,$$

which implies that $S_i^2 < 0$.

(d) Since $c_1(A) = 2$, there must be at least one S_i with $c_1(S_i) > 0$; since $c_1(S_i) = S_i^2 + 2$ by adjunction and $S_i^2 < 0$, this must be a -1 -sphere. \square

Remark 4.2.2. We thank Weiyi Zhang for pointing out that this proposition can also be deduced from [31, Lemma 4.10 and Corollary 4.11].

Lemma 4.2.3. *In a non-degenerate regulation, two broken rulings are either identical or disjoint.*

Proof. Suppose that S and S' are broken rulings of a non-degenerate regulation. Since $[S] = [S']$ and $[S] \cdot [S'] = [S]^2 = 0$, the only way for S and S' to intersect is if they share a common component. Suppose that they are not identical (but share a common component). Take a component T of S that is adjacent to a shared component, but is not contained in S' . Then $T \cdot S' > 0$. But non-degeneracy means that S' is homologous to a smooth ruling C , and $T \cdot C = 0$ by Proposition 4.2.1(a), so $T \cdot S' = 0$. This yields a contradiction. \square

Remark 4.2.4. The existence of a smooth ruling is necessary (see Example 4.1.3(2)). We thank Weiyi Zhang for pointing out [29, Theorem 1.7] which guarantees the existence of regulations with at least one smooth ruling on any rational symplectic 4-manifold other than \mathbb{CP}^2 .

In the sequel, we look at spheres without marked point. Note that by Gromov compactness, there is a finite number of broken rulings of a non-degenerate regulation.

Definition 4.2.5. Given a broken ruling $S \in \overline{\mathcal{M}}_{0,0}(A, J)$, pick a contractible neighbourhood of S in $\overline{\mathcal{M}}_{0,0}(A, J)$ which contains no other broken rulings and let $N \subset Y$ be the union of all rulings from this neighbourhood in the moduli space. We call such an N a *tubular neighbourhood* of S .

Lemma 4.2.6. *Let S be a broken ruling of a non-degenerate regulation in a class A and let N be a tubular neighbourhood of S . Let J' be a new tame almost complex structure which coincides with J outside N and for which S is still J' -holomorphic. Then there is still a non-degenerate J' -holomorphic regulation in the class A and it has no new broken rulings.*

Proof. Since the smooth rulings outside N are unaffected by the modification of the almost complex structure, they are still part of a non-degenerate J' -holomorphic regulation and so is S (because it is still part of the moduli space $\overline{\mathcal{M}}_{0,0}(A, J')$). If there are any new broken rulings then they must be disjoint from both S and from the rulings outside N , and so they must be contained in $N \setminus S$. But $N \setminus S$ is a sphere bundle over a non-compact surface (the punctured neighbourhood of $S \in \overline{\mathcal{M}}_{0,0}(A, J')$) and hence $H_2(N \setminus S; \mathbb{Z}) = \mathbb{Z}$, generated by the class A . Therefore there are no homology classes into which the rulings can break (since A has minimal area amongst multiples of A). \square

Proposition 4.2.7. *Let (Y, J) be an almost complex 4-manifold tamed by a symplectic form ω . Suppose Y admits a non-degenerate J -holomorphic regulation in the class A . Let $U \subset Y$ be a subset on which J is integrable. We can find another almost complex structure J' tamed by ω satisfying:*

- (i) $J'|_U = J|_U$.
- (ii) Y still admits a J' -holomorphic regulation, and has exactly the same broken rulings (identical as point sets) as the original regulation.
- (iii) J' is integrable on a neighbourhood of all the broken rulings.

Proof. Sikorav [45, Theorem 3] shows that one can make J' integrable on a neighbourhood of any given holomorphic curve; Chen and Zhang [11, Appendix A] modified this argument to produce a tamed J' . Since we are modifying the almost complex structure only on a tubular neighbourhood of the broken rulings, Lemma 4.2.6 guarantees that we do not produce any new broken rulings. \square

Corollary 4.2.8. *The dual graph of a broken ruling in a non-degenerate regulation is obtained from the graph $\begin{smallmatrix} 0 \\ \bullet \end{smallmatrix}$ by a sequence of the following moves (combinatorial blow-ups):*

- (1) *Add a new vertex labelled -1 connected by a single edge to an existing vertex i , whose label drops by 1.*
- (2) *Add a new vertex labelled -1 at the middle of an edge connecting two vertices i and j , whose labels both drop by 1.*

Proof. We know from Proposition 4.2.1(d) that any broken ruling S contains an embedded -1 -sphere E . Once we have made the almost complex structure integrable near S , we can blow down E holomorphically to obtain a new almost complex manifold with a non-degenerate regulation. Iterate this procedure until the ruling becomes smooth; then its dual graph is a single vertex labelled 0. Inverting this process, at each step we blow up a point which either lives at a smooth point of the ruling or a node of the ruling, which changes the dual graph by a combinatorial blow-up of type 1 or 2 respectively. \square

The possible dual graphs with at most three vertices are shown in Figure 15.

Remark 4.2.9. Note that by [32, Lemma 2.2] chain-shaped dual graphs obtained from iterated combinatorial blow-up are precisely the *zero continued fractions*; for example

$$2 - \frac{1}{1 - \frac{1}{2}} = 0.$$

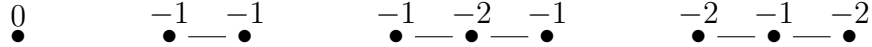
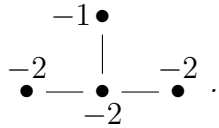


Figure 15: The dual graphs for broken rulings with at most three irreducible components.

Corollary 4.2.10. *If S is a broken ruling of a non-degenerate regulation and S has precisely one -1 -sphere amongst its irreducible components, then the same is true of all its blow-downs until we reach $\begin{smallmatrix} -1 & -1 \\ \bullet & \text{---} & \bullet \end{smallmatrix}$. Blowing back up, the next dual graph must be*

$\begin{smallmatrix} -2 & -1 & -2 \\ \bullet & \text{---} & \bullet & \text{---} & \bullet \end{smallmatrix}$, and all subsequent ones are obtained from this by combinatorially blowing-

up a point on the -1 -sphere; for example the next step might be $\begin{smallmatrix} -2 & -2 & -1 & -3 \\ \bullet & \text{---} & \bullet & \text{---} & \bullet & \text{---} & \bullet \end{smallmatrix}$ or



5 Pin-ellipsoids in the complex projective plane

5.1 Goal and strategy

In what follows, we specialise to the case where $X = \mathbb{CP}^2$ equipped with the Fubini–Study form giving a line area 1. In this preliminary section, we will outline the key technical results needed to prove Theorems 1.4.1, 1.5.2, 1.6.1 and Corollary 1.6.4.

Assume that we have a symplectic embedding $\iota: E_{p,q}(\alpha, \beta) \hookrightarrow X$ for some p, q, α, β , write U for the image of this embedding and $V = X \setminus U$. Choose a Delzant pavilion $\boldsymbol{\rho}, \boldsymbol{\lambda}$ and equip the pavilion blow-up $\tilde{X} := \text{Pav}_{\boldsymbol{\rho}, \boldsymbol{\lambda}}^\iota(X)$ with an almost complex structure \tilde{J} and symplectic form $\tilde{\omega}$ as in Definition 3.1.5. Let C_1, \dots, C_m be the exceptional curves of the pavilion.

Theorem 5.1.1. *Assume that \tilde{J} is chosen generically on V and that the Delzant pavilion is minimal. Then there exists a smoothly embedded \tilde{J} -holomorphic sphere $\tilde{C} \subset \tilde{X}$ with*

$$\tilde{C}^2 = 0 \quad \text{and} \quad \tilde{C} \cdot C_j = \begin{cases} 0 & \text{unless } j = i_{\text{culet}}, \\ 1 & \text{if } j = i_{\text{culet}}. \end{cases}$$

Remark 5.1.2. Note that Theorem 5.1.1 is obvious for a visible embedding ι^{vis} : one can then find \tilde{C} over a segment perpendicular to the line of $C_{i_{\text{culet}}}$ and to the edge \mathfrak{e}_1 , cf. Figure 12. Theorem 5.1.1 follows easily from the results of Evans and Smith [17, Theorem 4.15], as we will explain in Appendix 6, but we will give an alternative proof below which avoids working with orbifold holomorphic curves. As a consequence we will give a more direct, orbifold-free proof of the fact that p is a Markov number and q is one of its companion numbers (though, upon comparison with the orbifold proof from [17], it is clear that the two proofs are doing the same thing in different language).

Remark 5.1.3. In the case of two disjointly embedded pin-ellipsoids, we perform a pavilion blow-up as above at both of them to obtain a space \tilde{X} . By similar arguments, we obtain the existence of a holomorphic sphere \tilde{C} satisfying:

- $\tilde{C}^2 = -1$,
- $\tilde{C} = c_0 \mathcal{E} + \sum c_{1,i} C_{1,i} + \sum c_{2,i} C_{2,i}$ where c_0 is the smaller of the two solutions to

$$c_0^2 + p_1^2 + p_2^2 = 3c_0 p_1 p_2.$$

- \tilde{C} intersects each Wahl chain in the pavilion blow-up once transversely at a point belonging to one of the curves at the end of the chain.

This curve will be used in Section 5.5 to prove Theorem 1.6.1 and Corollary 1.6.4. Again, this curve is visible (living over an edge) if both pin-ellipsoids are visible.

Theorem 5.1.1 implies that \tilde{X} admits a regulation. The next result gives some properties of this regulation.

Theorem 5.1.4. *Assume that \tilde{J} is chosen generically on V and that the Delzant pavilion is minimal. Then the curve \tilde{C} from Theorem 5.1.1 is part of a \tilde{J} -holomorphic regulation with the following properties:*

- (a) *The culet curve $C_{i_{\text{culet}}}$ is a section.*
- (b) (i) *If $C_{i_{\text{culet}}}^2 = -4$ then there are no broken rulings.*
- (ii) *If $C_{i_{\text{culet}}}^2 = -7$ then $i_{\text{culet}} = 1$ (or m) and there is one broken ruling consisting of $C_2 \cup \dots \cup C_m \cup E$ (respectively $C_1 \cup \dots \cup C_{m-1} \cup E$) where E is an embedded -1 -sphere intersecting precisely one of the curves C_i in the broken ruling once transversely.*
- (iii) *If $C_{i_{\text{culet}}}^2 = -10$ then there are two broken rulings:*

$$C_1 \cup \dots \cup C_{i_{\text{culet}}-1} \cup E_1 \quad \text{and} \quad C_{i_{\text{culet}}+1} \cup \dots \cup C_m \cup E_2$$

where E_1 and E_2 are embedded -1 -spheres which intersect precisely one of the curves C_i in the broken ruling once transversely.

In all cases, the curves C_i which hit the -1 -curves E , E_1 and E_2 are completely determined by the numbers p and q .

Corollary 5.1.5. *If the pavilion is not minimal then we will still find a regulation with at most two broken rulings. The possible structures of the broken rulings is described in the proof and illustrated in Figure 18.*

Proof. Recall from Remark 2.1.5 that a non-minimal pavilion is obtained from a minimal one by a sequence of toric blow-ups, corresponding to adding further rays to the fan ρ . Since these blow-ups occur at intersection points between the curves C_1, \dots, C_m , they are disjoint from a general ruling of the regulation, so the proper transform of a general ruling is still a holomorphic curve of square zero, so the result is still ruled and the culet curve¹³ is still a section.

The broken rulings are given by taking the total transforms of either an existing broken ruling (we call this Type I) or of a smooth ruling (which we call Type II). Since the blow-ups are toric, the Type II broken rulings are chain-shaped and their dual graphs correspond to zero continued fractions as in Remark 4.2.9. The dual graphs for Type I broken rulings still have the form of a tree comprising a chain of spheres from the pavilion together with a -1 -sphere attached somewhere along the chain, but now the resolution curves from the pavilion can be -1 -curves. See Figure 18 for an example of a non-minimal pavilion blow-up with one Type I and one Type II broken ruling. \square

Definition 5.1.6. We will define a tree \mathcal{T} of symplectic curves in \tilde{X} as follows.

¹³Recall from Remark 2.4.2 that the culet curve for a non-minimal resolution is the proper transform of the culet curve from the minimal resolution.

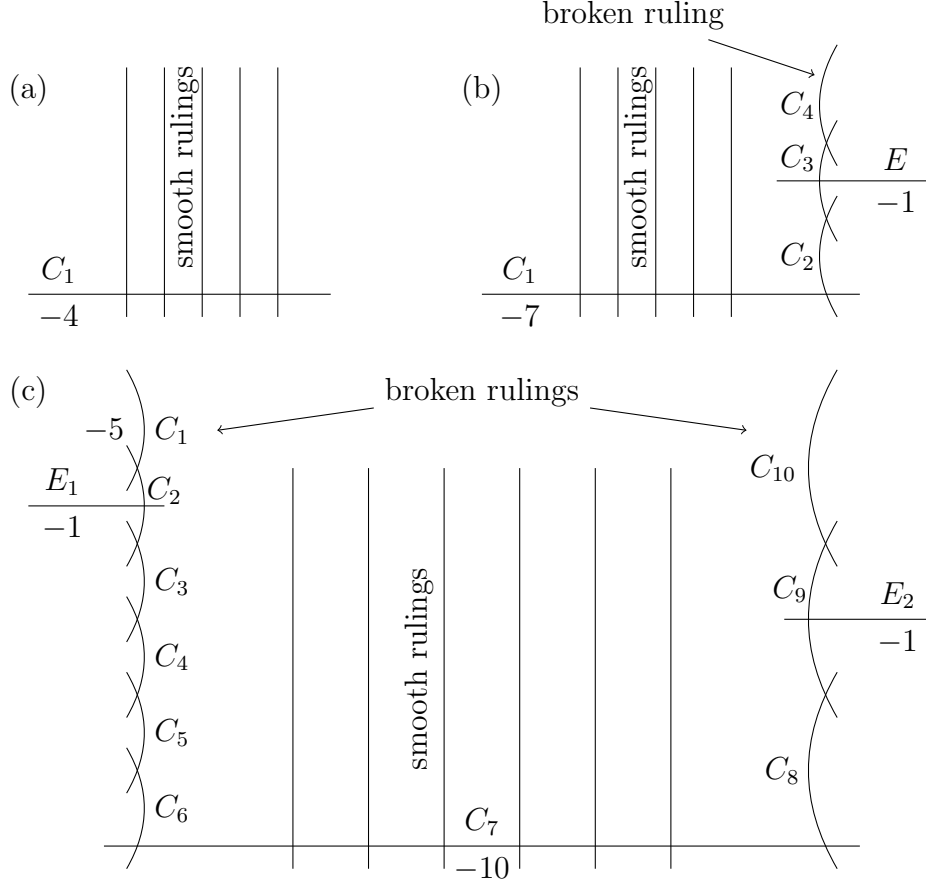


Figure 16: Examples illustrating the structure of the regulation described in Theorem 5.1.4 for the cases (a) weight 4 ($p = 2, q = 1$), (b) weight 7 ($p = 5, q = 1$) and (c) weight 10 ($p = 29, q = 7$). Curves are labelled with their name and self-intersection, except vertical straight lines (which represent smooth rulings with square 0) and -2 -spheres whose self-intersection is omitted.

- If there are two broken rulings then \mathcal{T} consists of $C_{i_{\text{culet}}}$ and the broken rulings.
- If there is precisely one broken ruling then we choose an unbroken ruling F and take \mathcal{T} to be the union of F , $C_{i_{\text{culet}}}$ and the broken ruling.
- If there are no broken rulings (which can happen only if $w = 4$ and the pavilion is minimal) then we choose two unbroken rulings F_1 and F_2 and take \mathcal{T} to be the union $F_1 \cup F_2 \cup C_1$.

Denote this splitting of \mathcal{T} into three parts by $\mathcal{T} = \mathcal{F}_1 \cup C_{i_{\text{culet}}} \cup \mathcal{F}_2$.

Corollary 5.1.7. *Let \mathcal{T} be the tree of curves from Definition 5.1.6. The complement $\tilde{X} \setminus \mathcal{T}$ is a minimal symplectic manifold.*

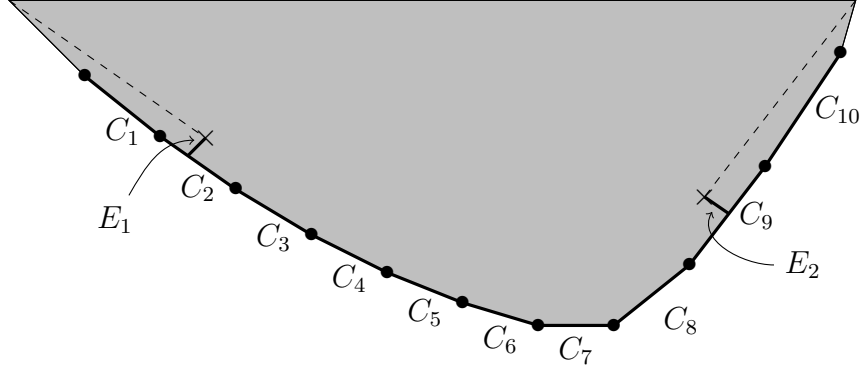


Figure 17: An almost toric base diagram for a minimal pavilion blow-up of a visible $E_{29,7}(\alpha, \beta) \subset \mathbb{CP}^2$. This is almost toric representation of Figure 16 (c).

Proof. The space \tilde{X} is obtained from a Hirzebruch surface by a sequence of blow-ups, since by Corollary 4.2.10 we can consecutively blow down the -1 -curves contained in the broken rulings until we arrive at a situation in which there are no broken rulings. Then, $\tilde{X} \setminus \mathcal{T}$ is identified with a subset in the complement of a section in a Hirzebruch surface. Since we can always arrange the consecutive blow-downs to happen away from the culet curve, $\tilde{X} \setminus \mathcal{T}$ lives in the normal neighbourhood of a symplectic sphere with positive self-intersection number. Therefore, $\tilde{X} \setminus \mathcal{T}$ is minimal. \square

Remark 5.1.8. It is possible to compute the minimal model that we mentioned in the proof of Corollary 5.1.7: it is diffeomorphic to the Hirzebruch surface \mathbb{F}_w whose negative section has square $-w$. This is diffeomorphic to either $S^2 \times S^2$ (if w is even) or $\mathbb{CP}^2 \# \overline{\mathbb{CP}^2}$ (if w is odd).

In the next few sections, we will show how Corollary 5.1.5 implies the Isotopy and Staircase Theorems 1.4.1 and 1.5.2 from the introduction. In Section 5.4, we will prove Theorem 5.1.1. In Section 5.5, we will modify the proof to handle multiple pin-balls and also give a proof of the Two Pin-Ball Theorem. Finally, in Section 5.6 we will prove Theorem 5.1.4.

5.2 Proof of the Isotopy Theorem (Theorem 1.4.1)

In this section, we explain how Corollary 5.1.5 solves the isotopy problem for pin-ellipsoids in \mathbb{CP}^2 . We begin by stating a further corollary of Corollary 5.1.5.

Corollary 5.2.1. *Let $\iota: E_{p,q}(\alpha, \beta) \hookrightarrow \mathbb{CP}^2$ be a symplectic embedding, let $\boldsymbol{\rho}, \boldsymbol{\lambda}$ be a (possibly non-minimal) choice of pavilion and let \tilde{X} be the pavilion blow-up along ι . Let \mathcal{T} be the tree of symplectic spheres from Definition 5.1.6. Then the complement $\tilde{X} \setminus \mathcal{T}$ is diffeomorphic to a disc bundle over the annulus and the self-intersections and symplectic areas of the spheres in \mathcal{T} depend only on p, q and the choice of pavilion.*

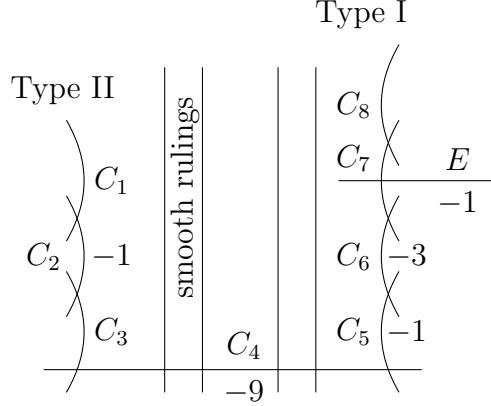


Figure 18: An example illustrating the structure of the regulation for a non-minimal pavilion blow-up, as described in Corollary 5.1.5. This example is obtained from Figure 16(b) by blowing up four times: once where the original broken ruling intersects the culet curve (yielding the Type I broken ruling) and three more times on a general smooth ruling (yielding the Type II broken ruling). Curves are labelled with their name and self-intersection, except vertical straight lines (which represent smooth rulings with square 0) and -2 -spheres whose self-intersection is omitted.

Proof. Since \mathcal{T} consists of a section and two rulings of the regulation on \tilde{X} , including all broken rulings, the restriction of the regulation to $\tilde{X} \setminus \mathcal{T}$ exhibits this complement as a disc bundle over the annulus.

The tree comprises the linear chain $C_1 \cup \dots \cup C_m$ together with some additional curves. These additional curves are of the following types:

- a proper transform of a smooth ruling in the minimal model, coming from a broken ruling of Type II;
- a -1 -curve attached to one of the curves C_i in the chain, coming from a broken ruling of Type I;
- a smooth ruling, if there are fewer than two broken rulings.

The dual graph of the linear chain is determined by the choice of pavilion, as are the positions in the dual graph where the additional curves attach. The symplectic areas of the curves C_i are also determined by the pavilion. Writing the additional curves in the form given by Equation (3.2), we can find the coefficients by computing their intersection numbers with the curves C_i and with a smooth ruling; then their symplectic areas can be computed using the fact that $\int_{\mathcal{E}} \tilde{\omega} = 1/p^2$ and the knowledge of the symplectic areas of the C_i coming from the pavilion. \square

For the rest of this subsection we assume that $\iota, \iota': E_{p,q}(\alpha, \beta) \hookrightarrow \mathbb{CP}^2$ are symplectic embeddings. Let $\boldsymbol{\rho}, \boldsymbol{\lambda}$ be a choice of pavilion for $E_{p,q}(\alpha, \beta)$. As before we denote the

symplectic manifolds obtained by performing the pavilion blow-up along these embeddings by $\tilde{X} = \text{Pav}_{\rho, \lambda}^t(\mathbb{CP}^2)$ and $\tilde{X}' = \text{Pav}_{\rho, \lambda}^{t'}(\mathbb{CP}^2)$.

Corollary 5.2.2. *There exists a symplectomorphism*

$$\Psi: ((\tilde{X}, \omega), \mathcal{T}) \rightarrow ((\tilde{X}', \omega'), \mathcal{T}')$$

which carries the tree \mathcal{T} of symplectic spheres in \tilde{X} coming from Corollary 5.2.1 to the tree \mathcal{T}' of symplectic spheres in \tilde{X}' .

Proof. Since the symplectomorphism type of the trees $\mathcal{T}, \mathcal{T}'$ of symplectic spheres depends only on the pavilion, the symplectic neighbourhood theorem gives symplectic embeddings $\psi: \nu \hookrightarrow \tilde{X}$ and $\psi': \nu \hookrightarrow \tilde{X}'$ of a plumbing ν of symplectic disk bundles over symplectic spheres into both pavilion blow-ups \tilde{X}, \tilde{X}' . Our goal is to extend the symplectomorphism $\psi' \circ \psi^{-1}: \psi(\nu) \rightarrow \psi'(\nu)$ to a symplectomorphism $\Psi: (\tilde{X}, \omega) \rightarrow (\tilde{X}', \omega')$. Recall from Definition 5.1.6 that the trees split as a union $\mathcal{T} = \mathcal{F}_1 \cup C_{i_{\text{culet}}} \cup \mathcal{F}_2$ and $\mathcal{T}' = \mathcal{F}'_1 \cup C'_{i_{\text{culet}}} \cup \mathcal{F}'_2$ of two rulings and the culet curve (a section). By the proof of Corollary 5.1.5, not only the two trees but also these two decompositions are homeomorphic. In particular, $\psi' \circ \psi^{-1}$ takes $C := C_{i_{\text{culet}}}$ to $C' := C'_{i_{\text{culet}}}$.

Step 1: Choice of regulations. Recall that the regulation of \tilde{X} was constructed with respect to an almost complex structure J . Denote the restriction of this almost complex structure to $\psi(\nu)$ by j . Extend $(\psi' \circ \psi^{-1})_* j$ to an almost complex structure J' on \tilde{X}' and consider the regulation of \tilde{X}' associated to J' . Note that $\psi' \circ \psi^{-1}$ takes rulings to rulings in a neighbourhood of \mathcal{F}_1 and \mathcal{F}_2 .

Step 2: Splitting \tilde{X} by splitting C . Since C is a section, the regulation determines a continuous projection map $\pi: \tilde{X} \rightarrow C$ that is smooth away from the rulings $\mathcal{F}_1, \mathcal{F}_2$. Let p_1, p_2 be the images under π of \mathcal{F}_1 and \mathcal{F}_2 . Choose small disjoint embedded closed curves γ_1, γ_2 in C around p_1, p_2 . They decompose C into a closed disc D_1 around p_1 , an annulus A , and a closed disc D_2 around p_2 . Since π is continuous, we can choose the γ_i so close to p_i that both $\pi^{-1}(D_i)$ are contained in $\psi(\nu)$. In this way we obtain a splitting

$$\tilde{X} = \pi^{-1}(D_1) \cup \pi^{-1}(A) \cup \pi^{-1}(D_2).$$

Choosing γ'_i to be the curves $(\psi' \circ \psi^{-1})(\gamma_i)$ in the section C' of \tilde{X}' , we obtain analogous splittings $C' = D'_1 \cup A' \cup D'_2$ and

$$\tilde{X}' = (\pi')^{-1}(D'_1) \cup (\pi')^{-1}(A') \cup (\pi')^{-1}(D'_2).$$

Note that $\psi' \circ \psi^{-1}$ restricts to a fibre-preserving map $\pi^{-1}(D_i) \rightarrow \pi'^{-1}(D'_i)$ and in particular to a fibre-preserving map $\pi^{-1}(\gamma_i) \rightarrow \pi'^{-1}(\gamma'_i)$.

Step 3: A good chart for ω near $\pi^{-1}(\gamma_i)$. Fix $i \in \{1, 2\}$. The S^2 -bundle $\pi: \pi^{-1}(\gamma_i) \rightarrow \gamma_i$ is the trivial S^2 -bundle over the circle γ_i , because the monodromy around γ_i is symplectic and hence preserves the orientation of the fibre. The same argument proves the first of the following two assertions.

- (i) The monodromy of the bundle $\gamma_i \times S^2 \rightarrow \gamma_i$ in $\pi_0(\text{Diff}(S^2))$ is trivial.
- (ii) The symplectic normal bundle $\mathcal{N} \rightarrow \gamma_i \times S^2$ with fibre $\{\theta\} \times (T_q S^2)^{\perp\omega}$ over $(\theta, q) \in \gamma_i \times S^2$ is trivial.

Proof of (ii): If \mathcal{F}_i is a broken ruling we successively blow down the exceptional divisors of the broken ruling $\pi^{-1}(p_i)$ as in § 4.2. The blow-downs are supported away from the wall $\pi^{-1}(\gamma_i)$. Furthermore, the broken ruling $\pi^{-1}(p_i)$ becomes one smooth fibre, and so the regulation over $\pi^{-1}(D_i)$ becomes a trivial symplectic sphere bundle over a disc. This implies assertion (ii).

The following lemma gives a one-sided normal form neighbourhood for the above loops of symplectic spheres.

Lemma 5.2.3. *Consider the closed disc D with symplectic form $\omega_D = dx \wedge dy$, the sphere S^2 with an area form ω_{S^2} whose total area agrees with the ω -area of a smooth fibre of π , and take the product symplectic form $\omega_D \oplus \omega_{S^2}$ on $D \times S^2$. Then there exists a neighbourhood U of $\partial D \times S^2$ in $D \times S^2$ and a diffeomorphism α from U to a neighbourhood of $\pi^{-1}(\gamma_i)$ in $\pi^{-1}(D_i)$ that pulls back ω to $\omega_D \oplus \omega_{S^2}$.*

Proof. The claim would be well-known if we only had to deal with one sphere $\{\theta\} \times S^2$ instead of $\gamma_i \times S^2$. In our case, we use assertions (i) and (ii) above to construct a smooth embedding $\underline{\alpha}: \partial D \times S^2 \rightarrow X$ onto $\pi^{-1}(\gamma_i)$ such that $\underline{\alpha}^*\omega = (\omega_D \oplus \omega_{S^2})|_{T(\partial D \times S^2)}$. The neighbourhood theorem for hypersurfaces from [21] (or also Exercise 3.4.17 in [39]) now implies that $\underline{\alpha}$ extends to the claimed diffeomorphism α on a neighbourhood U . \square

Step 4: Extending $\psi' \circ \psi^{-1}$. We first extend the symplectomorphism

$$\psi' \circ \psi^{-1}: \pi^{-1}(D_1) \cup \nu(C) \cup \pi^{-1}(D_2) \rightarrow \pi^{-1}(D'_1) \cup \nu(C') \cup \pi^{-1}(D'_2)$$

to a diffeomorphism $\Psi_0: \tilde{X} \rightarrow \tilde{X}'$. (This is possible since $\tilde{X} \setminus \mathcal{T}$ and $\tilde{X}' \setminus \mathcal{T}'$ are both disc bundles over an annulus by Corollary 5.2.1. We could assume that Ψ_0 preserves the fibres of π and π' , but this is not needed in the sequel.) We then have the two symplectic forms ω and $\Psi_0^*\omega'$ on \tilde{X} , that agree on $\pi^{-1}(D_1) \cup \nu(C) \cup \pi^{-1}(D_2)$. We are left with showing that there exists a diffeomorphism ρ of \tilde{X} that maps \mathcal{T} to \mathcal{T}' and satisfies $\rho^*\Psi_0^*\omega' = \omega$.

View $S^2 \times S^2$ as $C \times S^2 = (D_1 \cup A \cup D_2) \times S^2$ where C is equipped with the symplectic form pulled back from ω . By Lemma 5.2.3 we can construct two symplectic forms ω_1 and ω_2 on $S^2 \times S^2$ by taking on $A \times S^2$ the forms ω and $\Psi_0^*\omega'$, but taking on $(D_1 \cup D_2) \times S^2$ the split form $\omega_D \times \omega_{S^2}$. By a Moser argument, we can find smaller closed discs $D_i^< \subset D_i$ and a diffeomorphism μ of $S^2 \times S^2$ such that:

- μ is the identity on $(D_1^< \cup D_2^<) \times S^2$,
- μ preserves $C \subset S^2 \times S^2$, and

- $\mu^*\omega_1$ is a split form near C . Since ω_1 and ω_2 coincide near C , this is also true of $\mu^*\omega_2$.

Choose a closed neighbourhood K of C that is contained in this neighbourhood, and choose smaller closed discs $D_i^{\ll} \subset D_i^<$ around p_i . By Theorem 5.2.4 below, there exists a diffeomorphism Φ of $S^2 \times S^2$ that is the identity on $K \cup ((D_1^{\ll} \cup D_2^{\ll}) \times S^2)$ and pulls back $\mu^*\omega_2$ to $\mu^*\omega_1$. We now take the diffeomorphism ρ of \tilde{X} to be $\mu \circ \Phi \circ \mu^{-1}$ on $\tilde{X} \setminus \pi^{-1}(p_1 \cup p_2) = (S^2 \times S^2) \setminus (\{p_1 \cup p_2\} \times S^2)$ and equal to the identity on the broken rulings $\pi^{-1}(p_1 \cup p_2)$. Then $\Psi_0 \circ \rho$ still takes \mathcal{T} to \mathcal{T}' , and it pulls back ω' to ω .

We are left with proving the following improvement of the Gromov–McDuff Theorem [36, Theorem 9.4.7 (ii)].

Theorem 5.2.4. *Let $\omega_{a,b}$ be the usual split symplectic form on $S^2 \times S^2$ that gives the first factor area a and the second factor area b . Represent $(S^2 \times S^2, \omega_{a,b})$ by its moment image as in Figure 19. Let p_N and p_S the North and South poles of S^2 , and consider the three spheres*

$$S_1 = S^2 \times \{p_S\}, \quad S_2^N = \{p_N\} \times S^2, \quad S_2^S = \{p_S\} \times S^2$$

in $S^2 \times S^2$. Let ω be a symplectic form on $S^2 \times S^2$ that agrees with $\omega_{a,b}$ on a neighbourhood of $S_1 \cup S_2^N \cup S_2^S$. Then there exists a symplectomorphism $\Phi: (S^2 \times S^2, \omega_{a,b}) \rightarrow (S^2 \times S^2, \omega)$ that is the identity on a neighbourhood of $S_1 \cup S_2^N \cup S_2^S$.

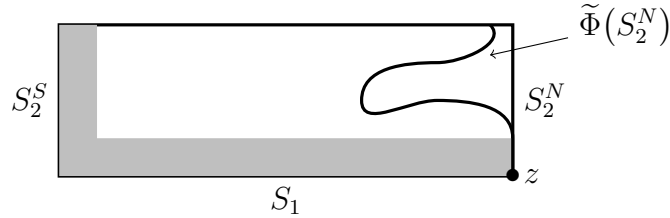


Figure 19: The moment rectangle for the manifold $S^2 \times S^2$, illustrating the proof of Theorem 5.2.4. The symplectomorphism $\tilde{\Phi}$ coming from the Gromov–McDuff Theorem, fixes the shaded region pointwise. We must isotope it to something fixing a neighbourhood of S_2^N by first isotoping $\tilde{\Phi}(S_2^N)$ back to S_2^N , then fixing the symplectic normal bundle of S_2^N , and finally straightening the symplectomorphism in a neighbourhood of S_2^N .

We note that this theorem (and in fact also a stronger version with four spheres taken out) has been proved independently in [14, Lemma 3.1.3].

Proof of Theorem 5.2.4. According to [36, Theorem 9.4.7] there exists a symplectomorphism $\tilde{\Phi}: (S^2 \times S^2, \omega_{a,b}) \rightarrow (S^2 \times S^2, \omega)$ that is the identity on a neighbourhood of $S_1 \cup S_2^S$. Set $z = (p_N, p_S) = S_1 \cap S_2^N$. For $t \in [0, 1]$ choose a smooth path J_t of ω -compatible almost complex structures such that

- (i) S_1 and S_2^S are J_t -holomorphic for all t ,

- (ii) $\tilde{\Phi}(S_2^N)$ is J_0 -holomorphic,
- (iii) S_2^N is J_1 -holomorphic.

Such a path exists since $S_1, S_2^S, S_2^N, \tilde{\Phi}(S_2^N)$ are embedded ω -symplectic spheres and since S_2^S is disjoint from $\tilde{\Phi}(S_2^N)$ and S_1 intersects S_2^N and $\tilde{\Phi}(S_2^N)$ transversely, positively, and only in z .

Let S_2^t be the unique J_t -holomorphic sphere in class $A := [S_2^N] \in H_2(S^2 \times S^2; \mathbb{Z})$ passing through z . This exists because $A^2 = 0$ so the Gromov–Taubes invariant counting holomorphic spheres in this class with a single point constraint is equal to 1 and curves in this class cannot bubble, S_2^S being J_t -holomorphic.¹⁴

The spheres S_2^t depend smoothly on t , because the path J_t is smooth in t and each S_2^t is automatically regular (being a square zero sphere). Now $\{S_2^t\}$ is a smooth path of embedded ω -symplectic spheres such that $S_2^0 = \tilde{\Phi}(S_2^N)$ and $S_2^1 = S_2^N$. By (i), each sphere S_2^t intersects S_1 transversally at z and is disjoint from S_2^S . We can therefore modify the path $\{S_2^t\}$ near z such that all S_2^t coincide with S_2^N near z , and such that the S_2^t are still disjoint from S_2^S and intersect S_1 only in z .

By [44, Proposition 0.3] or [40, Lemma 5.16] there exists a Hamiltonian isotopy φ^t of $(S^2 \times S^2, \omega)$ whose support is contained in any given neighbourhood of $\bigcup_{t \in [0,1]} S_2^t$ such that $\varphi^t(S_2^0) = S_2^t$. In particular, we can assume that the support of φ^t is disjoint from S_2^S . Since the S_2^t already agree near z , we can also assume that the support is disjoint from S_1 . Hence $\varphi^1 \circ \tilde{\Phi}$ is still the identity near $S_1 \cup S_2^S$ and takes S_2^N to itself. Let σ be the restriction of $\varphi^1 \circ \tilde{\Phi}$ to S_2^N . Since σ fixes a neighbourhood of z , it is the time-1 map of a Hamiltonian isotopy σ^t of S_2^N that fixes a neighbourhood of z . Extend σ^t to a Hamiltonian isotopy $\hat{\sigma}_t$ of $(S^2 \times S^2, \omega)$ that has support near S_2^N and is the identity near z . Then $\hat{\Phi} := \hat{\sigma}_1^{-1} \circ \varphi^1 \circ \tilde{\Phi}$ is a symplectomorphism $(S^2 \times S^2, \omega_{a,b}) \rightarrow (S^2 \times S^2, \omega)$ that is the identity near $S_2^S \cup S_1$ and is the identity along S_2^N .

The differential of $\hat{\Phi}$ at a point $p \in S_2^N$ with respect to the symplectic splitting of $T_p(S^2 \times S^2)$ is of the form

$$d_p \hat{\Phi} = \begin{pmatrix} \text{id}_2 & B \\ 0_2 & D \end{pmatrix} : T_p S_2^N \oplus (T_p S_2^N)^\omega \rightarrow T_p S_2^N \oplus (T_p S_2^N)^\omega.$$

Since $d_p \hat{\Phi}$ is symplectic, it leaves $(T_p S_2^N)^\omega$ invariant. Hence $B = 0_2$ and D is symplectic. The space $\text{Symp}(2; \mathbb{R})$ deformation retracts onto $U(1) = S^1$. Since the space of pointed maps from the 2-sphere to the circle is connected, we can isotopy $d\hat{\Phi}|_{S_2^N}$ at the bundle level to the identity along S_2^N . Using Moser's method as in the proof of the symplectic

¹⁴This is because a J_t -holomorphic bubble curve will necessarily remain disjoint from S_2^S , because z is not contained in S_2^S and by positivity of intersection, and must therefore live in a homology class which is a positive multiple of A . But the area cannot be larger than that of S_2^N , so there can be only one irreducible component.

neighbourhood theorem, we can then find a symplectic isotopy from $\widehat{\Phi}$ to the identity *near* S_2^N . Since the tubular neighbourhood of S_2^N has trivial first homology, we can make this isotopy Hamiltonian. We finally multiply the Hamiltonian function H_t , that we may choose to vanish near z , with a function χ that is 1 on a small tubular neighbourhood of S_2^N and vanishes outside a slightly larger tubular neighbourhood. The composition $\Phi := \phi_{\chi H} \circ \widehat{\Phi}$ is then a symplectomorphism $(S^2 \times S^2, \omega_{a,b}) \rightarrow (S^2 \times S^2, \omega)$ that is the identity *near* S_2^N . The proof of Theorem 5.2.4 is complete. \square

We are now ready to prove Theorem 1.4.1, that we restate as:

Corollary 5.2.5 (Hamiltonian uniqueness of pin-ellipsoids). *Given two symplectic embeddings $\iota, \iota': E_{p,q}(\alpha, \beta) \hookrightarrow \mathbb{CP}^2$ there exists a Hamiltonian diffeomorphism Φ of \mathbb{CP}^2 such that $\iota = \Phi \circ \iota'$.*

Proof. We first give the idea of the proof. Two embeddings ι, ι' as in the corollary yield splittings of \mathbb{CP}^2 , namely

$$\mathbb{CP}^2 = (\mathbb{CP}^2 \setminus U) \cup U$$

for $U = \iota(E_{p,q}(\alpha, \beta))$, and analogously for ι' . By Corollary 5.2.2 the two complements can be symplectically identified, and the embedded ellipsoids are trivially symplectically identified through the embeddings. We will adjust the first identification near the boundaries so that it agrees with the second one, and hence obtain a symplectomorphism Φ of $(\mathbb{CP}^2, \omega_{\text{FS}})$ that intertwines the ellipsoid embeddings. This symplectomorphism is Hamiltonian thanks to Gromov's result from [22] that the symplectomorphism group of $(\mathbb{CP}^2, \omega_{\text{FS}})$ is connected.

We now come to the actual proof. By definition of “symplectic embedding”, there exist $\hat{\alpha} > \alpha$, $\hat{\beta} > \beta$ such that the maps ι, ι' are restrictions of symplectic embeddings

$$\hat{\iota}, \hat{\iota}': E_{p,q}(\hat{\alpha}, \hat{\beta}) \hookrightarrow \mathbb{CP}^2.$$

Choose the almost toric offcut $\text{Off}_{\rho, \lambda}(E_{p,q}(\hat{\alpha}, \hat{\beta}))$ such that

$$E_{p,q}(\alpha, \beta) \subset \text{Off}_{\rho, \lambda}(E_{p,q}(\hat{\alpha}, \hat{\beta})) \subset E_{p,q}(\hat{\alpha}, \hat{\beta})$$

and such that $\overline{\text{Off}}_{\rho, \lambda}(E_{p,q}(\hat{\alpha}, \hat{\beta})) \subset \text{Int}(E_{p,q}(\hat{\alpha}, \hat{\beta}))$.¹⁵ Doing the pavilion blow-up, as introduced in Definition 3.1.5, we obtain two closed symplectic manifolds, which we denote by $(\tilde{X}, \tilde{\omega})$ and $(\tilde{X}', \tilde{\omega}')$. Denote by \mathcal{C}_{vis} the linear chain of symplectic spheres in the pavilion blow-up $\text{Pav}_{\rho, \lambda}(E_{p,q}(\hat{\alpha}, \hat{\beta}))$, and let $\mathcal{N}(\mathcal{C}_{\text{vis}})$ be a neighbourhood of \mathcal{C}_{vis} in $\text{Pav}_{\rho, \lambda}(E_{p,q}(\hat{\alpha}, \hat{\beta}))$.¹⁶

¹⁵Even though the edges of the offcut have rational slopes, we can clearly choose ρ, λ such that the offcut has these properties.

¹⁶The chain of spheres \mathcal{C}_{vis} is visible in the almost toric diagram as in Figure 10 (b). The combinatorial data of \mathcal{C}_{vis} is exactly that of \mathcal{T} and \mathcal{T}' , except that \mathcal{T} and \mathcal{T}' may in addition contain one or two (-1) -spheres, depending on the Manetti weight. Recall that these (-1) -spheres stem from the “ambient” topology of \mathbb{CP}^2 and are not contained in the linear chain corresponding to the choice of pavilion. Therefore, the “interface” between the embeddings of the pin-ellipsoids and the symplectomorphism of their complements will exactly be \mathcal{C}_{vis} .

In the following we denote the linear subchains of \mathcal{T} and \mathcal{T}' corresponding to \mathcal{C}_{vis} by \mathcal{C} and \mathcal{C}' . Trivially, the complements of the trees \mathcal{T} and \mathcal{T}' of symplectic spheres in these pavilion blow-ups are identified with the complement of the offcuts “downstairs” in \mathbb{CP}^2 . We write

$$j: \mathbb{CP}^2 \setminus \hat{i}(\overline{\text{Off}}_{\rho, \lambda}(E_{p,q}(\hat{\alpha}, \hat{\beta}))) \rightarrow (\tilde{X} \setminus \mathcal{C}, \tilde{\omega})$$

and analogously j' for these identifications. By Corollary 5.2.2, there exists a symplectomorphism $\psi: (\tilde{X}', \tilde{\omega}') \rightarrow (\tilde{X}, \tilde{\omega})$ that takes \mathcal{T}' to \mathcal{T} . In particular, ψ takes \mathcal{C} to \mathcal{C}' . Now consider the diagram of symplectic maps shown in Figure 20. Since the embedding \hat{i} is defined on all of $E_{p,q}(\hat{\alpha}, \hat{\beta})$, the embedding

$$j \circ \hat{i}: \mathcal{N}(\mathcal{C}_{\text{vis}}) \setminus \mathcal{C}_{\text{vis}} \hookrightarrow \tilde{X}$$

uniquely extends to a smooth embedding $\sigma: \mathcal{N}(\mathcal{C}_{\text{vis}}) \hookrightarrow \tilde{X}$. Since $j \circ \hat{i}$ is symplectic, σ is also symplectic, and $\sigma(\mathcal{C}_{\text{vis}}) = \mathcal{C}$. Using in addition that ψ is a symplectomorphism \mathcal{C}' to \mathcal{C} , we see in the same way that

$$\psi \circ j' \circ \hat{i}': \mathcal{N}(\mathcal{C}_{\text{vis}}) \setminus \mathcal{C}_{\text{vis}} \hookrightarrow \tilde{X} \quad (5.1)$$

extends to a symplectic embedding $\sigma': \mathcal{N}(\mathcal{C}_{\text{vis}}) \hookrightarrow \tilde{X}$ that also takes \mathcal{C}_{vis} to \mathcal{C} .

$$\begin{array}{ccc}
((\tilde{X}', \tilde{\omega}'), \mathcal{C}') & \xrightarrow{\psi} & ((\tilde{X}, \tilde{\omega}), \mathcal{C}) \\
\uparrow j' & & \uparrow j \\
\mathbb{CP}^2 \setminus \hat{i}'(\overline{\text{Off}}_{\rho, \lambda}(E_{p,q}(\hat{\alpha}, \hat{\beta}))) & & \mathbb{CP}^2 \setminus \hat{i}(\overline{\text{Off}}_{\rho, \lambda}(E_{p,q}(\hat{\alpha}, \hat{\beta}))) \\
\cap & & \cap \\
\mathbb{CP}^2 & & \mathbb{CP}^2 \\
\cup & & \cup \\
\hat{i}'(E_{p,q}(\hat{\alpha}, \hat{\beta})) & & \hat{i}(E_{p,q}(\hat{\alpha}, \hat{\beta})) \\
& \nwarrow \hat{i}' \quad \nearrow \hat{i} & \\
& E_{p,q}(\hat{\alpha}, \hat{\beta}) &
\end{array}$$

Figure 20: The diagram of symplectic maps used in the proof of Corollary 5.2.5.

Lemma 5.2.6. *There exists a compactly supported Hamiltonian diffeomorphism h of a neighbourhood $\mathcal{N}(\mathcal{C})$ such that near \mathcal{C} ,*

$$h \circ \sigma' = \sigma. \quad (5.2)$$

Proof. Set $\tau = \sigma \circ (\sigma')^{-1}|_{\mathcal{C}}$. Then $\tau(C_j) = C_j$ for all spheres C_j in \mathcal{C} , and τ fixes the transverse intersection points $C_j \cap C_{j+1}$. The group of orientation preserving diffeomorphisms of

a sphere that fix one or two points is connected. We therefore find a smooth path τ_t from $\text{id}_{\mathcal{C}}$ to τ . By Moser's deformation argument, we can assume that the τ_t are symplectic. Using Weinstein's symplectic neighbourhood theorem, we can extend τ_t to a smooth path of symplectic embeddings $\hat{\tau}_t: \mathcal{N}_t \rightarrow \mathcal{N}(\mathcal{C})$ of tubular neighbourhoods \mathcal{N}_t of \mathcal{C} that starts at the inclusion. Since $H_1(\mathcal{N}_t) = 0$, this path is generated by a Hamiltonian vector field. Multiplying the Hamiltonian function by a cut-off function that is 1 near \mathcal{C} and 0 outside a small neighbourhood of \mathcal{C} , we obtain a Hamiltonian diffeomorphism h supported near \mathcal{T} that agrees with $\sigma \circ (\sigma')^{-1}$ near \mathcal{C} . \square

In view of Equations (5.1) and (5.2) we can define the symplectomorphism $\Phi \in \text{Symp}(\mathbb{CP}^2, \omega_{\text{FS}})$ by

$$\mathbb{CP}^2 \setminus \hat{\iota}'(\overline{\text{Off}}_{\rho, \lambda}(E_{p,q}(\hat{\alpha}, \hat{\beta}))) \xrightarrow{j^{-1} \circ h \circ \psi \circ j'} \mathbb{CP}^2 \setminus \hat{\iota}(\overline{\text{Off}}_{\rho, \lambda}(E_{p,q}(\hat{\alpha}, \hat{\beta})))$$

and

$$\hat{\iota}'(\mathcal{N}) \xrightarrow{\hat{\iota} \circ (\hat{\iota}')^{-1}} \hat{\iota}(\mathcal{N}),$$

where \mathcal{N} is a sufficiently small neighbourhood of $\overline{\text{Off}}_{\rho, \lambda}(E_{p,q}(\hat{\alpha}, \hat{\beta}))$ in $E_{p,q}(\hat{\alpha}, \hat{\beta})$. By Lemma 5.2.6 this symplectomorphism is well-defined. Due to Gromov's theorem from [22] that $\text{Symp}(\mathbb{CP}^2, \omega_{\text{FS}})$ is connected, Φ is a Hamiltonian diffeomorphism, and hence the map we were looking for. \square

5.3 Proof of the Staircase Theorem (Theorem 1.5.2)

In this section, we will use Corollary 5.2.5 to prove the Staircase Theorem, which we restate in the following form:

Theorem 5.3.1 (Markov staircases). *Let (p_1, p_2, p_3) be a Markov triple with $q_1 := 3p_2p_3^{-1} \bmod p_1$ and let $(p'_1, p'_2, p'_3) = (p_1, p_3, 3p_3p_1 - p_2)$ be its mutation at p_2 . There is no symplectic embedding $E_{p_1, q_1}(\alpha, \beta) \hookrightarrow \mathbb{CP}^2$ if both $\alpha > \frac{p_3}{p_1p_2}$ and $\beta > \frac{p'_2}{p'_3p'_1}$.*

Fix the triple (p_1, p_2, p_3) , companion q_1 and mutant triple p'_1, p'_2, p'_3 as in the statement of Theorem 5.3.1. Consider the Vianna triangles $\mathfrak{D}(p_1, p_2, p_3)$ and $\mathfrak{D}(p'_1, p'_2, p'_3)$ whose edges \mathfrak{e}_i and \mathfrak{e}'_i have affine integral lengths

$$\begin{aligned} |\mathfrak{e}_1| &= \frac{p_1}{p_2p_3} & |\mathfrak{e}_2| &= \frac{p_2}{p_3p_1} & |\mathfrak{e}_3| &= \frac{p_3}{p_1p_2} \\ |\mathfrak{e}'_1| &= \frac{p'_1}{p'_2p'_3} & |\mathfrak{e}'_2| &= \frac{p'_2}{p'_3p'_1} & |\mathfrak{e}'_3| &= \frac{p'_3}{p'_1p'_2}. \end{aligned}$$

It suffices to show that if $E_{p_1, q_1}(\alpha, \beta)$ admits a symplectic embedding and $\alpha > |\mathfrak{e}_3|$ then $\beta \leq |\mathfrak{e}'_2|$. If we draw the two Vianna triangles $\mathfrak{D}(p_1, p_2, p_3)$ and $\mathfrak{D}(p'_1, p'_2, p'_3)$ superimposed then we can see they both contain $\mathfrak{A}_{p_1, q_1}(|\mathfrak{e}_3|, |\mathfrak{e}'_2|)$ (Figure 21).

Lemma 5.3.2. *Consider the triangle $\mathfrak{A}_{p_1, q_1}(|\mathfrak{e}_3|, |\mathfrak{e}'_2|)$ and recall that its girdle is the top side.*

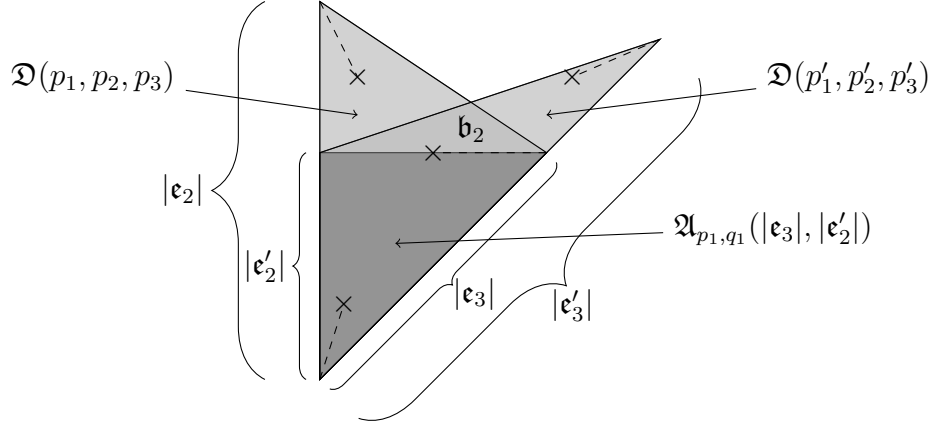


Figure 21: The Vianna triangles $\mathfrak{D}(p_1, p_2, p_3)$ and $\mathfrak{D}(p'_1, p'_2, p'_3)$ superimposed. The dark shaded region is a copy of $\mathfrak{A}_{p_1, q_1}(|\mathfrak{e}_3|, |\mathfrak{e}'_2|)$ in their intersection.

- (a) The primitive integer vector pointing along the girdle is $\begin{pmatrix} p'_3 \\ (p'_3 q_1 - 3p'_2)/p_1 \end{pmatrix}$.
- (b) The affine length of the girdle is equal to $\frac{p_1 p_3}{p_2 p'_3}$.
- (c) The affine displacement between the girdle and the vertex \mathbf{v}_1 is equal to p_3/p_1 .

Proof. The vertices of $\mathfrak{A}_{p, q}(|\mathfrak{e}_3|, |\mathfrak{e}'_2|)$ are at

$$\begin{pmatrix} 0 \\ 0 \end{pmatrix}, \quad |\mathfrak{e}_3| \begin{pmatrix} p_1^2 \\ p_1 q_1 - 1 \end{pmatrix}, \quad \begin{pmatrix} 0 \\ |\mathfrak{e}'_2| \end{pmatrix},$$

so the vector pointing along the girdle is

$$\begin{pmatrix} |\mathfrak{e}_3| p_1^2 \\ |\mathfrak{e}_3| p_1 q_1 - |\mathfrak{e}_3| - |\mathfrak{e}'_2| \end{pmatrix} = \frac{p_3}{p_1 p_2 p'_3} \begin{pmatrix} p'_3 p_1^2 \\ p'_3 p_1 q_1 - p'_3 - p_2 \end{pmatrix} = \frac{p_3}{p_2 p'_3} \begin{pmatrix} p'_3 p_1 \\ p'_3 q_1 - 3p_3 \end{pmatrix},$$

where we used the facts that $p'_1 = p_1$, $p'_2 = p_3$ and $p'_3 + p_2 = 3p_1 p_3$.

Since no Markov number is divisible by 3, and since the numbers in a Markov triple are always pairwise coprime, $\gcd(p'_3, p'_3 q_1 - 3p_3) = \gcd(3p_1 p_3 - p_2, 3p_3) = \gcd(p_2, p_3) = 1$.

We also have $\gcd(p_1, p'_3 q_1 - 3p_3) = \gcd(p_1, (3p_1 p_3 - p_2) q_1 - 3p_3) = \gcd(p_1, p_2 q_1 + 3p_3) = p_1$ since¹⁷ $q_1 = 3p_2 p_3^{-1} = -3p_3 p_2^{-1} \pmod{p_1}$. Therefore the vector along the girdle is

$$\frac{p_1 p_3}{p_2 p'_3} \begin{pmatrix} p'_3 \\ (p'_3 q_1 - 3p_3)/p_1 \end{pmatrix}$$

¹⁷Note that $p_2^2 + p_3^2 = 3p_1 p_2 p_3 - p_1^2 = 0 \pmod{p_1}$ so $p_2 p_3^{-1} = -p_3 p_2^{-1} \pmod{p_1}$.

where $\frac{p_1 p_3}{p_2 p'_3}$ is the integral affine length and $u := \begin{pmatrix} p'_3 \\ (p'_3 q_1 - 3p_3)/p_1 \end{pmatrix}$ is a primitive integer vector. The affine displacement between the girdle and the vertex at the origin is therefore

$$u^\perp \cdot \begin{pmatrix} 0 \\ |\mathfrak{e}'_2| \end{pmatrix} = \begin{pmatrix} -(p'_3 q_1 - 3p_3)/p_1 \\ p'_3 \end{pmatrix} \cdot \begin{pmatrix} 0 \\ p_3/(p_1 p'_3) \end{pmatrix} = p_3/p_1. \quad \square$$

Lemma 5.3.3. *If $\alpha > |\mathfrak{e}_3|$ and $\beta > |\mathfrak{e}'_2|$ then there exists a Delzant pavilion for $E_{p_1, q_1}(\alpha, \beta)$ (which introduces new edges $\mathfrak{f}_1, \dots, \mathfrak{f}_m$ with inward normals $\boldsymbol{\rho} = (\rho_1, \dots, \rho_m)$ corresponding to curves C_1, \dots, C_m) and an index i such that:*

- (a) *the edge \mathfrak{f}_i is parallel to the branch cut \mathfrak{b}_2 in the Vianna triangle $\mathfrak{D}(p_1, p_2, p_3)$;*
- (b) $\int_{C_i} \tilde{\omega} > \frac{p_1 p_3}{p_2 p'_3}$;
- (c) *if we define*

$$b_i = -C_i^2, \quad e_i/e_{i-1} = [b_{i-1}, \dots, b_1] \text{ and } f_i/f_{i+1} = [b_{i+1}, \dots, b_m]$$

then $e_i = p'_3$ and $f_i = p_2$.

Proof. The fact that $\alpha > |\mathfrak{e}_3|$ and $\beta > |\mathfrak{e}'_2|$ means that the almost toric base diagram $\mathfrak{A}_{p_1, q_1}(|\mathfrak{e}_3|, |\mathfrak{e}'_2|)$ is strictly contained in $\mathfrak{A}_{p_1, q_1}(\alpha, \beta)$. The top side of this subdiagram is precisely where the branch cut \mathfrak{b}_2 would run in the Vianna triangle $\mathfrak{D}(p_1, p_2, p_3)$ (see Figure 21). Since the containment of the subdiagram is strict, this means that we can make a pavilion cut parallel to \mathfrak{b}_2 just above this top side (with further very small cuts near the ends of this side to ensure the pavilion is Delzant). The symplectic area of the corresponding curve C_i is given by the affine length of the side. Since our cut is slightly above the top side of $\mathfrak{A}_{p_1, q_1}(|\mathfrak{e}_3|, |\mathfrak{e}'_2|)$ (whose affine length is $\frac{p_1 p_3}{p_2 p'_3}$ by Lemma 5.3.2) and since we can take our remaining cuts to be arbitrarily small, we can ensure that $\int_{C_i} \tilde{\omega} > \frac{p_1 p_3}{p_2 p'_3}$.

Finally, since the integer vector along the girdle is $\begin{pmatrix} p'_3 \\ (p'_3 q_1 - 3p_3)/p_1 \end{pmatrix}$, we can compute e_i and f_i as

$$\begin{aligned} e_i &= \begin{pmatrix} p'_3 \\ (p'_3 q_1 - 3p_3)/p_1 \end{pmatrix} \wedge \begin{pmatrix} 0 \\ 1 \end{pmatrix} = p'_3, \\ f_i &= \begin{pmatrix} p'_3 \\ (p'_3 q_1 - 3p_3)/p_1 \end{pmatrix} \wedge \begin{pmatrix} p_1^2 \\ p_1 q_1 - 1 \end{pmatrix} \\ &= p'_3(p_1 q_1 - 1) - p_1(p'_3 q_1 - 3p_3) = 3p_3 p_1 - p'_3 = p_2. \end{aligned} \quad \square$$

We now complete the proof. Let $\boldsymbol{\rho}$ be the normal vectors and $\boldsymbol{\lambda}$ the choice of constants giving the pavilion from Lemma 5.3.3. Let $\boldsymbol{\lambda}_t = (t\lambda_1, \dots, t\lambda_m)$ for $t \in [0, 1]$ and consider the family of pavilion cuts $(\text{Pav}'_{\boldsymbol{\rho}, \boldsymbol{\lambda}_t}(\mathbb{CP}^2), \tilde{\omega}_t)$. When t is sufficiently small, there is a

visible symplectic embedding $\iota_{\text{vis}}: \text{Off}_{\rho, \lambda_t}(E_{p,q}(\alpha, \beta)) \hookrightarrow \mathbb{CP}^2$ given by the neighbourhood of a vertex of a Vianna triangle. By Corollary 5.2.5, the restriction

$$\iota|_{\text{Off}_{\rho, \lambda_t}(E_{p,q}(\alpha, \beta))}: \text{Off}_{\rho, \lambda_t}(E_{p,q}(\alpha, \beta)) \hookrightarrow \mathbb{CP}^2$$

is Hamiltonian isotopic to ι_{vis} , so $\text{Pav}_{\rho, \lambda_t}^t(\mathbb{CP}^2)$ is symplectomorphic to $\text{Pav}_{\rho, \lambda_t}^{\iota_{\text{vis}}}(\mathbb{CP}^2)$. In the pavilion blow-up $\text{Pav}_{\rho, \lambda_t}^{\iota_{\text{vis}}}(\mathbb{CP}^2)$ along the visible offcut, there is a visible symplectic -1 -sphere S_t , living over an arc in the almost toric base diagram which connects the node coming out of v_2 to the edge \mathbf{f}_i corresponding to C_i . This is because \mathbf{f}_i is parallel to \mathbf{b}_2 ; see [16, Example 9.1 and Figure 9.1] and Figure 22.

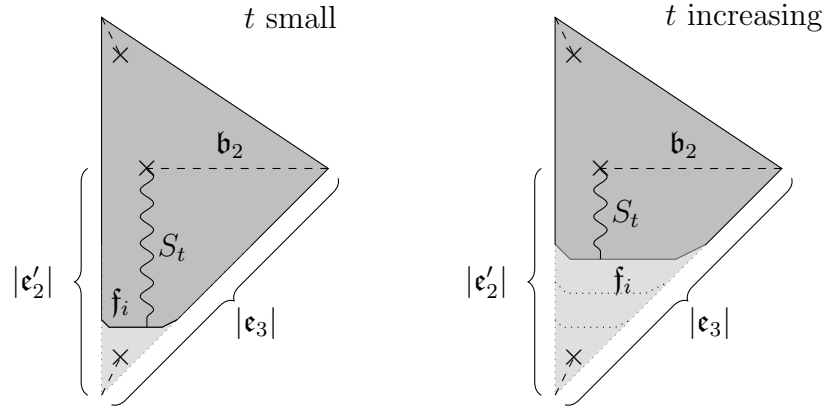


Figure 22: The pavilion blow-up $\text{Pav}_{\rho, \lambda_t}^{\iota_{\text{vis}}}(\mathbb{CP}^2)$ along a visible $E_{p,q}(\alpha, \beta)$ in \mathbb{CP}^2 for two different values of t . The visible sphere S_t lives over an arc connecting a node to the edge \mathbf{f}_i . As t increases, the pavilion cuts move upwards and the symplectic area of S gets smaller. If $\alpha > |\mathbf{e}_3|$ and $\beta > |\mathbf{e}'_2|$, we could push \mathbf{f}_i up above the branch cut \mathbf{b}_2 and S_t would end up with negative area.

This symplectic sphere S_t intersects C_i and none of the other curves C_j . As in Equation (3.2), we can write

$$[S_t] = s_0 \mathcal{E} + \sum_{j=1}^m s_j [C_j] \in H_2(\text{Pav}_{\rho, \lambda_t}^t(\mathbb{CP}^2); \mathbb{Q})$$

and $\sigma_j := [S_t] \cdot [C_j]$, so $\boldsymbol{\sigma} = (\sigma_1, \dots, \sigma_m) = (0, \dots, 0, 1, 0, \dots, 0)$ with the 1 in the i th place. Since S_t is a symplectic -1 -sphere, the spherical Gromov–Taubes invariant $\text{Gr}([S_t])$ counting holomorphic spheres in $\text{Pav}_{\rho, \lambda_t}^t(\mathbb{CP}^2)$ in the class $[S_t]$ is equal to 1, see for instance [34, Proposition 4.1]. Since Gromov–Taubes invariants are deformation invariant, there is still a holomorphic sphere in this homology class for $\text{Pav}_{\rho, \lambda_1}^t(\mathbb{CP}^2)$. This means that

$$0 < \int_{[S_1]} \tilde{\omega}_1 = s_0 \int_{\mathcal{E}} \tilde{\omega}_1 + \sum_{j=1}^m s_j \int_{C_j} \tilde{\omega}_1.$$

Since $\mathbf{s} = M^{-1}\boldsymbol{\sigma}$, and since by Lemma 3.2.4 the entries of M^{-1} are all negative, we get

$$0 < s_0 \int_{\mathcal{E}} \tilde{\omega}_1 + s_i \int_{C_i} \tilde{\omega}_1.$$

Recall from Remark 3.2.5 that $p_1^2 \mathcal{E}$ can be represented by a cycle in V (the complement of our embedding). Hence $s_0 \int_{\mathcal{E}} \tilde{\omega}_t$ is constant in t ; in particular, it is equal to the limit of the areas of the visible $\tilde{\omega}_t$ -symplectic spheres S_t as $t \rightarrow 0$; by [48, Proposition 7.8], this equals the affine displacement $\frac{p_3}{p_1}$ between the girdle and the bottom vertex computed in Lemma 5.3.2(c). Therefore,

$$0 < \frac{p_3}{p_1} + s_i \int_{C_i} \tilde{\omega}_1.$$

By Lemma 5.3.3(b), this tells us that

$$-s_i \frac{p_1 p_3}{p_2 p'_3} < \frac{p_3}{p_1}.$$

But $s_i = M_{ii}^{-1} = -\frac{e_i f_i}{p_1^2} = -\frac{p_2 p'_3}{p_1^2}$ by Lemma 3.2.4 and Lemma 5.3.3(c), so we get

$$\frac{p_3}{p_1} < \frac{p_3}{p_1},$$

which is a contradiction. This shows that we cannot have both $\alpha > \frac{p_3}{p_1 p_2}$ and $\beta > \frac{p'_2}{p'_3 p'_1}$, as required.

5.4 Proof of Theorem 5.1.1 (Evans–Smith *sans* orbifolds)

Recall the notation from Definitions 3.1.4–3.1.5: given a symplectic embedding

$$\iota: E_{p,q}(\alpha, \beta) \hookrightarrow X := \mathbb{CP}^2,$$

we let $U = \iota(E_{p,q}(\alpha, \beta))$, let $V = X \setminus U$, and let \bar{U} and \bar{V} be the symplectic completions of U and V ; we also write $\Sigma = \partial U$. We pick a neck-stretching sequence of almost complex structures J_t as in Definition 3.1.4.

Lemma 5.4.1. *For each t , pick a J_t -holomorphic line L_t in the class $H \in H_2(\mathbb{CP}^2; \mathbb{Z})$. As $t \rightarrow \infty$, there is a subsequence $t_i \rightarrow \infty$ such that the sequence L_{t_i} converges (in the sense of Gromov–Hofer convergence [8, Section 9.1]) to a holomorphic limit building with a nonempty component in \bar{U} and a nonempty component in \bar{V} (and potentially components in intermediate symplectisation levels).*

Proof. Convergence to a limit building is the content of the SFT compactness theorem [8, 12]. There must be a component in \bar{V} because \bar{U} is exact and therefore unable to contain a closed holomorphic curve. There must be components in \bar{U} because the anticanonical bundle of X restricted to the complement of a line can be trivialised, whilst the first Chern class of \bar{U} is nontrivial (though it is torsion; see [17, Lemma 2.13]). \square

Let C be one of the components of the SFT limit curve living in \bar{V} . Fix a minimal Delzant pavilion $\boldsymbol{\rho}, \boldsymbol{\lambda}$, let \tilde{X} be the pavilion blow-up and let $\tilde{U} \subset \tilde{X}$ be the girdled resolution with complement V . Let \tilde{C} be the corresponding closed curve in \tilde{X} given by Lemma 3.1.7. Our strategy will be to carefully analyse the adjunction formula for \tilde{C} , using the discrepancies of the singularity to compute $K \cdot \tilde{C}$ where $K = -\text{PD}(c_1(\tilde{X}))$ is the canonical class.

For that purpose, we write $K_{\mathbb{Q}}$ and $\tilde{C}_{\mathbb{Q}}$, as in Equation (3.2), in the form

$$K_{\mathbb{Q}} = -3p\mathcal{E} + \sum k_i C_i, \quad \tilde{C}_{\mathbb{Q}} = c_0\mathcal{E} + \sum c_i C_i.$$

The coefficient of \mathcal{E} in $K_{\mathbb{Q}}$ comes from the facts that $K_{\mathbb{CP}^2} = -3H$ and $H = p\mathcal{E}$. The numbers k_i are called the discrepancies of the singularity and can be computed to be $k_i = -1 + \frac{e_i + f_i}{p^2}$, see [24, Section 2.1]. Here, e_i and f_i are defined as in Lemma 3.2.4. Note that these all lie in the interval $(-1, 0)$ since we have taken the minimal resolution; if we had taken a non-minimal resolution then some of the discrepancies would have been positive.

Lemma 5.4.2. *We have $0 < c_0 \leq p$.*

Proof. The symplectic form on \bar{V} extends to a closed 2-form ϖ on \tilde{X} which vanishes on $\bigcup_{i=1}^m C_i$ (this is essentially the form on the pavilion blow-up with $\boldsymbol{\lambda} = \mathbf{0}$). The integral $\int_{\tilde{C}} \varpi$ agrees with the symplectic area of $C \subset \bar{V}$, which is bounded above by the symplectic area of a line in \mathbb{CP}^2 (which we are normalising to be 1). We have $\int_{\tilde{C}} \varpi = c_0/p$ since the symplectic area of the line (which is homologous to $p\mathcal{E}$) is 1. Note that ϖ is non-negative on \tilde{J} -complex lines in tangent spaces and vanishes only on points of $\bigcup_{i=1}^m C_i$, so $c_0/p = \int_{\tilde{C}} \varpi > 0$. \square

Proposition 5.4.3. *The curve \tilde{C} is an embedded sphere of self-intersection $\tilde{C}^2 \leq 0$.*

Proof. The curve \tilde{C} has arithmetic genus zero (since we obtained it by stretching a holomorphic sphere). The adjunction formula for \tilde{C} is

$$\sum_{x \in \text{Sing}(\tilde{C})} \delta_x = \frac{\tilde{C}^2 + K \cdot \tilde{C}}{2} + 1$$

where δ_x is the multiplicity of the singular point $x \in \tilde{C}$. We have:

$$\begin{aligned} \tilde{C}^2 &= c_0^2/p^2 + \left(\sum_{i=1}^m c_i C_i \right)^2 \\ \tilde{C} \cdot K &= \frac{-3c_0}{p} + \sum_{i=1}^m \chi_i k_i, \end{aligned}$$

where $\chi_i = \tilde{C} \cdot C_i$. Since the intersection matrix $M_{ij} = C_i \cdot C_j$ is negative definite, $(\sum_{i=1}^m c_i C_i)^2 \leq 0$. By positivity of intersections, $\chi_i = \tilde{C} \cdot C_i \geq 0$ for all i , so negativity of the discrepancies implies $\sum_{i=1}^m \chi_i k_i \leq 0$. Therefore the adjunction formula becomes

$$\sum_{x \in \text{Sing}(\tilde{C})} \delta_x \leq \frac{c_0^2 - 3pc_0}{2p^2} + 1.$$

Since c_0 satisfies $0 < c_0 \leq p$ by Lemma 5.4.2, we find that $c_0^2 - 3pc_0$ is strictly negative. Since the numbers δ_x are positive integers, we deduce that $\text{Sing}(\tilde{C}) = \emptyset$. This shows that \tilde{C} is an embedded sphere.

The self-intersection of \tilde{C} is $c_0^2/p^2 + (\sum_{i=1}^m c_i C_i)^2$. Since M_{ij} is negative definite, and since $c_0 \leq p$, this is ≤ 1 . Therefore $\tilde{C}^2 \leq 1$ and $\tilde{C}^2 \leq 0$ unless $c_0 = p$ and $\mathbf{c} = 0$. In the latter case, \tilde{C} would be homologous to H . The following shows that this is impossible. Recall that $U = \iota(E_{p,q}(\alpha, \beta))$ deformation-retracts onto a CW complex called a pin-wheel, which has a fundamental class in homology with coefficients in \mathbb{Z}_ℓ for any prime ℓ dividing p (note that, despite the name, p is not assumed to be prime). The pin-wheel has nonzero self-intersection, so the fundamental class of this pin-wheel has nonzero \mathbb{Z}_ℓ intersection number with a line (which generates \mathbb{Z}_ℓ -homology). This shows that \tilde{C} cannot be both homologous to H and disjoint from $\bigcup_{i=1}^m C_i$, which concludes the proof that $\tilde{C}^2 \leq 0$. \square

Remark 5.4.4. Choosing the almost complex structure on V generically, we can ensure that the curve \tilde{C} has square 0 or -1 , because the expected dimension of the moduli space is only positive in these two cases.

Proposition 5.4.5. *At least one of the components C of the SFT limit yields a curve $\tilde{C} \subset \tilde{X}$ which has square zero.*

Proof. We can impose an arbitrary point constraint on the line before we stretch, so that we find SFT-limit curves through every point of \bar{V} . If all of these were to lift to curves of negative square then, since there is only a countable number of such curves (at most one in each homology class), we could not find one through every point. This is a contradiction. \square

To summarise, we have found an embedded $\tilde{C} \subset \tilde{X}$ with $\tilde{C}^2 = 0$. Recall that we write $\tilde{C} = c_0 \mathcal{E} + \sum c_i C_i$ with $0 < c_0 \leq p$, and we define $\chi_i = \tilde{C} \cdot C_i$, $\mathbf{c}^T = (c_1, \dots, c_m)$, $\boldsymbol{\chi}^T = (\chi_1, \dots, \chi_m)$ and $M_{ij} = C_i \cdot C_j$, so that $\boldsymbol{\chi} = M\mathbf{c}$. A formula for M_{ij}^{-1} was given in Lemma 3.2.4 in terms of the numbers e_i, f_i defined there. The fact that $\tilde{C}^2 = 0$ implies

$$0 = \tilde{C}^2 = \frac{c_0^2}{p^2} + \boldsymbol{\chi}^T M^{-1} \boldsymbol{\chi}.$$

Finally, the adjunction formula tells us that

$$0 = \frac{\tilde{C}^2 + K \cdot \tilde{C}}{2} + 1,$$

that is

$$1 = \frac{3pc_0 - c_0^2}{2p^2} - \frac{1}{2}\boldsymbol{\chi}^T M^{-1} \boldsymbol{\chi} - \frac{1}{2}\mathbf{k}^T \boldsymbol{\chi} \quad (5.3)$$

where $\mathbf{k}^T = (k_1, \dots, k_m)$ is the vector of (negative) discrepancies defined by $K = -3p\mathcal{E} + \sum k_i C_i$.

Lemma 5.4.6. *We have (a) $\chi_i \leq 1$ for all i and (b) $\chi_i = 1$ for precisely one i .*

Proof. All the entries of $-M^{-1}$ are positive and also $\chi_i \geq 0$, so the second and third terms on the right-hand side of Equation (5.3) contribute at least

$$\sum_{i=1}^m \left(\frac{1}{2p^2} \chi_i^2 e_i f_i + \frac{1}{2} \chi_i \left(1 - \frac{e_i + f_i}{p^2} \right) \right) \quad (5.4)$$

to a sum whose total is 1.

If $\chi_i \geq 2$ then

$$\frac{1}{2p^2} \chi_i^2 e_i f_i + \frac{1}{2} \chi_i \left(1 - \frac{e_i + f_i}{p^2} \right) \geq 1 + \frac{1}{p^2} (2e_i f_i - e_i - f_i) \geq 1,$$

since $e_i, f_i \geq 1$. This is not possible, since the first term in Equation (5.3) is positive. Therefore $\chi_i \leq 1$ for all i . This proves (a).

If $\chi_i = 1$ then

$$\frac{1}{2p^2} \chi_i^2 e_i f_i + \frac{1}{2} \chi_i \left(1 - \frac{e_i + f_i}{p^2} \right) = \frac{1}{2} \left(1 + \frac{1}{p^2} (e_i f_i - e_i - f_i) \right) \geq \frac{1}{2} (1 - 1/p^2).$$

Let r be the number of indices i with $\chi_i \neq 0$. Then Equation (5.3) implies

$$1 \geq \frac{1}{2p^2} (3pc_0 - c_0^2) + \frac{r}{2} \left(1 - \frac{1}{p^2} \right).$$

The function $3pc_0 - c_0^2$ is an increasing function of c_0 on the interval $1 \leq c_0 \leq p$ and with minimum $3p - 1$, so

$$1 \geq \frac{r}{2} \left(1 - \frac{1}{p^2} \right) + \frac{3p - 1}{2p^2}.$$

If $r = 2$, the right hand side is > 1 . If $r \geq 3$, the right hand side is also > 1 , since then (using $p \geq 2$) we have $\frac{r}{2} - \frac{r}{2p^2} \geq \frac{3}{2} - \frac{3}{8} = \frac{9}{8} > 1$. The only possibility is that $r = 1$, which proves (b). \square

Lemma 5.4.7. *There exist integers p_2, p_3 such that (p, p_2, p_3) is a Markov triple.*

Proof. We now know that the curve \tilde{C} intersects precisely one of the curves C_i (and does so once transversely), that is $\chi_i = 1$ and $\chi_j = 0$ for $j \neq i$. Therefore,

$$0 = \tilde{C}^2 = \frac{c_0^2}{p^2} + \chi^T M^{-1} \chi = \frac{1}{p^2} (c_0^2 - e_i f_i),$$

so

$$c_0^2 = e_i f_i.$$

Equation (5.3) becomes

$$1 = \frac{3pc_0 - c_0^2}{2p^2} + \frac{e_i f_i}{2p^2} + \frac{1}{2} - \frac{e_i + f_i}{2p^2},$$

that is,

$$p^2 + e_i + f_i = 3p\sqrt{e_i f_i}.$$

Set $w_0 = p^2$, $w_1 = e_i$ and $w_2 = f_i$; we find

$$\frac{(w_0 + w_1 + w_2)^2}{w_0 w_1 w_2} = 9.$$

Now [25, Lemma 2.8] implies that w_0, w_1, w_2 is a squared Markov triple, that is $e_i = p_2^2$ and $f_i = p_3^2$ for some Markov triple (p, p_2, p_3) . \square

Corollary 5.4.8. *The singularity $\frac{1}{p^2}(1, pq - 1)$ has the form $\frac{1}{p^2}(p_3^2, p_2^2)$, so $q = \pm 3p_2 p_3^{-1} \mod p$, and the curve C_i which \tilde{C} hits is the culet curve.*

Proof. Consider the toric singularity $\frac{1}{p^2}(1, pq - 1)$, whose cone is bounded by the rays $\mathbb{R}_{\geq 0}(1, 0)$ and $\mathbb{R}_{\geq 0}(1 - pq, p^2)$. The curve C_i in the minimal resolution corresponds to a ray in this cone, say $\mathbb{R}_{\geq 0}(-t, s)$. Add the *opposite* ray $\mathbb{R}_{\geq 0}(t, -s)$ into the fan, and instead of getting a resolution, we get a compactification of the toric singularity (the fan is now complete). In terms of the moment polygon, this is equivalent to making a symplectic cut parallel to the (s, t) -direction whose inward normal points *downwards*. See Figure 23.

Since the partial resolution corresponding to the ray $\mathbb{R}_{\geq 0}(-t, s)$ would introduce the cyclic singularities $\frac{1}{e_i}(1, e_{i-1}^{-1} \mod e_i)$ and $\frac{1}{f_i}(1, f_{i+1} \mod f_i)$ (by definition of e_i and f_i from Lemma 3.2.4), the compactification will have dual singularities

$$\frac{1}{e_i}(1, e_i - e_{i-1}^{-1}), \quad \frac{1}{f_i}(1, f_i - f_{i+1}).$$

Since $\gcd(p^2, e_i, f_i) = 1$, the result is a weighted projective space $\mathbb{P}(p^2, e_i, f_i)$. Since p^2, e_i, f_i is a Markov triple (p_1^2, p_2^2, p_3^2) , the original singularity is $\frac{1}{p_1^2}(p_3^2, p_2^2)$ and the two new singularities are dual to the Wahl singularities $\frac{1}{p_2^2}(p_1^2, p_3^2)$ and $\frac{1}{p_3^2}(p_2^2, p_1^2)$, so by the discussion in Section 2.4, the curve C_i is the culet curve. The fact that $q = \pm 3p_2 p_3^{-1} \mod p$ follows as in Equation (2.5). \square

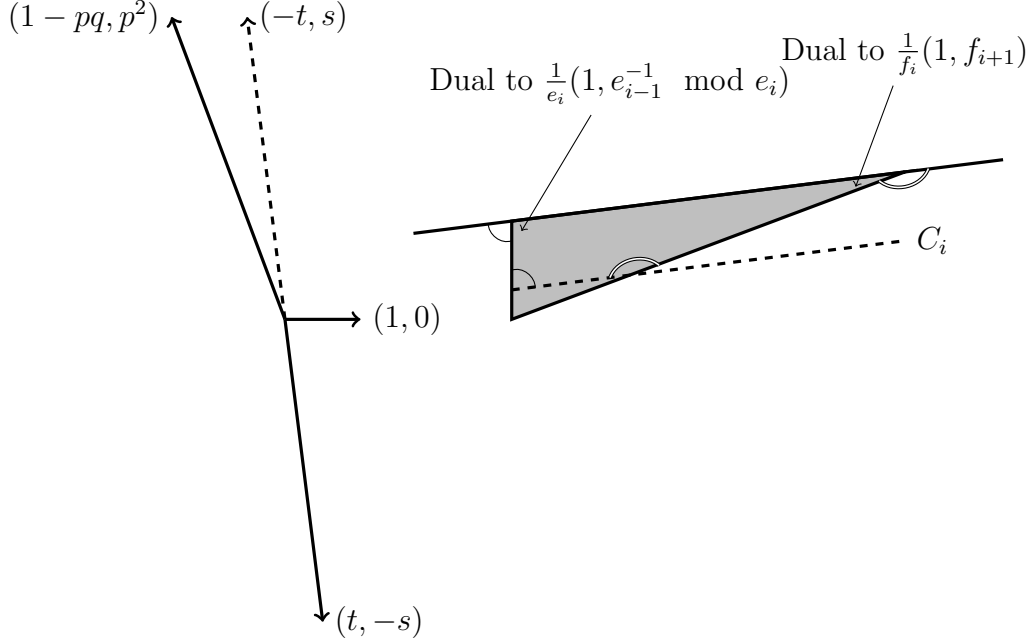


Figure 23: Left: The fan for the compactification of the toric $\frac{1}{p^2}(1, pq - 1)$ singularity. Right: The moment polygon for the compactification. The two new singularities (top left and top right corners of the triangle) are dual to the singularities $\frac{1}{e_i}(1, e_{i-1}^{-1} \bmod e_i)$ and $\frac{1}{f_i}(1, f_{i+1})$ that would be introduced by the partial resolution with exceptional locus C_i .

This completes the proof of Theorem 5.1.1 and also reproves the theorem of Evans and Smith that $E_{p,q}(\alpha, \beta)$ can only embed in \mathbb{CP}^2 if p is a Markov number and q a companion.

5.5 Proof of the Two Pin-Ball Theorem (Theorem 1.6.1)

For this subsection we assume that we have a symplectic embedding of two pin-balls

$$\iota: B_{p_1, q_1}(\alpha_1) \sqcup B_{p_2, q_2}(\alpha_2) \hookrightarrow \mathbb{CP}^2,$$

where $1 < p_1 < p_2$, and we denote $\Delta = p_1 p_2$. We take the same setup as in the beginning of Section 5.4, that is, we take C to be a component of the SFT limit curve in \bar{V} obtained by the neck-stretching procedure and denote the corresponding closed curve in the minimal resolution \tilde{X} by \tilde{C} . As explained in Remark 3.2.6, we write

$$K_{\mathbb{Q}} = -3\Delta\mathcal{E} + \sum_{i=1}^{m_1} k_{1,i}C_{1,i} + \sum_{i=1}^{m_2} k_{2,i}C_{2,i} \quad \text{and} \quad \tilde{C}_{\mathbb{Q}} = c_0\mathcal{E} + \sum_{i=1}^{m_1} c_{1,i}C_{1,i} + \sum_{i=1}^{m_2} c_{2,i}C_{2,i}. \quad (5.5)$$

Repeating the proofs of Lemma 5.4.2 and Proposition 5.4.3 verbatim, we obtain $0 < c_0 \leq \Delta$ and that \tilde{C} is an embedded sphere with $\tilde{C}^2 \leq 0$. Writing $\chi_j = M_j(c_{j,1}, \dots, c_{j,m_j})$ and

$\mathbf{k}_j = (k_{j,1}, \dots, k_{j,m_j})$, the adjunction formula gives us an analogue of Equation (5.3):

$$1 = \frac{3\Delta c_0 - c_0^2}{2\Delta^2} - \frac{1}{2} (\boldsymbol{\chi}_1^T M_1^{-1} \boldsymbol{\chi}_1 + \mathbf{k}_1^T \boldsymbol{\chi}_1) - \frac{1}{2} (\boldsymbol{\chi}_2^T M_2^{-1} \boldsymbol{\chi}_2 + \mathbf{k}_2^T \boldsymbol{\chi}_2). \quad (5.6)$$

In their proof of [17, Theorem 4.16] Evans and Smith show the existence of an orbifold curve whose proper transform is the curve \tilde{C} we want; it hits each Wahl chain precisely once transversely: the first chain at a point of either $C_{1,1}$ or C_{1,m_1} , the second at a point of either $C_{2,1}$ or C_{2,m_2} (this translates into the property that $K_z = K_{z'} = 0$ in the notation of that paper). As in the previous section, one could repeat all their arguments in the minimal resolution, without referring to orbifolds, but we omit this derivation. Using this we find that Equation (5.6) for \tilde{C} is equivalent to

$$3c_0 p_1 p_2 = c_0^2 + p_1^2 + p_2^2, \quad (5.7)$$

which is just the Markov equation. This means that there are exactly two solutions for c_0 , and because $c_0 < \frac{\Delta}{3p_1} = \frac{p_2}{3}$ by the proof of [17, Lemma 4.11.B], we know that c_0 is the smaller of the two solutions to (5.7).

Now the SFT-limit curve C has area $\int_{c_0\mathcal{E}} \tilde{\omega} = c_0/(p_1 p_2)$. For $i = 1, 2$, let \overline{N}_i be the negative end of \overline{V} coming from the neck around $B_{p_i, q_i}(\alpha_i)$ and let D_i be the unique non-compact connected component of $C \cap \overline{N}_i$. Each D_i is properly embedded.

Lemma 5.5.1. *We have $\alpha_i \leq \text{Area}(D_i)$ for $i = 1, 2$.*

Proof. Add in the orbifold points x_1 and x_2 to obtain girdled orbifolds \widehat{N}_i , which are locally modelled on $\mathbb{C}^2/\mathbb{Z}_{p_i^2}$. For each $i = 1, 2$, take the uniformising cover $\mathbb{C}^2 \rightarrow \mathbb{C}^2/\mathbb{Z}_{p_i^2}$ and take the preimage of D_i ; this is a union of punctured curves in a Euclidean ball $B \subset \mathbb{C}^2$. In fact, the preimage consists of a single punctured curve D'_i : since \tilde{C} intersects one of the end-curves of the Wahl chain, D_i is asymptotic to the quotient of either the punctured z_1 or z_2 axis in \mathbb{C}^2 , so that $\pi_1(D_i)$ maps surjectively to $\mathbb{Z}_{p_i^2}$.

Since D'_i is a finite-energy curve, removal of singularities tells us that it compactifies to give a properly embedded holomorphic curve $D''_i \subset B \subset \mathbb{C}^2$ passing through the origin. The monotonicity formula for minimal surfaces now tells us that the area of this holomorphic curve is at least the area of a complex line intersected with B . Therefore the area of D_i is bounded from below by the area of the projection of a complex line to the girdled orbifold \widehat{N}_i , which is α_i . \square

As a corollary,

$$\alpha_1 + \alpha_2 < \text{Area}(C) = \frac{c_0}{p_1 p_2},$$

because the curve C passes through the region between the two necks. As explained in Remark 1.6.2, this proves the Two Pin-Ball Theorem (Theorem 1.6.1).

5.6 Proof of Theorem 5.1.4

The strategy of the proof is to mimic, as closely as possible, an argument of Manetti [33] but staying in the world of symplectic geometry. Given a symplectic embedding $\iota : E_{p,q}(\alpha, \beta) \hookrightarrow X$ for some p, q, α, β , choose a minimal pavilion in the sense of Definition 2.1.7.

By Theorem 5.1.1, there exists a square zero \tilde{J} -holomorphic sphere $\tilde{C} \subset \tilde{X}$ which hits $C_{i_{\text{culet}}}$ once transversely and is disjoint from the other curves C_j , $j \neq i_{\text{culet}}$. By Theorem 4.1.4, \tilde{C} is part of a \tilde{J} -holomorphic regulation on \tilde{X} . By Lemma 3.1.8, we can choose J generically on V so as to ensure that the only irregular genus zero J -curves are C_1, \dots, C_m : all the other embedded J -holomorphic spheres are either -1 -spheres or have non-negative square. By Proposition 4.2.1(c), the broken rulings can only involve spheres of negative square, so the broken rulings are built out of the curves C_1, \dots, C_m and some -1 -spheres.

Lemma 5.6.1. *Every curve C_j except the culet curve $C_{i_{\text{culet}}}$ appears as an irreducible component in one of the broken rulings.*

Proof. The curves C_j other than $C_{i_{\text{culet}}}$ are disjoint from \tilde{C} . Since $\tilde{C}^2 = 0$, we can impose an arbitrary point constraint $x \in \tilde{X}$ and find a ruling passing through x . If $x \in C_j$ then we find a ruling S intersecting C_j . Since $[S] = [\tilde{C}]$, we find $S \cdot C_j = 0$, and thus the ruling S must contain C_j as an irreducible component. \square

We now use Proposition 4.2.7 to ensure that \tilde{J} is integrable in a neighbourhood of the -1 -curves in the broken rulings, keeping it integrable along C_1, \dots, C_m (where it is already integrable). Recall from Proposition 4.2.1(d) that every broken ruling contains at least one -1 -sphere. Now we can successively holomorphically contract -1 -spheres in broken rulings until we reach an almost complex 4-manifold Y with a non-degenerate holomorphic regulation with no broken rulings. This must have second Betti number 2 (in fact, it must be diffeomorphic to either $S^2 \times S^2$ or $\mathbb{CP}^2 \# \overline{\mathbb{CP}^2}$, see Remark 5.1.8).

Lemma 5.6.2. *The contraction from our resolved surface \tilde{X} to the minimal model Y contracts $m - 1$ curves.*

Proof. Let k be the number of curves contracted in going from \tilde{X} to Y . The second Betti number of \tilde{X} is $k + 2$. But the second Betti number of \tilde{X} is equal to $1 + m$ since it is obtained from \mathbb{CP}^2 by pavilion blow-up, introducing the chain of m spheres C_1, \dots, C_m . Therefore $k + 2 = m + 1$ and $k = m - 1$. \square

Lemma 5.6.3. *There are at most two broken rulings on \tilde{X} . More precisely,*

- *If $i_{\text{culet}} = 1 = m$ then there are no broken rulings.*

- If $i_{\text{culet}} = 1 < m$ (respectively $1 < i_{\text{culet}} = m$) then there is precisely one broken ruling comprising C_2, \dots, C_m (respectively C_1, \dots, C_{m-1}) and one additional \tilde{J} -holomorphic -1 -sphere E .
- If $1 < i_{\text{culet}} < m$ then there are precisely two broken rulings: one comprising $C_1, \dots, C_{i_{\text{culet}}-1}$ and an additional -1 -sphere E_1 , the other comprising $C_{i_{\text{culet}}+1}, \dots, C_m$ and an additional -1 -sphere E_2 .

Proof. By Proposition 4.2.1, each broken ruling is a tree of embedded \tilde{J} -holomorphic spheres with negative self-intersection, which are therefore either amongst the curves C_1, \dots, C_m or else -1 -spheres. All of the curves C_i other than the culet curve $C_{i_{\text{culet}}}$ appear amongst the irreducible components of some broken rulings by Lemma 5.6.1.

If $m = 1$ then $i_{\text{culet}} = 1$ and by Lemma 5.6.2 we have $\tilde{X} = Y$, so there are no broken rulings. This situation arises only for pin-ellipsoids with $p = 2$.

If $i_{\text{culet}} = 1 < m$ (respectively $1 < i_{\text{culet}} = m$) then by Lemma 4.2.3 the curves C_2, \dots, C_m (respectively C_1, \dots, C_{m-1}) will belong to a single broken ruling. Since these curves all have $C_i^2 \leq -2$, Proposition 4.2.1(d) shows that this broken ruling must also contain a -1 -sphere E . We need to contract all but one of the curves in this ruling to get to the minimal model Y . This is $m - 1$ curves, so there can be no other broken rulings by Lemma 5.6.2. Moreover, the broken ruling is precisely $E \cup \bigcup_{i=2}^m C_i$. See Figure 16(b) for an example; this situation arises precisely for pin-ellipsoids with $p \geq 5$ along the Fibonacci branch of the Markov tree.

If $i_{\text{culet}} \neq 1, m$ then there will be two broken rulings containing the subchains $C_1, \dots, C_{i_{\text{culet}}-1}$ and $C_{i_{\text{culet}}+1}, \dots, C_m$. Each of these broken rulings will also contain a -1 -sphere, say E_1 and E_2 . In each broken ruling we need to contract all but one of the curves, which means we contract a total of $i_{\text{culet}} - 1$ curves in the first and $m - i_{\text{culet}}$ curves in the second ruling, making a total of $m - 1$ curves. Again, Lemma 5.6.2 tells us there can be no further rulings and the two rulings we have found contain no further curves. See Figure 16(c) for an example. \square

Remark 5.6.4. Moreover, we can identify which of the curves C_1, \dots, C_m intersect the -1 -spheres E_1 and E_2 in the broken rulings. Since the dual graph of the broken ruling is a tree, E_1 and E_2 can each intersect at most one of the curves in the chain, and blowing down E_1 (respectively E_2) will turn the subchain $C_1, \dots, C_{i_{\text{culet}}-1}$ (respectively $C_{i_{\text{culet}}+1}, \dots, C_m$) into a zero continued fraction by Remark 4.2.9. Recall that $C_1, \dots, C_{i_{\text{culet}}-1}$ and $C_{i_{\text{culet}}+1}, \dots, C_m$ form dual Wahl chains. It is well-known (see for example [49, Proposition-Definition 2.3 and Proposition 2.4]) that a dual Wahl chain has a unique position where it can be combinatorially blown down to obtain a zero-continued fraction, so this gives the positions where E_1 and E_2 intersect the subchains.

This completes the proof of Theorem 5.1.4.

6 Appendix

6.1 Alternative proof of Theorem 5.1.1

In this appendix, we explain how Theorem 5.1.1 follows from [17, Theorem 4.15]. Given a symplectic embedding $\iota : E_{p,q}(\alpha, \beta) \hookrightarrow \mathbb{CP}^2$, they found a Markov triple (p, b, c) and constructed a \widehat{J} -holomorphic orbifold curve \widehat{C} in the orbifold \widehat{X} (see Figure 14 for the notation) satisfying the following properties:

- (ES1) Near the orbifold point $p \in \widehat{X}$, \widehat{C} has precisely one branch (in the terminology of [17], $|Z| = 1$).
- (ES2) If we look at the lift of \widehat{C} to the local uniformising cover $\mathbb{C}^2 \rightarrow \mathbb{C}^2/G$, there exist local coordinates (z_1, z_2) transforming under the action of $\zeta \in G$ as $(\zeta^{m_1} z_1, \zeta^{m_2} z_2)$ with respect to which the lift is given by $z \mapsto (z^{b^2}, a_1 z^{c^2})$. In particular, the Puiseux series has length one and the link of the singularity of the curve in the cover is a (b^2, c^2) -torus knot.
- (ES3) The real dimension of the moduli space containing \widehat{C} is equal to its virtual dimension which equals 2.

Remark 6.1.1. We take this opportunity to correct [17, Remark 3.15]. Namely, as described in [17, Section 3.3], the germ of the orbifold curve $f : \widehat{C} \rightarrow \widehat{X}$ near an orbifold point $z \in \widehat{C}$ involves a choice of homomorphism $\rho_z : H_z \rightarrow G_z$, where H_z is the isotropy group of \widehat{C} at z and G_z is the isotropy group of \widehat{X} near $f(z)$; a lift \tilde{f}_α of f to the local uniformising cover near $f(z)$ satisfies the equivariance condition [17, Eq. (2)]

$$\tilde{f}_\alpha(\zeta x) = \rho_z(\zeta) \tilde{f}_\alpha(x).$$

In [17, Remark 3.15], this was applied to $\tilde{f}_\alpha(x) = (x^Q, \sum a_i x^{R_i})$ and the cyclic quotient singularity $\frac{1}{p^2}(1, pq - 1)$ to say that

$$\left(\zeta^Q x^Q, \sum a_i \zeta^{R_i} x^{R_i} \right) = \left(\zeta x^Q, \zeta^{pq-1} \sum a_i x^{R_i} \right)$$

and deduce that $Q \equiv 1 \pmod{p^2}$, $R_i \equiv pq - 1 \pmod{p^2}$ (or vice versa). However, this assumes that ρ_z is the identity. More generally, ρ_z could have the form $\rho_z(\zeta) = \zeta^n$ for some n . If $\gcd(n, p^2) = p^2/d$ then at best we can deduce that

$$R_i/Q = (pq - 1)^{\pm 1} \pmod{d}.$$

In fact, this is all that was used in what followed. It should have been clear that the stronger conclusion is false from the fact that eventually $Q = b^2$, $R_1 = c^2$, for example if $(p, b, c) = (2, 5, 29)$ then neither 2^2 nor 5^2 is congruent to 1 modulo 29^2 .

6.1.0.1 The uniformising cover. Make an integral affine transformation of the Vianna triangle $\mathfrak{D}(p_1, p_2, p_3)$ as in 2.4 to make the edge \mathfrak{e}_1 horizontal with the rest of the triangle below. Let \mathbf{w}_2 and \mathbf{w}_3 be the primitive integer vectors pointing out of \mathfrak{v}_1 along \mathfrak{e}_2 and \mathfrak{e}_3 respectively; note that $\mathbf{w}_2 = (-u_2, p_3^2)$ and $\mathbf{w}_3 = (u_3, p_2^2)$ for some u_2, u_3 , since $(p_2\mathbf{w}_2)/(p_3p_1)$ and $(p_3\mathbf{w}_3)/(p_1p_2)$ must reach the same height p_2p_3/p_1 (compare with [9, Paragraph 2 of the proof of Proposition 2.5] for the computation of this height). Consider the uniformising cover $\mathbb{C}^2 \rightarrow \mathbb{C}^2/G$ for the orbifold singularity $\frac{1}{p_1^2}(p_2^2, p_3^2)$. The cover \mathbb{C}^2 is also toric, its moment polygon is the positive quadrant, and the uniformising cover is induced by the integral affine map given by the matrix whose columns are \mathbf{w}_2 and \mathbf{w}_3 . Under this map, a symplectic cut along the $(p_2^2, -p_3^2)$ direction in the moment image of \mathbb{C}^2 maps to a horizontal cut in the moment image of $\frac{1}{p_1^2}(p_2^2, p_3^2)$, that is the culet cut.

Proposition 6.1.2. *If $\widehat{C} \subset \widehat{X}$ is a curve with Properties (ES1–3) then the proper transform $\widetilde{C} \subset \widetilde{X}$ satisfies the following properties:*

- (a) *\widetilde{C} is a smooth sphere which intersects the culet curve $C_{i_{\text{culet}}}$ once transversely and is disjoint from the other curves C_j , $j \neq i_{\text{culet}}$.*
- (b) *\widetilde{C} lives in a moduli space of real dimension equal to its virtual dimension, which equals 2. In particular, \widetilde{C} is a square zero \widetilde{J} -holomorphic sphere, and therefore appears as a smooth ruling in a \widetilde{J} -holomorphic regulation.*

Proof. (a) By Property (ES2), the germ of the lifted curve in the uniformising cover $\mathbb{C}^2 \rightarrow \mathbb{C}^2/G$ is parametrised by $z \mapsto (z^{b^2}, a_1 z^{c^2})$. We can resolve the singularity of the germ by performing a weighted blow-up. Consider the surface

$$\left\{ (z_1, z_2, [w_1 : w_2]) : z_1^{c^2} w_2^{b^2} = w_1^{c^2} z_2^{b^2} \right\} \subset \mathbb{C}^2 \times \mathbb{P}^1(b^2, c^2).$$

The total transform of our germ under the projection of this surface to \mathbb{C}^2 is given by the equations $z_1^{c^2} w_2^{b^2} = w_1^{c^2} z_2^{b^2}$ and $z_1^{c^2} = z_2^{b^2}$. In the chart $w_2 = 1$, we have $z_1^{c^2} = w_1^{c^2} z_2^{b^2} = z_2^{b^2}$, so the proper transform becomes $w_1^{c^2} = 1$; this looks like a curve with c^2 irreducible components $w_1 = \mu$ as μ runs over the set μ_{c^2} of c^2 th roots of unity, but there is a residual action of μ_{c^2} (the rescalings preserving the condition $w_2 = 1$) which relates all of these, so the proper transform of the germ has a single, smooth irreducible component in this chart which intersects the exceptional curve $z_2 = 0$ once transversely; we find the same component in the other chart $w_1 = 1$. This weighted blow-up corresponds to making a symplectic cut of \mathbb{C}^2 along the hypersurface living over the line parallel to the vector $(b^2, -c^2)$, which projects under the partial resolution of the uniformising cover to the culet curve, as explained in 6.1.0.1.

(b) The same analysis applies to the proper transforms of the other curves \widehat{C}_t in the moduli space of \widehat{C} , so that the proper transforms \widetilde{C}_t live in the same moduli space. Moreover, if \widetilde{C}_s is in the same moduli space of \widetilde{C} then its projection to \widehat{X} lives in the same moduli

space as \widehat{C} , so the moduli spaces are diffeomorphic and the dimension computation follows from Property (ES3). The fact that \widetilde{C} is a sphere of square zero follows from the fact that a sphere of square n lives in a moduli space of virtual real dimension $2n + 2$ (which equals the actual dimension as long as $n \geq -1$ by automatic transversality). \square

This completes the alternative proof of Theorem 5.1.1.

References

- [1] M. Abreu. Kähler geometry of toric manifolds in symplectic coordinates. In *Symplectic and contact topology: interactions and perspectives (Toronto, ON/Montreal, QC, 2001)*, volume 35 of *Fields Inst. Commun.*, pages 1–24. Amer. Math. Soc., Providence, RI, 2003.
- [2] N. Adaloglou. Embeddings and disjunction of Lagrangian pinwheels via rational blow-ups. *arXiv:2405.02110*, 2024.
- [3] N. Adaloglou. Uniqueness of Lagrangians in $T^*\mathbb{R}P^2$. *Ann. Math. Qué.*, 49(1):215–222, 2025.
- [4] N. Adaloglou and J. Hauber. Pinwheels in symplectic rational and ruled surfaces and non-squeezing of rational homology balls. *arXiv:2503.16250*, 2025.
- [5] M. Aigner. *Markov’s theorem and 100 years of the uniqueness conjecture*. Springer, Cham, 2013. A mathematical journey from irrational numbers to perfect matchings.
- [6] P. Biran. Lagrangian barriers and symplectic embeddings. *Geom. Funct. Anal.*, 11(3):407–464, 2001.
- [7] M. S. Borman, T.-J. Li, and W. Wu. Spherical Lagrangians via ball packings and symplectic cutting. *Selecta Math. (N.S.)*, 20(1):261–283, 2014.
- [8] F. Bourgeois, Y. Eliashberg, H. Hofer, K. Wysocki, and E. Zehnder. Compactness results in symplectic field theory. *Geom. Topol.*, 7:799–888, 2003.
- [9] J. Brendel and F. Schlenk. Pinwheels as Lagrangian barriers. *Commun. Contemp. Math.*, 26(5):Paper No. 2350020, 21, 2024.
- [10] Encyclopaedia Britannica. “facet”. In *Micropedia*, volume 4. Encyclopaedia Britannica, Inc., 15th edition, 1990.
- [11] H. Chen and W. Zhang. Kodaira dimensions of almost complex manifolds II. *Comm. Anal. Geom.*, 32(3):751–790, 2024.
- [12] K. Cieliebak and K. Mohnke. Compactness for punctured holomorphic curves. *J. Symplectic Geom.*, 3(4):589–654, 2005.

- [13] D. Cristofaro-Gardiner and R. Hind. Boundaries of open symplectic manifolds and the failure of packing stability. *arXiv:2307.01140*, 2023.
- [14] Dan Cristofaro-Gardiner, Nicki Magill, and Dusa McDuff. Curvy points, the perimeter, and the complexity of convex toric domains, 2025.
- [15] Y. Eliashberg, A. Givental, and H. Hofer. Introduction to Symplectic Field Theory. In *GAFa 2000*, pages 560–673. Basel: Birkhäuser, 2000.
- [16] J. D. Evans. *Lectures on Lagrangian torus fibrations*, volume 105 of *London Mathematical Society Student Texts*. Cambridge University Press, Cambridge, 2023.
- [17] J. D. Evans and I. Smith. Markov numbers and Lagrangian cell complexes in the complex projective plane. *Geom. Topol.*, 22(2):1143–1180, 2018.
- [18] J. D. Evans and I. Smith. Bounds on Wahl singularities from symplectic topology. *Algebr. Geom.*, 7(1):59–85, 2020.
- [19] R. Fintushel and R. J. Stern. Rational blowdowns of smooth 4-manifolds. *J. Differential Geom.*, 46(2):181–235, 1997.
- [20] W. Fulton. *Introduction to toric varieties*, volume 131 of *Annals of Mathematics Studies*. Princeton University Press, Princeton, NJ, 1993. The William H. Roever Lectures in Geometry.
- [21] Mark J. Gotay. On coisotropic imbeddings of presymplectic manifolds. *Proc. Amer. Math. Soc.*, 84(1):111–114, 1982.
- [22] M. Gromov. Pseudo holomorphic curves in symplectic manifolds. *Invent. Math.*, 82(2):307–347, 1985.
- [23] P. Hacking and Y. Prokhorov. Smoothable del Pezzo surfaces with quotient singularities. *Compos. Math.*, 146(1):169–192, 2010.
- [24] P. Hacking, J. Tevelev, and G. Urzúa. Flipping surfaces. *J. Algebraic Geom.*, 26(2):279–345, 2017.
- [25] J. Hausen, K. Király, and M. Wrobel. On degenerations of the projective plane. *arXiv:2405.04862*, 2024.
- [26] R. Hind. Lagrangian isotopies in Stein manifolds. *arxiv:0311093*, 2003.
- [27] T. Khodorovskiy. Bounds on embeddings of rational homology balls in symplectic 4-manifolds. *arXiv:1307.4321*, 2013.
- [28] T. Khodorovskiy. Symplectic rational blow-up. *arXiv:1303.2581*, 2013.
- [29] J. Li, T.-J. Li, and W. Wu. The space of tamed almost complex structures on symplectic 4-manifolds via symplectic spheres. *Riv. Math. Univ. Parma (N.S.)*, 13(2):651–670, 2022.

- [30] T.-J. Li and W. Wu. Lagrangian spheres, symplectic surfaces and the symplectic mapping class group. *Geom. Topol.*, 16(2):1121–1169, 2012.
- [31] Tian-Jun Li and Weiyi Zhang. J -holomorphic curves in a nef class. *Int. Math. Res. Not.*, 2015(22):12070–12104, 2015.
- [32] P. Lisca. On symplectic fillings of lens spaces. *Trans. Amer. Math. Soc.*, 360(2):765–799, 2008.
- [33] M. Manetti. Normal degenerations of the complex projective plane. *J. Reine Angew. Math.*, 419:89–118, 1991.
- [34] D. McDuff. Lectures on Gromov invariants for symplectic 4-manifolds. In *Gauge theory and symplectic geometry (Montreal, PQ, 1995)*, volume 488 of *NATO Adv. Sci. Inst. Ser. C: Math. Phys. Sci.*, pages 175–210. Kluwer Acad. Publ., Dordrecht, 1997. With notes by Wladyslaw Lorek.
- [35] D. McDuff and E. Opshtein. Nongeneric J -holomorphic curves and singular inflation. *Algebr. Geom. Topol.*, 15(1):231–286, 2015.
- [36] D. McDuff and D. Salamon. *J -holomorphic curves and symplectic topology*, volume 52 of *American Mathematical Society Colloquium Publications*. American Mathematical Society, Providence, RI, 2004.
- [37] D. McDuff and F. Schlenk. The embedding capacity of 4-dimensional symplectic ellipsoids. *Ann. of Math. (2)*, 175(3):1191–1282, 2012.
- [38] D. McDuff and K. Siegel. Singular algebraic curves and infinite symplectic staircases. *arXiv:2404.14702*, 2024.
- [39] Dusa McDuff and Dietmar Salamon. *Introduction to symplectic topology*. Oxford Graduate Texts in Mathematics. Oxford University Press, Oxford, third edition, 2017.
- [40] M. McLean. The growth rate of symplectic homology and affine varieties. *Geom. Funct. Anal.*, 22(2):369–442, 2012.
- [41] G. Mikhalkin and M. Shkolnikov. Wave fronts and caustics in the tropical plane. *arXiv:2310.17269*, 2023.
- [42] F. Schlenk. Symplectic embedding problems, old and new. *Bull. Amer. Math. Soc. (N.S.)*, 55(2):139–182, 2018.
- [43] V. Shevchishin and G. Smirnov. Symplectic triangle inequality. *Proc. Amer. Math. Soc.*, 148(4):1389–1397, 2020.
- [44] B. Siebert and G. Tian. On the holomorphicity of genus two Lefschetz fibrations. *Ann. of Math. (2)*, 161(2):959–1020, 2005.
- [45] J.-C. Sikorav. Singularities of J -holomorphic curves. *Math. Z.*, 226(3):359–373, 1997.

- [46] M. Symington. Symplectic rational blowdowns. *J. Differential Geom.*, 50(3):505–518, 1998.
- [47] M. Symington. Generalized symplectic rational blowdowns. *Algebr. Geom. Topol.*, 1:503–518, 2001.
- [48] M. Symington. Four dimensions from two in symplectic topology. In *Topology and geometry of manifolds (Athens, GA, 2001)*, volume 71 of *Proc. Sympos. Pure Math.*, pages 153–208. Amer. Math. Soc., Providence, RI, 2003.
- [49] G. Urzúa and J. P. Zúñiga. The birational geometry of Markov numbers. *arXiv:2310.17957*, 2023.
- [50] R. Vianna. On exotic Lagrangian tori in \mathbb{CP}^2 . *Geom. Topol.*, 18(4):2419–2476, 2014.
- [51] R. Vianna. Infinitely many exotic monotone Lagrangian tori in \mathbb{CP}^2 . *J. Topol.*, 9(2):535–551, 2016.
- [52] W. Zhang. Moduli space of J -holomorphic subvarieties. *Selecta Math. (N.S.)*, 27(2):Paper No. 29, 44, 2021.

N. Adaloglou, MATHEMATISCH INSTITUUT, LEIDEN,
`n.adaloglou@math.leidenuniv.nl`

J. Brendel, D-MATH, ETH ZÜRICH,
`joe.brendel@math.ethz.ch`

J. Evans, SCHOOL OF MATHEMATICAL SCIENCES, LANCASTER UNIVERSITY,
`j.d.evans@lancaster.ac.uk`

J. Hauber, INSTITUT DE MATHÉMATIQUES, UNIVERSITÉ DE NEUCHÂTEL,
`johannes.hauber@unine.ch`

F. Schlenk, INSTITUT DE MATHÉMATIQUES, UNIVERSITÉ DE NEUCHÂTEL,
`schlenk@unine.ch`